

# The genomic history of the Iberian Peninsula over the past 8000 years

Iñigo Olalde<sup>1\*</sup>, Swapan Mallick<sup>1,2,3</sup>, Nick Patterson<sup>2</sup>, Nadin Rohland<sup>1</sup>, Vanessa Villalba-Mouco<sup>4,5</sup>, Marina Silva<sup>6</sup>, Katharina Dulias<sup>6</sup>, Ceiridwen J. Edwards<sup>6</sup>, Francesca Gandini<sup>6</sup>, Maria Pala<sup>6</sup>, Pedro Soares<sup>7</sup>, Manuel Ferrando-Bernal<sup>8</sup>, Nicole Adamski<sup>1,3</sup>, Nasreen Broomandkhoshbacht<sup>1,3</sup>, Olivia Cheronet<sup>9</sup>, Brendan J. Culleton<sup>10</sup>, Daniel Fernandes<sup>9,11</sup>, Ann Marie Lawson<sup>1,3</sup>, Matthew Mah<sup>1,2,3</sup>, Jonas Oppenheimer<sup>1,3</sup>, Kristin Stewardson<sup>1,3</sup>, Zhao Zhang<sup>1</sup>, Juan Manuel Jiménez Arenas<sup>12,13,14</sup>, Isidro Jorge Toro Moyano<sup>15</sup>, Domingo C. Salazar-García<sup>16</sup>, Pere Castanyer<sup>17</sup>, Marta Santos<sup>17</sup>, Joaquim Tremoleda<sup>17</sup>, Marina Lozano<sup>18,19</sup>, Pablo García Borja<sup>20</sup>, Javier Fernández-Eraso<sup>21</sup>, José Antonio Mujika-Alustiza<sup>21</sup>, Cecilio Barroso<sup>22</sup>, Francisco J. Bermúdez<sup>22</sup>, Enrique Viguera Mínguez<sup>23</sup>, Josep Burch<sup>24</sup>, Neus Coromina<sup>24</sup>, David Vivó<sup>24</sup>, Artur Cebrià<sup>25</sup>, Josep Maria Fullola<sup>25</sup>, Oretó García-Puchol<sup>26</sup>, Juan Ignacio Morales<sup>25</sup>, F. Xavier Oms<sup>25</sup>, Tona Majó<sup>27</sup>, Josep Maria Vergès<sup>18,19</sup>, Antònia Díaz-Carvajal<sup>28</sup>, Imma Ollich-Castanyer<sup>28</sup>, F. Javier López-Cachero<sup>25</sup>, Ana Maria Silva<sup>29,30,31</sup>, Carmen Alonso-Fernández<sup>32</sup>, Germán Delibes de Castro<sup>33</sup>, Javier Jiménez Echevarría<sup>32</sup>, Adolfo Moreno-Márquez<sup>34</sup>, Guillermo Pascual Berlanga<sup>35</sup>, Pablo Ramos-García<sup>36</sup>, José Ramos Muñoz<sup>34</sup>, Eduardo Vijande Vila<sup>34</sup>, Gustau Aguilera Arzo<sup>37</sup>, Ángel Esparza Arroyo<sup>38</sup>, Katina T. Lillios<sup>39</sup>, Jennifer Mack<sup>40</sup>, Javier Velasco-Vázquez<sup>41</sup>, Anna Waterman<sup>42</sup>, Luis Benítez de Lugo Enrich<sup>43,44</sup>, María Benito Sánchez<sup>45</sup>, Bibiana Agustí<sup>46,47</sup>, Ferran Codina<sup>47</sup>, Gabriel de Prado<sup>47</sup>, Almudena Estalrich<sup>48</sup>, Álvaro Fernández Flores<sup>49</sup>, Clive Finlayson<sup>50,51,52,53</sup>, Geraldine Finlayson<sup>50,52,53</sup>, Stewart Finlayson<sup>50,54</sup>, Francisco Giles-Guzmán<sup>50</sup>, Antonio Rosas<sup>55</sup>, Virginia Barciela González<sup>56,57</sup>, Gabriel García Atiénzar<sup>56,57</sup>, Mauro S. Hernández Pérez<sup>56,57</sup>, Armando Llanos<sup>58</sup>, Yolanda Carrión Marco<sup>59</sup>, Isabel Collado Beneyto<sup>60</sup>, David López-Serrano<sup>61</sup>, Mario Sanz Tormo<sup>35</sup>, António C. Valera<sup>62</sup>, Concepción Blasco<sup>43</sup>, Corina Liesau<sup>43</sup>, Patricia Ríos<sup>43</sup>, Joan Daura<sup>25</sup>, María Jesús de Pedro Michó<sup>63</sup>, Agustín A. Diez-Castillo<sup>64</sup>, Raúl Flores Fernández<sup>35</sup>, Joan Francès Farré<sup>65</sup>, Rafael Garrido-Pena<sup>43</sup>, Victor S. Gonçalves<sup>30</sup>, Elisa Guerra-Doce<sup>33</sup>, Ana Mercedes Herrero-Corral<sup>66</sup>, Joaquim Juan-Cabanilles<sup>67</sup>, Daniel López-Reyes<sup>68</sup>, Sarah B. McClure<sup>69</sup>, Marta Merino Pérez<sup>70</sup>, Arturo Oliver Foix<sup>37</sup>, Montserrat Sanz Borràs<sup>25</sup>, Ana Catarina Sousa<sup>30</sup>, Julio Manuel Vidal Encinas<sup>71</sup>, Douglas J. Kennett<sup>69</sup>, Martin B. Richards<sup>6</sup>, Kurt Werner Alt<sup>72,73</sup>, Wolfgang Haak<sup>4,74</sup>, Ron Pinhasi<sup>9</sup>, Carles Lalueza-Fox<sup>8\*</sup>, David Reich<sup>1,2,3\*</sup>

**\*Corresponding authors.** Email: inigo\_olalde@hms.harvard.edu (I.O.); carles.lalueza@upf.edu (C.L.-F.); reich@genetics.med.harvard.edu (D.R.)

<sup>1</sup>Department of Genetics, Harvard Medical School, Boston, Massachusetts 02115, USA. <sup>2</sup>Broad Institute of MIT and Harvard, Cambridge, Massachusetts 02142, USA. <sup>3</sup>Howard Hughes Medical Institute, Harvard Medical School, Boston, Massachusetts 02115, USA. <sup>4</sup>Max Planck Institute for the Science of Human History, Jena 07745, Germany. <sup>5</sup>Departamento de Ciencias de la Antigüedad, Grupo Primeros Pobladores del Valle del Ebro (PPVE), Instituto de Investigación en Ciencias Ambientales (IUCA), Universidad de Zaragoza, Zaragoza 50009, Spain. <sup>6</sup>Department of Biological and Geographical Sciences, School of Applied Sciences, University of Huddersfield, Huddersfield HD1 3DH, UK. <sup>7</sup>Centre of Molecular and Environmental Biology, Department of Biology, University of Minho, Braga 4710-057, Portugal. <sup>8</sup>Institute of Evolutionary Biology, CSIC-Universitat Pompeu Fabra, Barcelona 08003, Spain. <sup>9</sup>Department of Evolutionary Anthropology, University of Vienna, Vienna 1090, Austria. <sup>10</sup>Department of Anthropology & Institute for Energy and the Environment, The Pennsylvania State University, University Park, PA 16802, USA. <sup>11</sup>Research Center for Anthropology and Health, Department of Life Science, University of Coimbra, Coimbra 3000-456, Portugal. <sup>12</sup>Departamento de Prehistoria y Arqueología, Universidad de Granada, Granada 18071, Spain. <sup>13</sup>Instituto Universitario de la Paz y los Conflictos, Universidad de Granada, Granada 18071, Spain. <sup>14</sup>Department of Anthropology - Anthropologisches Institut & Museum, Universität Zürich, Zürich CH-8057, Switzerland. <sup>15</sup>Museo Arqueológico y Etnológico de Granada, Granada 18010, Spain. <sup>16</sup>Departamento de Geografía, Prehistoria y Arqueología, Grupo de Investigación en Prehistoria, (UPV-EHU)/IKERBASQUE-Basque Foundation for Science, Vitoria 01006, Spain. <sup>17</sup>Museu d'Arqueologia de Catalunya-Empúries, L'Escala 17130, Spain. <sup>18</sup>Institut Català de Paleoecologia Humana i Evolució Social (IPHES), Tarragona 43007, Spain. <sup>19</sup>Àrea de Prehistòria, Universitat Rovira i Virgili (URV), Tarragona 43002, Spain. <sup>20</sup>Departamento de Prehistoria e Historia Antigua, Universidad Nacional de Educación a Distancia, Valencia 46014, Spain. <sup>21</sup>Departamento de Geografía, Prehistoria y Arqueología, Universidad del País Vasco, Vitoria 01006, Spain. <sup>22</sup>Fundación Instituto de Investigación de Prehistoria y Evolución Humana (FIPEH), Lucena 14900, Spain. <sup>23</sup>Àrea de Genètica, Facultat de Ciències, Universitat de Màlaga, Màlaga 29071 Spain. <sup>24</sup>Institut de Recerca Històrica, Universitat de Girona, Girona 17004, Spain. <sup>25</sup>SERP, Departament d'Història i Arqueologia, Facultat de Geografia i Història, Universitat de Barcelona, Barcelona 08001, Spain. <sup>26</sup>PREMEDOC Research Group, Departament de

Prehistòria, Arqueologia i Historia Antiga, Universitat de València, València 46010, Spain. <sup>27</sup>Archaeom. Departament de Prehistòria, Universitat Autònoma de Barcelona, Cerdanyola del Vallès 08193, Spain. <sup>28</sup>Universitat de Barcelona-GRAMP / Museu Arqueològic de l'Esquerda, Roda de Ter 08510, Spain. <sup>29</sup>Laboratory of Prehistory, Research Center for Anthropology and Health, Department of Life Sciences, University of Coimbra, Coimbra 3000-456, Portugal. <sup>30</sup>UNIARQ, Faculdade de Letras, Universidade de Lisboa, Lisboa 1600-214, Portugal. <sup>31</sup>CEF, Department of Life Sciences, University of Coimbra, Coimbra 3000-456, Portugal. <sup>32</sup>Cronos S.C. Arqueología y Patrimonio, Burgos 09003, Spain. <sup>33</sup>Departamento de Prehistoria, Facultad de Filosofía y Letras, Universidad de Valladolid, Valladolid 47011, Spain. <sup>34</sup>Departamento de Historia, Geografía y Filosofía, Universidad de Cádiz, Cádiz 11003, Spain. <sup>35</sup>Professional archaeologist. <sup>36</sup>School of Dentistry, University of Granada, Colegio Máximo, Campus Universitario de Cartuja, Granada 18071, Spain. <sup>37</sup>Servicio de Investigaciones Arqueológicas y Prehistóricas de la Diputación de Castellón, Castellón de la Plana 12003, Spain. <sup>38</sup>GIR PrehUSAL, Dept. Prehistoria, Hª Antigua y Arqueología, Universidad de Salamanca, Salamanca 37071, Spain. <sup>39</sup>Department of Anthropology, University of Iowa, Iowa City, Iowa 52240, USA. <sup>40</sup>Office of the State Archaeologist, University of Iowa, Iowa City, Iowa 52240, USA. <sup>41</sup>Dept. Ciencias Históricas, Universidad de Las Palmas de Gran Canaria, Las Palmas 35071, Spain. <sup>42</sup>Mt. Mercy University, Cedar Rapids, Iowa 52402, USA. <sup>43</sup>Departamento de Prehistoria y Arqueología, Universidad Autónoma de Madrid, Madrid 28049, Spain. <sup>44</sup>Departamento de Prehistoria y Arqueología, Universidad Nacional de Educación a Distancia, Madrid 28040, Spain. <sup>45</sup>Departamento de Medicina Legal, Psiquiatria y Anatomía Patológica, Universidad Complutense de Madrid, Madrid 28040, Spain. <sup>46</sup>INSITU S.C.P.. <sup>47</sup>Museu d'Arqueologia de Catalunya-Ullastret, Ullastret 17114, Spain. <sup>48</sup>Instituto Internacional de Investigaciones Prehistóricas de Cantabria IIIPC (Universidad de Cantabria-Gobierno de Cantabria-Santander), Santander 39005, Spain. <sup>49</sup>Arqueología y Gestión S.L.L., Fuentes de Andalucía 41420, Spain. <sup>50</sup>The Gibraltar National Museum, Gibraltar GX11 1AA, Gibraltar. <sup>51</sup>Department of Anthropology, University of Toronto, Toronto ON M5S 2S2, Canada. <sup>52</sup>School of Natural Sciences and Psychology, Liverpool John Moores University, Liverpool L3 3AF, UK. <sup>53</sup>Institute of Life and Earth Sciences, University of Gibraltar, Gibraltar GX11 1AA, Gibraltar. <sup>54</sup>Department of Life Sciences, Anglia Ruskin University, Cambridge CB1 1PT, UK. <sup>55</sup>Paleoanthropology Group, Department of Paleobiology, Museo Nacional de Ciencias Naturales (MNCN)–Consejo Superior de Investigaciones Científicas (CSIC), Madrid 28006, Spain. <sup>56</sup>Departamento de Prehistoria, Arqueología e Historia Antigua, Facultad de Filosofía y Letras, Universidad de Alicante, San Vicente del Raspeig 03690, Spain. <sup>57</sup>Instituto Universitario de Investigación en Arqueología y Patrimonio Histórico (INAPH), San Vicente del Raspeig 03690, Spain. <sup>58</sup>Instituto Alavés de Arqueología, Vitoria-Gasteiz 01008, Spain. <sup>59</sup>Departament de Prehistòria, Arqueologia i Historia Antiga, Universitat de València, València 46010, Spain. <sup>60</sup>Museu Arqueològic Vicent Casanova, Bocairent 46880, Spain. <sup>61</sup>Estrats. Treballs d'Arqueologia SL, El Campello 03560, Spain. <sup>62</sup>Era – Arqueologia, Oeiras 1495–705, Portugal. <sup>63</sup>Museu de Prehistòria de València, València 46003, Spain. <sup>64</sup>GRAM Research Group, Departament de Prehistòria, Arqueologia i Historia Antiga, Universitat de València, València 46010, Spain. <sup>65</sup>Museu i Poblats Ibèrics de Ca n'Oliver, Cerdanyola del Vallès 08290, Spain. <sup>66</sup>Departamento de Prehistoria, Universidad Complutense de Madrid, Madrid 28040, Spain. <sup>67</sup>Museu de Prehistoria/SIP, Diputació de València, València 46003, Spain. <sup>68</sup>Arqueovitis scl. Avinyonet del Penedès 08793, Spain. <sup>69</sup>Department of Anthropology, University of California, Santa Barbara, California 93106, USA. <sup>70</sup>Unitat d'Antropologia Física, Departament de Biologia Animal, Facultat de Biologia, Universitat de Barcelona, Barcelona 08028, Spain. <sup>71</sup>Junta de Castilla y León, Servicio de Cultura de León, León 24008, Spain. <sup>72</sup>Center of Natural and Cultural Human History, Danube Private University, Krems 3500, Austria. <sup>73</sup>Department of Biomedical Engineering and Integrative Prehistory and Archaeological Science, Basel University, Basel 4123, Switzerland. <sup>74</sup>Australian Centre for Ancient DNA, School of Biological Sciences, University of Adelaide, Adelaide 5005, Australia

*We assembled genome-wide data from 271 ancient Iberians of whom 176 are from the largely unsampled period after 2000 BCE, thereby providing a high resolution time transect of the Peninsula. We document high genetic substructure between northwestern and southeastern hunter-gatherers prior to the spread of farming. We reveal sporadic contacts between Iberia and North Africa by ~2500 BCE, and by ~2000 BCE the replacement of 40% of Iberia's ancestry and nearly 100% of its Y-chromosomes by people with Steppe ancestry. In the Iron Age, we show that Steppe ancestry had spread not only into Indo-European-speaking regions but also into non-Indo-European-speaking ones, and we reveal that present-day Basques are best described as a typical Iron Age population without the admixture events that later impacted the rest of Iberia. Beginning at least in the Roman period, we document how the ancestry of the Peninsula was transformed by gene flow from North Africa and the eastern Mediterranean.*

The Iberian Peninsula, lying at the extreme southwestern corner of Europe, provides an excellent context in which to assess the final impact of population movements entering the continent from the east as well as interactions with North Africa. To study the genetic impact of prehistoric and historic events in Iberia, we prepared next-generation sequencing libraries treated with uracil-DNA glycosylase (UDG) (1) and enriched them for ~1.2 million single nucleotide polymorphisms (SNPs) (2, 3) to generate genome-wide data from 4 Mesolithic, 44 Neolithic, 47 Copper Age, 53 Bronze Age, 24 Iron Age, and 99 historical period Iberians (Fig. 1A-B and tables S1-2). We also generated 26 radiocarbon dates (table S3). We co-analyzed the new genomic data with previously reported data from 1107 ancient individuals, including 132 from Iberia (Fig. 1B) (2, 4–9), and 2862 present-day individuals (10). We filtered from the analysis datasets individuals covered by <10,000 single nucleotide polymorphisms (SNPs), evidence of contamination, or first-degree relatives of others (table S1). We analyzed the data with Principal Component Analysis (PCA) (Fig. 1C-D), *f*-statistics (11), and *qpAdm* (12), and summarize the results in Fig. 1E. We confirmed the robustness of key findings by repeating analyses after removing SNPs in CpG dinucleotides (table S5) that are susceptible to cytosine-to-thymine errors even in UDG-treated libraries (1).

Previous knowledge of the genetic structure of Mesolithic Iberia is from 3 individuals from the northwest: LaBraña1 (2), Canes1 (5) and Chan (5). We add LaBraña2, who was a brother of the previously reported LaBraña1 (figs. S1-2 and table S6), as well as Cueva de la Carigüela (fig. S10), Cingle del Mas Nou and Cueva de la Cocina from the southeast. In northwest Iberia, we document a previously unappreciated ancestry shift before the arrival of farming (Figs. 2A, S5 and table S7). The oldest individual Chan was similar to the ~17000 BCE El Mirón, whereas the La Braña brothers from ~1300 years later were closer to central European hunter-gatherers like the Hungarian KO1, with an even more extreme shift ~700 years later in Canes1. This likely reflects gene flow impacting northwest Iberia but not the southeast, where individuals remained close to El Mirón (Fig. 2A). More data from the Mesolithic period, and especially from

currently unsampled areas, would provide additional insight into the geographical impact and archaeological correlates of this ancestry shift.

In the Neolithic and Copper Age, we model populations as mixtures of groups related to Anatolian Neolithic, El Mirón and KO1 (Fig. 2A and table S8). We replicate previous findings of the arrival of Anatolian Neolithic-associated ancestry in multiple regions of Iberia in the Early Neolithic (7, 8, 12); however, sampling from this period remains limited and studies of larger sample sizes and additional sites will be important in order to shed additional light on the interaction between the incoming farmers and indigenous hunter-gatherers. In the Middle Neolithic and Copper Age, we reproduce previous reports of an increase of hunter-gatherer-related ancestry after 4000 BCE (6, 7, 12, 13), with higher proportions in groups from the north and center. By using as a reference frame our observations about population substructure in the Mesolithic, we show that the hunter-gatherer-related ancestry during those periods was more closely related to later northwestern (Canes1-like) than to the El Mirón-like hunter-gatherers (Fig. 2A), providing clues about the source of this ancestry.

Our Copper Age dataset includes a newly reported 2473-2030 cal BCE male (I4246) from Camino de las Yeseras (14) in central Iberia, who clusters with modern and ancient North Africans in the PCA (Fig. 1C and fig. S3), and like ~3000 BCE Moroccans (8) can be well modeled as having ancestry from both Late Pleistocene North Africans (15) and Early Neolithic Europeans (tables S9-10). His genome-wide ancestry and uniparental markers (tables S1 and S4) are unique among Copper Age Iberians, including individuals from sites with many analyzed individuals such as Sima del Ángel, and point to a North African origin. Our genetic evidence of sporadic contacts from North Africa during the Copper Age fits with the presence of African ivory at Iberian sites (16), and is confirmed by a Bronze Age individual (I7162) from Loma del Puerco in southern Iberia who had 25% ancestry related to individuals like I4246 (Fig. 1D; table S16). However, these early movements from North Africa had a limited impact on Copper and Bronze Age Iberians, as North African ancestry only became widespread in the past ~2000 years.

From the Bronze Age (~2200-900 BCE) we increase the available dataset (6, 7, 17) from 7 to 60 individuals and show how ancestry from the Pontic-Caspian steppe ("Steppe ancestry") appeared throughout Iberia in this period (Fig. 1C-D), albeit with less impact in the south (table S13). The earliest evidence is in 14 individuals dated to ~2500-2000 BCE who co-existed with local people without Steppe ancestry (Fig. 2B). These groups lived in close proximity and admixed to form the Bronze Age population after 2000 BCE with ~40% ancestry from incoming groups (Fig. 2B and fig. S6). Y-chromosome turnover was even more dramatic (Fig. 2B), as the lineages common in Copper Age Iberia (I2, G2, H) were nearly completely replaced by one lineage, R1b-M269. These patterns point to a higher contribution of incoming males than females, also supported by a lower proportion of non-local ancestry on the X-chromosome

(table S14 and fig. S7), a paradigm that can be exemplified by a Bronze Age tomb from Castillejo del Bonete containing a male with Steppe ancestry and a female with ancestry similar to Copper Age Iberians. While ancient DNA can document that sex-biased admixture occurred, archaeological and anthropological research will be needed to understand the processes that generated it.

In the Iron Age, we document a consistent trend of increased ancestry related to North/Central European populations with respect to the preceding Bronze Age (Figs. 1C-D and 2B). The increase was 10–19% (95% confidence intervals given here and in what follows) in 15 individuals along the eastern Mediterranean coast where non-Indo-European Iberian languages were spoken; 11–31% in 2 individuals at the Tartessian site of La Angorrilla in the southwest with unknown language attribution; and 28–43% in 3 individuals at La Hoya in the north where Indo-European Celtiberian languages were likely spoken (fig. S6 and tables S11-12). This documents gene flow into Iberia during the Late Bronze Age or Early Iron Age, possibly associated with the introduction of the Urnfield tradition (18). Unlike central or northern Europe where Steppe ancestry likely marked the introduction of Indo-European languages (12), our results indicate that in Iberia increases in Steppe ancestry were not always accompanied by switches to Indo-European languages. This is consistent with present-day Basques who speak the only non-Indo-European language in western Europe but overlap genetically with Iron Age populations (Fig. 1D) showing substantial levels of Steppe ancestry.

In the historical period, our transect begins with 24 individuals from the Greek colony of Empúries in the northeast from 500 BCE to 600 CE (19) who fall into two ancestry groups (Fig. 1C-D and fig. S8): one similar to Bronze Age individuals from the Aegean, and the other similar to the population of Iron Age Iberia that includes the nearby non-Greek site of Ullastret, confirming historical sources indicating that this town was inhabited by a multi-ethnic population (19). The impact of mobility from the Central/Eastern Mediterranean during the Classical period is also evident in 10 individuals from the 7th-8th centuries CE site of L'Esquerda in the northeast, who show a shift from the Iron Age population in the direction of present-day Italians and Greeks (Fig. 1D), accounting for approximately one quarter of their ancestry (Fig. 2C and table S17). The same shift is also observed in present-day populations from Iberia outside the Basque area and is plausibly a consequence of the Roman presence in Iberia, which had a profound cultural impact and, according to our data, a substantial genetic impact too.

In contrast to the demographic changes in the Classical period, movements into Iberia during the decline of the Roman Empire had less long-term demographic impact. Nevertheless, individual sites bear witness to events in this period, for example at the 6th century site of Pla de l'Horta in the northeast. These individuals, archaeologically interpreted as Visigoths, are shifted from those at L'Esquerda in the direction of north/central Europe (Figs. 1D, 2C and table

S18), and we observe the Asian mtDNA haplogroup C4a1a also found in Early Medieval Bavaria (20), supporting a recent link with groups with ultimate ancestry from central/eastern Europe.

In the southeast, we recovered genomic data from 45 individuals dated between the 3rd-16th centuries CE. All the analyzed individuals fell outside the genetic variation of preceding Iberian Iron Age populations (Figs. 1C-D and S3) and harbored ancestry from both southern European and North African populations (Fig. 2D), as well as additional Levantine-related ancestry that could reflect Jewish contributions (21). These results demonstrate that by the Roman period, southern Iberia had experienced a major influx of North African ancestry, probably related to the well-known mobility patterns during the Roman Empire (22) or the earlier Phoenician-Punic presence (23); the latter is also supported by the observation of the Phoenician-associated Y-chromosome J2 (24). Gene flow from North Africa continued into the Muslim period, as is clear from Muslim burials with elevated North African and sub-Saharan African ancestry (Figs. 2D, S4 and table S22), and uniparental markers typical of North Africa not present among pre-Islamic individuals (Figs. 2D and S11). Present-day populations from southern Iberia harbor less North African ancestry (25) than the ancient Muslim burials, plausibly reflecting expulsion of *moriscos* (former Muslims converted to Christianity) and repopulation from the north, as supported by historical sources and genetic analysis of present-day groups (25). The impact of Muslim rule is also evident in northeast Iberia in seven individuals from Sant Julià de Ramis from the 8-12th centuries CE who, unlike previous ancient individuals from the same region, show North African-related ancestry (Fig. 2C and table S19) and a complete overlap in PCA with present-day Iberians (Fig. 1D).

Our time transect allowed us to track frequency changes of phenotypically important variants over the last 4,000 years (fig. S9), a period which has been minimally sampled in the ancient DNA literature not just of Iberia but of Europe more generally. Prior to this work, it was known that the lactase persistence allele at (rs4988235), which is present at moderate or high frequencies in most European populations today and is one of the strongest known signals of selection in Europeans (26), occurred at extremely low frequencies in Europe through the Bronze Age (2), raising the question of when it became common. Here we show that in Iberia the allele continued to be at low frequency in the Iron Age (fig. S9), and only approached present-day frequencies in the last 2,000 years, pointing to recent strong selection.

Beyond the specific insights about Iberia, this study serves as a model for how a high-resolution ancient DNA transect continuing into historical periods can be used to provide a detailed description of the formation of present-day populations (Fig. 1E); future application of similar strategies will provide equally valuable insights in other world regions.

254

255 **Fig. 1. Overview of the Ancient Iberian Genetic Time Transect.** (A) Geographic distribution  
256 and (B) dates of new and previously reported samples. Random jitter is added for sites with  
257 multiple individuals. Sites mentioned in the text are labeled. (C) Principal Component Analysis  
258 of 989 present-day west Eurasian individuals (grey dots), with ancient individuals from Iberia  
259 and other regions (pale yellow) projected onto the first two principal components. (D) Section  
260 of the PCA in (C). (E) Schematic representation of events documented in this study.

261

262

263

264

265

266 **Fig. 2. Genome-wide admixture proportions using *qpAdm*.** (A) Modeling Mesolithic,  
267 Neolithic and Copper Age populations as a mixture of Anatolia\_N, El Mirón and KO1.  
268 Percentages indicate proportion of El Mirón + KO1 ancestry. (B) Proportion of ancestry derived  
269 from central European Beaker/Bronze Age populations in Iberians from the Middle Neolithic to  
270 the Iron Age (table S15). Colors indicate the Y-chromosome haplogroup for each male (table  
271 S4). (C) Ancestry proportions for individuals from three sites in northeast Iberia dated between  
272 the 6th and 12th centuries CE. (D) Ancestry proportions for individuals from southeast Iberia  
273 from the 3-16th centuries CE (tables S20-S21). Each bar represents one individual with  
274 associated mtDNA (top) and Y-chromosome (bottom). In bold, haplogroups with a likely recent  
275 non-local origin.

276

## References

1. N. Rohland, E. Harney, S. Mallick, S. Nordenfelt, D. Reich, Partial uracil – DNA – glycosylase treatment for screening of ancient DNA. *Philos. Trans. R. Soc. London B.* **370** (2015), doi:10.1098/rstb.2013.0624.
2. I. Mathieson, I. Lazaridis, N. Rohland, S. Mallick, N. Patterson, S. A. Roodenberg, E. Harney, K. Stewardson, D. Fernandes, M. Novak, K. Sirak, C. Gamba, E. R. Jones, B. Llamas, S. Dryomov, J. Pickrell, J. L. Arsuaga, J. M. B. de Castro, E. Carbonell, F. Gerritsen, A. Khokhlov, P. Kuznetsov, M. Lozano, H. Meller, O. Mochalov, V. Moiseyev, M. A. R. Guerra, J. Roodenberg, J. M. Vergès, J. Krause, A. Cooper, K. W. Alt, D. Brown, D. Anthony, C. Lalueza-Fox, W. Haak, R. Pinhasi, D. Reich, Genome-wide patterns of selection in 230 ancient Eurasians. *Nature.* **528**, 499–503 (2015).
3. Q. Fu, M. Hajdinjak, O. T. Moldovan, S. Constantin, S. Mallick, P. Skoglund, N. Patterson, N. Rohland, I. Lazaridis, B. Nickel, B. Viola, K. Prüfer, M. Meyer, J. Kelso, D. Reich, S. Pääbo, An early modern human from Romania with a recent Neanderthal ancestor. *Nature.* **524**, 216–219 (2015).
4. Q. Fu, C. Posth, M. Hajdinjak, M. Petr, S. Mallick, D. Fernandes, A. Furtwängler, W. Haak, M. Meyer, A. Mittnik, B. Nickel, A. Peltzer, N. Rohland, V. Slon, S. Talamo, I. Lazaridis, M. Lipson, I. Mathieson, S. Schiffels, P. Skoglund, A. P. Derevianko, N. Drozdov, V. Slavinsky, A. Tsybankov, R. G. Cremonesi, F. Mallegni, B. Gély, E. Vacca, M. R. G. Morales, L. G. Straus, C. Neugebauer-Maresch, M. Teschler-Nicola, S. Constantin, O. T. Moldovan, S. Benazzi, M. Peresani, D. Coppola, M. Lari, S. Ricci, A. Ronchitelli, F. Valentin, C. Thevenet, K. Wehrberger, D. Grigorescu, H. Rougier, I. Crevecoeur, D. Flas, P. Semal, M. A. Mannino, C. Cupillard, H. Bocherens, N. J. Conard, K. Harvati, V. Moiseyev, D. G. Drucker, J. Svoboda, M. P. Richards, D. Caramelli, R. Pinhasi, J. Kelso, N. Patterson, J. Krause, S. Pääbo, D. Reich, The genetic history of Ice Age Europe. *Nature.* **534**, 200–205 (2016).
5. G. González-Fortes, E. R. Jones, E. Lightfoot, C. Bonsall, C. Lazar, A. Grandal-d'Anglade, M. D. Garralda, L. Drak, V. Siska, A. Simalcsik, A. Boroneanț, J. R. Vidal Romaní, M. Vaquero Rodríguez, P. Arias, R. Pinhasi, A. Manica, M. Hofreiter, Paleogenomic Evidence for Multi-generational Mixing between Neolithic Farmers and Mesolithic Hunter-Gatherers in the Lower Danube Basin. *Curr. Biol.* **27**, 1801–1810 (2017).
6. R. Martiniano, L. M. Cassidy, R. Ó'Maoldúin, R. McLaughlin, N. M. Silva, L. Manco, D. Fidalgo, T. Pereira, M. J. Coelho, M. Serra, J. Burger, R. Parreira, E. Moran, A. C. Valera, E. Porfírio, R. Boaventura, A. M. Silva, D. G. Bradley, The population genomics of archaeological transition in west Iberia: Investigation of ancient substructure using imputation and haplotype-based methods. *PLoS Genet.* **13**, e1006852 (2017).
7. C. Valdiosera, T. Günther, J. C. Vera-Rodríguez, I. Ureña, E. Iriarte, R. Rodríguez-Varela, L. G. Simões, R. M. Martínez-Sánchez, E. M. Svensson, H. Malmström, L. Rodríguez, J.-M. Bermúdez de Castro, E. Carbonell, A. Alday, J. A. Hernández Vera, A. Götherström, J.-M. Carretero, J. L. Arsuaga, C. I. Smith, M. Jakobsson, Four millennia of Iberian biomolecular prehistory illustrate the impact of prehistoric migrations at the far end of Eurasia. *Proc. Natl. Acad. Sci. U.S.A.* **115**, 201717762 (2018).
8. R. Fregel, F. L. Mendez, Y. Bokbot, D. Martin-Socas, M. D. Camalich-Massieu, J. Santana, J. Morales, M. C. Avila-Arcos, P. A. Underhill, B. Shapiro, G. L. Wojcik, M. Rasmussen, A. E. R. Soares, J. Kapp, A. Sockell, F. J. Rodriguez-Santos, A. Mikdad, A. Trujillo-Mederos, C. D. Bustamante, Ancient genomes



- 329 from North Africa evidence prehistoric migrations to the Maghreb from both the  
330 Levant and Europe. *Proc. Natl. Acad. Sci. U.S.A.* **115**, 6774–6779 (2018).
- 331 9. I. Olalde, S. Brace, M. E. Allentoft, I. Armit, K. Kristiansen, T. Booth, N.  
332 Rohland, S. Mallick, A. Szécsényi-Nagy, A. Mittnik, E. Altena, M. Lipson, I.  
333 Lazaridis, T. K. Harper, N. Patterson, N. Broomandkhoshbacht, Y. Diekmann, Z.  
334 Faltyskova, D. Fernandes, M. Ferry, E. Harney, P. de Knijff, M. Michel, J.  
335 Oppenheimer, K. Stewardson, A. Barclay, K. W. Alt, C. Liesau, P. Ríos, C.  
336 Blasco, J. V. Miguel, R. M. García, A. A. Fernández, E. Bánffy, M. Bernabò-  
337 Brea, D. Billoin, C. Bonsall, L. Bonsall, T. Allen, L. Büster, S. Carver, L. C.  
338 Navarro, O. E. Craig, G. T. Cook, B. Cunliffe, A. Denaire, K. E. Dinwiddy, N.  
339 Dodwell, M. Ernée, C. Evans, M. Kuchařík, J. F. Farré, C. Fowler, M.  
340 Gazenbeek, R. G. Pena, M. Haber-Uriarte, E. Haduch, G. Hey, N. Jowett, T.  
341 Knowles, K. Massy, S. Pfrengle, P. Lefranc, O. Lemerrier, A. Lefebvre, C. H.  
342 Martínez, V. G. Olmo, A. B. Ramírez, J. L. Maurandi, T. Majó, J. I. McKinley,  
343 K. McSweeney, B. G. Mende, A. Mod, G. Kulcsár, V. Kiss, A. Czene, R. Patay,  
344 A. Endrődi, K. Köhler, T. Hajdu, T. Szeniczey, J. Dani, Z. Bernert, M. Hoole, O.  
345 Cheronet, D. Keating, P. Velemínský, M. Dobeš, F. Candilio, F. Brown, R. F.  
346 Fernández, A.-M. Herrero-Corral, S. Tusa, E. Carnieri, L. Lentini, A. Valenti, A.  
347 Zanini, C. Waddington, G. Delibes, E. Guerra-Doce, B. Neil, M. Brittain, M.  
348 Luke, R. Mortimer, J. Desideri, M. Besse, G. Brücken, M. Furmanek, A.  
349 Hałuszko, M. Mackiewicz, A. Rapiński, S. Leach, I. Soriano, K. T. Lillios, J. L.  
350 Cardoso, M. P. Pearson, P. Włodarczak, T. D. Price, P. Prieto, P.-J. Rey, R.  
351 Risch, M. A. Rojo Guerra, A. Schmitt, J. Serralougue, A. M. Silva, V. Smrčka, L.  
352 Vergnaud, J. Zilhão, D. Caramelli, T. Higham, M. G. Thomas, D. J. Kennett, H.  
353 Fokkens, V. Heyd, A. Sheridan, K.-G. Sjögren, P. W. Stockhammer, J. Krause,  
354 R. Pinhasi, W. Haak, I. Barnes, C. Lalueza-Fox, D. Reich, The Beaker  
355 phenomenon and the genomic transformation of northwest Europe. *Nature*. **555**,  
356 190–196 (2018).
- 357 10. I. Lazaridis, N. Patterson, A. Mittnik, G. Renaud, S. Mallick, K. Kirsanow, P. H.  
358 Sudmant, J. G. Schraiber, S. Castellano, M. Lipson, B. Berger, C. Economou, R.  
359 Bollongino, Q. Fu, K. I. Bos, S. Nordenfelt, H. Li, C. de Filippo, K. Prüfer, S.  
360 Sawyer, C. Posth, W. Haak, F. Hallgren, E. Fornander, N. Rohland, D. Delsate,  
361 M. Francken, J.-M. Guinet, J. Wahl, G. Ayodo, H. a. Babiker, G. Bailliet, E.  
362 Balanovska, O. Balanovsky, R. Barrantes, G. Bedoya, H. Ben-Ami, J. Bene, F.  
363 Berrada, C. M. Bravi, F. Brisighelli, G. B. J. Busby, F. Cali, M. Churnosov, D. E.  
364 C. Cole, D. Corach, L. Damba, G. van Driem, S. Dryomov, J.-M. Dugoujon, S. a.  
365 Fedorova, I. Gallego Romero, M. Gubina, M. Hammer, B. M. Henn, T. Hervig,  
366 U. Hodoglugil, A. R. Jha, S. Karachanak-Yankova, R. Khusainova, E.  
367 Khusnutdinova, R. Kittles, T. Kivisild, W. Klitz, V. Kučinskas, A.  
368 Kushniarevich, L. Laredj, S. Litvinov, T. Loukidis, R. W. Mahley, B. Melegh, E.  
369 Metspalu, J. Molina, J. Mountain, K. Näkkäläjärvi, D. Nesheva, T. Nyambo, L.  
370 Osipova, J. Parik, F. Platonov, O. Posukh, V. Romano, F. Rothhammer, I. Rudan,  
371 R. Ruizbakiev, H. Sahakyan, A. Sajantila, A. Salas, E. B. Starikovskaya, A.  
372 Tarekegn, D. Toncheva, S. Turdikulova, I. Uktveryte, O. Utevska, R. Vasquez,  
373 M. Villena, M. Voevoda, C. a. Winkler, L. Yepiskoposyan, P. Zalloua, T.  
374 Zemunik, A. Cooper, C. Capelli, M. G. Thomas, A. Ruiz-Linares, S. a. Tishkoff,  
375 L. Singh, K. Thangaraj, R. Villems, D. Comas, R. Sukernik, M. Metspalu, M.  
376 Meyer, E. E. Eichler, J. Burger, M. Slatkin, S. Pääbo, J. Kelso, D. Reich, J.  
377 Krause, Ancient human genomes suggest three ancestral populations for present-  
378 day Europeans. *Nature*. **513**, 409–413 (2014).
- 379 11. N. Patterson, P. Moorjani, Y. Luo, S. Mallick, N. Rohland, Y. Zhan, T.  
380 Genschoreck, T. Webster, D. Reich, Ancient admixture in human history.

*Genetics*. **192**, 1065–93 (2012).

12. W. Haak, I. Lazaridis, N. Patterson, N. Rohland, S. Mallick, B. Llamas, G. Brandt, S. Nordenfelt, E. Harney, K. Stewardson, Q. Fu, A. Mittnik, E. Bánffy, C. Economou, M. Francken, S. Friederich, R. G. Pena, F. Hallgren, V. Khartanovich, A. Khokhlov, M. Kunst, P. Kuznetsov, H. Meller, O. Mochalov, V. Moiseyev, N. Nicklisch, S. L. Pichler, R. Risch, M. a. Rojo Guerra, C. Roth, A. Szécsényi-Nagy, J. Wahl, M. Meyer, J. Krause, D. Brown, D. Anthony, A. Cooper, K. W. Alt, D. Reich, Massive migration from the steppe was a source for Indo-European languages in Europe. *Nature*. **522**, 207–211 (2015).
13. M. Lipson, A. Szécsényi-Nagy, S. Mallick, A. Pósa, B. Stégmár, V. Keerl, N. Rohland, K. Stewardson, M. Ferry, M. Michel, J. Oppenheimer, N. Broomandkhoshbacht, E. Harney, S. Nordenfelt, B. Llamas, B. G. Mende, K. Köhler, K. Oross, M. Bondár, T. Marton, A. Osztás, J. Jakucs, T. Paluch, F. Horváth, P. Csengeri, J. Koós, K. Sebok, A. Anders, P. Raczký, J. Regenye, J. P. Barna, S. Fábián, G. Serlegi, Z. Toldi, E. G. Nagy, J. Dani, E. Molnár, G. Pálfi, L. Márk, B. Melegh, Z. Bánfai, J. Fernández-Eraso, J. A. Mujika-Alustiza, C. A. Fernández, J. J. Echevarría, R. Bollongino, J. Orschiedt, K. Schierhold, H. Meller, A. Cooper, J. Burger, E. Bánffy, K. W. Alt, C. Lalueza-Fox, W. Haak, D. Reich, Parallel ancient genomic transects reveal complex population history of early European farmers. *Nature*. **551**, 368–372 (2017).
14. C. Blasco, C. Liesau, G. Delibes de Castro, E. Baquedano, M. Rodriguez, in *El campaniforme en la Península Ibérica y su contexto europeo*, M. Rojo, R. Garrido, I. García, Eds. (Universidad de Valladolid-Junta de Castilla y León, Valladolid, 2005), pp. 457–479.
15. M. van de Loosdrecht, A. Bouzouggar, L. Humphrey, C. Posth, N. Barton, A. Aximu-Petri, B. Nickel, S. Nagel, E. H. Talbi, M. A. El Hajraoui, S. Amzazi, J.-J. Hublin, S. Pääbo, S. Schiffels, M. Meyer, W. Haak, C. Jeong, J. Krause, Pleistocene North African genomes link Near Eastern and sub-Saharan African human populations. *Science*. **360**, 548–552 (2018).
16. C. Liesau, E. Moreno, T. X. Schuhmacher, D. Marzoli, J. A. López Padilla, Eds., *Marfiles campaniformes de Camino de Las Yeseras (San Fernando de Henares, Madrid). Marfil y elefantes en la Península Ibérica y el Mediterráneo Occident. Actas del Coloq. Int.* (2012), pp. 87–98.
17. T. Günther, C. Valdiosera, H. Malmström, I. Ureña, R. Rodríguez-Varela, Ó. O. Sverrisdóttir, E. a. Daskalaki, P. Skoglund, T. Naidoo, E. M. Svensson, J. M. Bermúdez de Castro, E. Carbonell, M. Dunn, J. Storå, E. Iriarte, J. L. Arsuaga, J.-M. Carretero, A. Götherström, M. Jakobsson, Ancient genomes link early farmers from Atapuerca in Spain to modern-day Basques. *Proc. Natl. Acad. Sci. U.S.A.* **112**, 11917–11922 (2015).
18. G. Ruiz Zapatero, in *Iberia. Protohistory of the far west of Europe: from Neolithic to Roman conquest*, M. Almagro-Gorbea, Ed. (Universidad de Burgos. Fundación Atapuerca, 2014), pp. 195–215.
19. M. Almagro-Basch, *Ampurias. Historia de la ciudad y guía de las excavaciones* (Instituto Español de Prehistoria del CSIC y Servicio de Investigaciones Arqueológicas de la Diputación Provincial, Barcelona, 1951).
20. K. R. Veeramah, A. Rott, M. Groß, L. Van Dorp, S. López, K. Kirsanow, C. Sell, J. Blöcher, D. Wegmann, V. Link, Z. Hofmanová, J. Peters, B. Trautmann, A. Gairhos, J. Haberstroh, B. Paffgen, G. Hellenthal, B. Haas-Gebhard, M. Harbeck, J. Burger, Population genomic analysis of elongated skulls reveals extensive female-biased immigration in early medieval Bavaria. *Proc. Natl. Acad. Sci. U.S.A.* **155**, 3494–3499 (2018).
21. J. S. Gerber, *The Jews of Spain: a History of the Sephardic Experience* (The Free

- Press, New York, 1992).
22. L. de Ligt, L. E. Tacoma, Eds., *Migration and Mobility in the Early Roman Empire* (Brill, Leiden, 2016).
  23. M. R. Bierling, S. Gitin, *The Phoenicians in Spain An Archaeological Review of the Eighth–Sixth Centuries B.C.E* (Eisenbrauns, 2002).
  24. P. A. Zalloua, D. E. Platt, M. El Sibai, J. Khalife, N. Makhoul, M. Haber, Y. Xue, H. Izaabel, E. Bosch, S. M. Adams, E. Arroyo, A. M. López-Parra, M. Aler, A. Picornell, M. Ramon, M. A. Jobling, D. Comas, J. Bertranpetit, R. S. Wells, C. Tyler-Smith, Identifying Genetic Traces of Historical Expansions: Phoenician Footprints in the Mediterranean. *Am. J. Hum. Genet.* **83**, 633–642 (2008).
  25. C. Bycroft, C. Fernández-Rozadilla, C. Ruiz-Ponte, I. Quintela-García, Á. Carracedo, P. Donnelly, S. Myers, Patterns of genetic differentiation and the footprints of historical migrations in the Iberian Peninsula. *bioRxiv*, 250191 (2018).
  26. T. Bersaglieri, P. C. Sabeti, N. Patterson, T. Vanderploeg, S. F. Schaffner, J. A. Drake, M. Rhodes, D. E. Reich, J. N. Hirschhorn, Genetic signatures of strong recent positive selection at the lactase gene. *Am. J. Hum. Genet.* **74**, 1111–20 (2004).
  27. C. Bronk Ramsey, OxCal 4.23 Online Manual (2013), (available at [https://c14.arch.ox.ac.uk/oxcalhelp/hlp\\_contents.html](https://c14.arch.ox.ac.uk/oxcalhelp/hlp_contents.html)).
  28. P. J. Reimer, E. Bard, A. Bayliss, J. W. Beck, P. G. Blackwell, C. Bronk, R. Caitlin, E. B. Hai, R. L. Edwards, Intcal13 and marine13 radiocarbon age calibration curves 0 – 50,000 years cal CP. *Radiocarbon.* **55**, 1869–1887 (2013).
  29. F. Giles, J. C. Finlayson, J. Rodríguez Vidal, A. Santiago, J. M. Gutiérrez López, D. Fa, E. Mata, G. Finlayson, F. Giles Guzmán, Referencias a las dataciones en los sistemas kársticos con ocupaciones humanas del Peñón de Gibraltar. *Bol SEDECK.* **2** (2001), pp. 86–90.
  30. F. J. Giles Guzmán, F. Giles Pacheco, J. M. Gutiérrez López, M. C. Reinoso del Río, C. Finlayson, G. Finlayson, J. Rodríguez Vidal, S. Finlayson, Bray, una cueva sepulcral de la Edad del Bronce en el Peñón de Gibraltar. *SAGVNTVM. Papeles del Lab. Arqueol. Val.* **49** (2017), p. 29.
  31. F. G. Guzmán, J. M. G. López, S. Finlayson, F. G. Pacheco, C. Finlayson, G. Finlayson, C. R. del Río, T. L. Holmes, El uso sepulcral de las cavidades de Gibraltar durante la Prehistoria Reciente. *Actas del I Congr. Int. Hist. la Serranía Ronda Las Ocup. por Soc. prehistóricas, protohistóricas y la antigüedad en la Serranía Ronda y Béticas Occident.* (2017), pp. 323–344.
  32. M. Hoyos, J. Lario, J. L. Goy, C. Zazo, C. J. Dabrio, C. Hillaire-Marcel, P. G. Silva, L. Somoza, T. Bardají, Sedimentación kárstica: Procesos morfosedimentarios en la zona del Estrecho de Gibraltar. *Gibraltar Dur. Quat. AEQUA Monogr.* **2** (1994), pp. 36–48.
  33. A. S. Pérez, J. Lario, F. Giles Pacheco, C. Finlayson, J. M. Gutiérrez López, R. Durell, I. Bramble, J. P. Latín, J. Aguilera García, El depósito neolítico de Rich Sand Cave (Punta Europa-Gibraltar). *Almoraima* (2001), pp. 31–36.
  34. M. S. Hernández Pérez, G. García Atiénzar, V. Barciela González, *Cabezo Redondo (Villena, Alicante)* (Universidad de Alicante, 2016).
  35. A. Romero Rameta, in *Cabezo Redondo (Villena, Alicante)*, M. S. Hernández Pérez, G. García Atiénzar, V. Barciela González, Eds. (Universidad de Alicante, 2016), pp. 85–87.
  36. D. C. Salazar-García, O. García-Puchol, M. P. de Miguel-Ibáñez, S. Talamo, Earliest evidence of Neolithic collective burials from eastern Iberia: radiocarbon dating at the archaeological site of Les Llometes (Alicante, Spain). *Radiocarbon.* **58**, 679–692 (2016).

- 485 37. V. Pascual Pérez, Hallazgos prehistóricos en les Llometes (Alcoy). *Arch. Prehist.*  
486 *Levantina*. **10**, 39–58 (1963).
- 487 38. C. Núñez, M. Baeta, S. Cardoso, L. Palencia-Madrid, N. García-Romero, A.  
488 Llanos, M. M. de Pancorbo, Mitochondrial DNA Reveals the Trace of the  
489 Ancient Settlers of a Violently Devastated Late Bronze and Iron Ages Village.  
490 *PLoS One*. **11**, e0155342 (2016).
- 491 39. M. J. S. Barreiro, *Cronología radiométrica, ecología y clima del Paleolítico*  
492 *cantábrico* (Ministerio de Educación, cultura y deporte, 2003), vol. 19.
- 493 40. E. Hernández-Pacheco, La vida de nuestros antecesores paleolíticos según los  
494 resultados de las excavaciones en la caverna de la Paloma (Asturias). *Mem. Com.*  
495 *Investig. Paleontológicas y Prehistóricas*. **31** (1923).
- 496 41. I. Barandiarán, La Cueva de La Paloma (Asturias). *Munibe*. **2**, 255–283 (1971).
- 497 42. M. I. Martínez Navarrete, T. Chapa Brunet, in *La Cueva de La Paloma. Soto de*  
498 *Las Regueras (Asturias)* (1980), pp. 115–204.
- 499 43. M. Hoyos, M. I. Martínez, T. Chapa, P. Castaños, F. B. Sanchiz, La Cueva de La  
500 Paloma, Soto de las Regueras (Asturias). *Excavaciones Arqueol. en España*. **116**  
501 (1980), pp. 65–100.
- 502 44. L. Domingo, P. Pérez-Dios, M. H. Fernández, J. Martín-Chivelet, J. E. Ortiz, T.  
503 Torres, Late Quaternary climatic and environmental conditions of northern  
504 Spain: An isotopic approach based on the mammalian record from La Paloma  
505 cave. *Palaeogeogr. Palaeoclimatol. Palaeoecol.* **440**, 417–430 (2015).
- 506 45. P. Castaños, in *La Cueva de La Paloma. Excavaciones Arqueológicas en España*  
507 (1980), vol. 116, pp. 65–100.
- 508 46. R. E. M. Hedges, R. A. Housley, C. B. Ramsey, G. J. Van Klinken, Radiocarbon  
509 dates from the Oxford AMS system: Archaeometry datelist 18. *Archaeometry*.  
510 **36**, 337–374 (1994).
- 511 47. J. I. Morales, A. Cebrià, J. Mestres, X. Oms, E. Allue, La Cova del Guineu,  
512 12,000 anys de presència humana a la capçalera del Foix. *III Monogr. del Foix*  
513 (2013), pp. 172–183.
- 514 48. F. X. Oms, A. Cebrià, J. Mestres, J. I. Morales, M. Pedro, J. M. Vergès,  
515 Campaniforme i metal·lúrgia en un espai sepulcral del III mil·lenni cal. BC: la  
516 Cova de la Guineu (Font-rubí, Alt Penedès). *Jornades d'Arqueologia del*  
517 *Penedès*, 109–116 (2016).
- 518 49. X. Carlús, F. J. López Cachero, M. Oliva, A. Palomo, A. Rodríguez, N. Terrats,  
519 C. Lara, N. Villena, Cabanes, Sitges i Tombes. El paratge de Can Roqueta  
520 (Sabadell, Vallès occidental), del 1300 al 500 aC. *Quad. d'Arqueologia*. **4**  
521 (2007).
- 522 50. X. Carlús, F. J. López Cachero, N. Terrats, M. Oliva, A. Palomo, A. Rodríguez,  
523 Diacronia durant la prehistòria recent a Can Roqueta (Sabadell-Barberà del  
524 Vallés, Vallès Occidental) entre el VI i el I Mil·lenni Cal ANE. *Cypsela*. **17**  
525 (2008), pp. 115–142.
- 526 51. A. Palomo, A. Rodríguez, Can Roqueta II (Sabadell-Vallès Occidental): un  
527 jaciment excepcional de l'edat del bronze. *Pirineus i Veïns al III mil·lenni aC,*  
528 *XII Col·loqui Int. d'Arqueologia Puigcerdà, Inst. d'Estudis Ceretans* (2002), pp.  
529 275–283.
- 530 52. A. Palomo, A. Rodríguez, Can Roqueta II (Sabadell, Vallès Occidental). *Trib.*  
531 *d'Arqueologia* (2004), pp. 77–98.
- 532 53. J. Daura, M. Sanz, A. W. G. Pike, M. E. Subirà, J. J. Fornós, J. M. Fullola, R.  
533 Julià, J. Zilhão, Stratigraphic context and direct dating of the Neandertal  
534 mandible from Cova del Gegant (Sitges, Barcelona). *J. Hum. Evol.* **59**, 109–122  
535 (2010).
- 536 54. J. Daura, M. Sanz, I. Soriano, M. Pedro, Á. Rubio, M. Oliva, J. Francisco Gibaja,

- 537 I. Queralt, R. Álvarez, F. J. López-Cachero, Objetos de oro y epicampaniforme  
538 en la Cova del Gegant. Relaciones en la costa mediterránea de la Península  
539 Ibérica durante la Edad del Bronce. *Trab. Prehist.* **74**, 149–167 (2017).
- 540 55. I. Ollich, M. Ocaña, M. Ramisa, M. Rocafiguera, *A banda i banda del Ter*,  
541 *Història de Roda* (Ajuntament de Roda de Ter / Eumo Editorial, 1995).
- 542 56. I. Ollich i Castanyer, in *Arqueologia funerària al nord-est peninsular (segles VI-*  
543 *XII)*, N. Molist, G. Ripoll, Eds. (Monografies d'Olèrdola, 3.2. Museu  
544 d'Arqueologia de Catalunya, 2012), pp. 275–286.
- 545 57. J. . Mestres, in *Memòria de les excavacions arqueològiques a l'àrea de la*  
546 *muralla 2012-2013 (en preparació)* (2013).
- 547 58. A. Szécsényi-Nagy, C. Roth, G. Brandt, C. Rihuete-Herrada, C. Tejedor-  
548 Rodríguez, P. Held, Í. García-Martínez-De-Lagrán, H. Arcusa Magallón, S.  
549 Zesch, C. Knipper, E. Bánffy, S. Friederich, H. Meller, P. Bueno Ramírez, R.  
550 Barroso Bermejo, R. De Balbín Behrmann, A. M. Herrero-Corral, R. Flores  
551 Fernández, C. Alonso Fernández, J. Jiménez Echevarria, L. Rindlisbacher, C.  
552 Oliart, M. I. Fregeiro, I. Soriano, O. Vicente, R. Micó, V. Lull, J. Soler Díaz, J.  
553 A. López Padilla, C. Roca De Togores Muñoz, M. S. Hernández Pérez, F. J.  
554 Jover Maestre, J. Lomba Maurandi, A. Avilés Fernández, K. T. Lillios, A. M.  
555 Silva, M. Magalhães Ramalho, L. M. Oosterbeek, C. Cunha, A. J. Waterman, J.  
556 Roig Buxó, A. Martínez, J. Ponce Martínez, M. Hunt Ortiz, J. C. Mejías-García,  
557 J. C. Pecero Espín, R. Cruz-Auñón Briones, T. Tomé, E. Carmona Ballester, J.  
558 L. Cardoso, A. C. Araújo, C. Liesau Von Lettow-Vorbeck, C. Blasco Bosqued, P.  
559 Ríos Mendoza, A. Pujante, J. I. Royo-Guillén, M. A. Esquembre Beviá, V. M.  
560 Dos Santos Goncalves, R. Parreira, E. Morán Hernández, E. Méndez Izquierdo, J.  
561 Vega Y Miguel, R. Mendiña García, V. Martínez Calvo, O. López Jiménez, J.  
562 Krause, S. L. Pichler, R. Garrido-Pena, M. Kunst, R. Risch, M. A. Rojo-Guerra,  
563 W. Haak, K. W. Alt, The maternal genetic make-up of the Iberian Peninsula  
564 between the Neolithic and the Early Bronze Age. *Sci. Rep.* **7**, 15644 (2017).
- 565 59. A. Sánchez-Polo, A. Blanco-González, Death, Relics, and the Demise of Huts:  
566 Patterns of Planned Abandonment in Middle BA Central Iberia. *Eur. J. Archaeol.*  
567 **17**, 4–26 (2014).
- 568 60. A. L. Palomino, M. J. Negredo, F. J. Abarquero, Cabañas, basureros, silos y  
569 tumbas en el yacimiento de El Cerro, La Horra (Burgos): a vueltas sobre el  
570 significado de un campo de hoyos en la Edad del Bronce de la Meseta. *Numantia*.  
571 **7** (1999), pp. 21–41.
- 572 61. A. Esparza Arroyo, J. Velasco Vázquez, G. Delibes de Castro, J. A. Rodríguez  
573 Marcos, J. Fernández Manzano, Eds., Planteamiento y primeros resultados de un  
574 proyecto de investigación sobre la muerte en Cogotas I. *Cogotas I una Cult. la*  
575 *Edad del Bronce en la Península Ibérica* (2012), pp. 259–320.
- 576 62. O. Arteaga, H. Schulz, A. M. Roos, Geoarqueología Dialéctica en la Bahía de  
577 Cádiz. *Geoarqueología y proceso histórico en la Bahía Cádiz. Rev. Atlántica-*  
578 *Mediterránea Prehist. y Arqueol. Soc.* **10** (2008), pp. 21–116.
- 579 63. E. Vijande Vila, El poblado de Campo de Hockey (San Fernando, Cádiz):  
580 resultados preliminares y líneas de investigación futuras para el conocimiento de  
581 las formaciones sociales tribales en la Bahía de Cádiz (tránsito V-IV milenios  
582 a.e). *Rev. Atlántica-Mediterránea Prehist. y Arqueol. Soc.* **11** (2009), pp. 265–  
583 284.
- 584 64. E. Vijande Vila, S. Domínguez-Bella, J. J. Cantillo Duarte, J. Martínez López, A.  
585 Barrera Tocino, Social inequalities in the Neolithic of southern Europe: The  
586 grave goods of the Campo de Hockey necropolis (San Fernando, Cádiz, Spain).  
587 *Comptes Rendus Palevol.* **14**, 147–161 (2015).
- 588 65. R. Benítez Mota, E. Mata Almonte, B. González Toraya, Intervención

- 589 arqueológica de urgencia en la Loma del Puerco (Chiclana de la Frontera, Cádiz).  
590 *Anu. Arqueol. Andalucía/1992*, 90–96 (1995).
- 591 66. T. Majó i Ortín, Estudi dels esquelets infantils ibèrics dels Estrets-Racó de Rata  
592 (Vilafamés, Castelló). *Quad. Prehistòria i Arqueol. Castelló*. **17** (1996), pp. 339–  
593 348.
- 594 67. A. Oliver, El poblado ibérico del Puig de la Misericordia de Vinaròs. *Assoc. Cult.*  
595 *Amics Vinaròs, Vinaròs* (1994).
- 596 68. C. Olària, F. Gusi, J. L. López, L. Oosterbeek, Ed., Epipaleolithic and Mesolithic  
597 Burial's from 12,000 to 7000 BP in Levantin territory art rock. *Proc. XV World*  
598 *Congr. Int. Union Prehist. Protohistoric Sci.* (2010), pp. 115–123.
- 599 69. D. C. Salazar-García, J. E. Aura, C. R. Olària, S. Talamo, J. V Morales, M. P.  
600 Richards, Isotope evidence for the use of marine resources in the Eastern Iberian  
601 Mesolithic. *J. Archaeol. Sci.* **42**, 231–240 (2014).
- 602 70. L. Benítez de Lugo Enrich, C. Esteban, Arquitecturas simbólicas orientadas  
603 astronómicamente durante el Neolítico Final, el Calcolítico y la Edad del Bronce  
604 en el sur de la Meseta. *SPAL-Revista Prehist. y Arqueol.*, 61–87 (2018).
- 605 71. I. Montero Ruiz, L. Benítez de Lugo Enrich, H. J. Álvarez García, P. C.  
606 Gutiérrez-Neira, M. Murillo-Barroso, N. Palomares Zumajo, G. Menchén  
607 Herreros, J. Moraleda Sierra, D. C. Salazar-García, Cobre para los muertos.  
608 Estudio arqueométrico del material metálico procedente del monumento  
609 megalítico prehistórico de Castillejo del Bonete (Terrinches, Ciudad Real).  
610 *Zephyrus*. **73**, 109 (2014).
- 611 72. L. Benítez de Lugo Enrich, M. Mejías Moreno, J. López Gutiérrez, H. J. Álvarez  
612 García, N. Palomares Zumajo, E. Mata Trujillo, J. Moraleda Sierra, G. Menchén  
613 Herreros, S. Fernández Martín, D. C. Salazar García, Aportaciones  
614 hidrogeológicas al estudio arqueológico de los orígenes de la Edad del Bronce de  
615 La Mancha: la cueva monumentalizada de Castillejo del Bonete (Terrinches,  
616 Ciudad Real, España). *Trab. Prehist.* **71**, 76–94 (2014).
- 617 73. L. Benítez de Lugo Enrich, N. Palomares Zumajo, H. J. Álvarez García, R.  
618 Barroso Bermejo, M. Benito Sánchez, H.-A. Blain, P. Bueno Ramírez, R. de  
619 Balbín Behrmann, S. Fernández Martín, J. A. López Sáez, Paleoeología y  
620 cultura material en el complejo tumular prehistórico del Castillejo del Bonete  
621 (Terrinches, Ciudad Real). *Menga Rev. Prehist. Andalucía* (2015).
- 622 74. D. C. Salazar-García, L. Benítez de Lugo Enrich, H. J. Alvarez García, M. Benito  
623 Sánchez, Estudio diacrónico de la dieta de los pobladores antiguos de Terrinches  
624 (Ciudad Real) a partir del análisis de isótopos estables sobre restos óseos  
625 humanos. *Rev. Española Antropol. Física*. **34**, 6–14 (2013).
- 626 75. G. Delvene, E. Baeza, L. Benítez de Lugo Enrich, in *Yacimientos*  
627 *paleontológicos excepcionales en la Península Ibérica (XXXIV Jornadas de*  
628 *Paleontología y IV Congreso ibérico de Paleontología)* (Instituto Geológico y  
629 Minero de España, Madrid, 2018), pp. 31–38.
- 630 76. C. Barroso Ruíz, D. Botella Ortega, M. Caparrós, A. M. Moigne, V. Celiberti, A.  
631 Testu, D. Barsky, O. Notter, J. A. Riquelme Cantal, M. P. Rodríguez, M. I.  
632 Carretero León, G. Monge Gómez, S. Khatib, T. Saos, S. Gregoire, S. Bailón, J.  
633 A. García Solano, A. L. Cabral Mesa, A. Djerrab, I. George Hedley, S.  
634 Abdessadok, G. Batalla LLasat, N. Astier, L. Bertin, N. Boulbes, D. Cauche, A.  
635 Filoux, C. Hanquet, C. Milizia, J. Moutoussamy, E. Rossoni, L. Verdú Bermejo,  
636 H. de Lumley, The Cueva del Angel (Lucena, Spain): An Acheulean hunters  
637 habitat in the South of the Iberian Peninsula. *Quat. Int.* **243**, 105–126 (2011).
- 638 77. A. M. Moigne, P. Valensi, P. Auguste, J. García-Solano, A. Tuffreau, A.  
639 Lamotte, C. Barroso, M. H. Moncel, Bone retouchers from Lower Palaeolithic  
640 sites: Terra Amata, Orgnac 3, Cagny-l'Épinette and Cueva del Angel. *Quat. Int.*

- 641 **409**, 195–212 (2016).
- 642 78. C. Falguères, B. Ghaleb, O. Tombret, E. Ben Arous, M. Richard, A. M. Moigne,  
643 T. Saos, M. Frouin, M. Caparros, C. Barroso-Ruiz, ESR/U-series dates on Equus  
644 teeth from the Middle Pleistocene Acheulean site of Cueva del Angel, Spain.  
645 *Quat. Geochronol.* **49**, 297–302 (2019).
- 646 79. J. Burch, G. García, J. M. Nolla, L. Palahí, J. Sagrera i Aradilla, M. Sureda, D.  
647 Vivó, I. Miquel, *Excavacions arqueològiques a la muntanya de Sant Julià de*  
648 *Ramis. El castellum* (Ajuntament de Sant Julià de Ramis, 2006).
- 649 80. J. Llinàs Pol, A. Tarrés Farrés, C. Montalbán Martínez, J. Frigola Triola, J.  
650 Merino Serra, B. Agustí Farjas, Pla de l'Horta (Sarrià de Ter, Girona): una  
651 necrópolis con inhumaciones visigodas en la Tarraconense oriental. *Arch.*  
652 *Español Arqueol.* **81**, 289–304 (2009).
- 653 81. M. García-Sánchez, Restos humanos del paleolítico medio y superior y del  
654 eneolítico de Piñar (Granada). *Trab. del Inst. "Bernardino Sahagún" Antropol. y*  
655 *Etnogr.* **15** (1960), pp. 19–78.
- 656 82. F. Molina González, J. A. Cámara Serrano, J. A. Afonso Marrero, T. Nájera  
657 Colino, Las sepulturas del Cerro de la Virgen (Orce, Granada). Diferencias  
658 cronológicas y sociales. *Rev. Atlántico-Mediterránea.* **16** (2014), pp. 121–142.
- 659 83. J. E. Ferrer Palma, A. Arribas, *La necrópolis megalítica del pantano de los*  
660 *Bermejales* (Granada, 1997).
- 661 84. J. J. Álvarez García, A. García Porras, La zawiya del "Cobertizo Viejo"  
662 (Granada). *Anu. Arqueol. Andalucía.* **1** (2003), pp. 429–436.
- 663 85. M. T. Bonet García, Intervención preventiva en la calle Panaderos no. 21-23.  
664 Albayzín, Granada. *Anu. Arqueol. Andalucía 06* (2010), pp. 1715–1723.
- 665 86. J. M. Peña Rodríguez, M. López López, M. O. Rodríguez Ariza, Excavación  
666 arqueológica de urgencia en Cueva Romero (Huéscar, Granada ). *Anu. Arqueol.*  
667 *Andalucía.* **97** (2016), pp. 309–319.
- 668 87. J. M. Román Punzón, *El Mundo funerario rural en la provincia de Granada*  
669 *durante la antigüedad tardía* (Universidad de Granada, Granada, 2004).
- 670 88. A. Rodríguez Aguilera, S. Bordes García, Intervención arqueológica de urgencia  
671 en el yacimiento arqueológico del Maraute (Torrenueva-Motril, provincia de  
672 Granada). *Anu. Arqueol. Andalucía 1999* (2002), pp. 292–303.
- 673 89. J. M. Román Punzón, Redescubriendo la Granada tardoantigua. Eliberri entre los  
674 siglos IV al VIII d.C. *Cuad. Prehist. la Univ. Granada*, 497–533 (2014).
- 675 90. A. Rodríguez Aguilera, S. Bordes García, F. Quero Endrino, El programa de  
676 medidas correctoras de impacto arqueológico de la autovía Bailén-Motril: tramo  
677 Dúrcal-Ízbor. *Bibataubín. Rev. Patrim. Cult. e Investig.* **2**, 33–41 (2001).
- 678 91. I. Toro Moyano, M. Ramos Linaza, Excavación de urgencia en la necrópolis  
679 visigoda de las Delicias (Ventas de Zafarraya, Alhama de Granada) 1985. *Anu.*  
680 *Arqueol. Andalucía/1985*, 143–149 (1987).
- 681 92. M. Ramos Lizana, I. Toro Moyano, C. PÉREZ TORRES, Excavación de  
682 urgencia en la necrópolis de Las Delicias de Ventas de Zafarraya (Alhama de  
683 Granada, Granada). 2ª campaña (1986). *Anu. Arqueol. Andalucía/1996*, 258–261  
684 (1990).
- 685 93. Á. Fernández Flores, A. Rodríguez Azogue, M. Casado Ariza, E. Prados Pérez,  
686 *La necrópolis de época tartésica de La Angorrilla. Alcalá del Río, Sevilla*  
687 (Universidad de Sevilla, Sevilla, 2014).
- 688 94. J. Fernández-Eraso, J. A. Mujika-Alustiza, L. Zapata-Peña, M. J. Iriarte-  
689 Chiapusso, A. Polo-Díaz, P. Castaños, A. Tarriño-Vinagre, S. Cardoso, J. Sesma-  
690 Sesma, J. García-Gazolaz, Beginnings, settlement and consolidation of the  
691 production economy in the Basque region. *Quat. Int.* **364**, 162–171 (2015).
- 692 95. J. A. Mujika-Alustiza, J. M. Edeso-Fito, *Los primeros agricultores y ganaderos*

- en Gipuzkoa del Neolítico a la Edad del Hierro (Diputación de Gipuzkoa, Donostia-San Sebastián, 2011).
96. T. Fernández-Crespo, J. A. Mujika, J. Ordoño, Aproximación al patrón alimentario de los inhumados en la cista de la Edad del Bronce de Ondarre (Aralar, Guipúzcoa) a través del análisis de isótopos estables de carbono y nitrógeno sobre colágeno óseo. *Trab. Prehist.* **73**, 325–334 (2016).
  97. I. Olalde, M. E. Allentoft, F. Sánchez-Quinto, G. Santpere, C. W. K. Chiang, M. DeGiorgio, J. Prado-Martinez, J. A. Rodríguez, S. Rasmussen, J. Quilez, O. Ramírez, U. M. Marigorta, M. Fernández-Callejo, M. E. Prada, J. M. V. Encinas, R. Nielsen, M. G. Netea, J. Novembre, R. a Sturm, P. Sabeti, T. Marquès-Bonet, A. Navarro, E. Willerslev, C. Lalueza-Fox, Derived immune and ancestral pigmentation alleles in a 7,000-year-old Mesolithic European. *Nature*. **507**, 225–8 (2014).
  98. G. Delibes de Castro, J. Fernández Manzano, J. . Rodríguez Marcos, Cerámica de la plenitud Cogotas I: el yacimiento de San Román de Hornija (Valladolid). *Boletín del Semin. Estud. Arte y Arqueol.* **56**, 64–105 (1990).
  99. G. Delibes de Castro, Una inhumación triple de facies Cogotas I en San Román de la Hornija (Valladolid). *Trab. Prehist.* **35**, 225–250 (1978).
  100. Á. Esparza Arroyo, J. Velasco Vázquez, G. Delibes de Castro, Exposition de cadáveres en el yacimiento de Tordillos (Aldeaseca de la Frontera, Salamanca). Perspectiva bioarqueológica y posibles implicaciones para el estudio del ritual funerario de Cogotas I. *Zephyrus*. **69**, 95–128 (2012).
  101. J. M. Vergès i Bosch, L. Muñoz Encinar, M. Pedro, A. Bargalló, M. Fontanals i Torroja, J. I. Morales, A. Ollé, E. Allué, H.-A. Blain, J. M. López García, La cova dels Galls Carboners (Mont-Ral, Alt Camp), una cavitat d'inhumació col·lectiva durant l'edat del Bronze. *Butlletí Arqueol. R. Soc. Arqueol. Tarraconense* (2016), pp. 17–44.
  102. J. Canyellas, L. Piñol, J. M. Vergès, La vil·la d'Alcover i la necropolis de Mas Gassol. *Quad. Vilaniu*. **29** (1996), pp. 27–41.
  103. P. García Borja, Á. Pérez Fernández, V. Biosca Cirujeda, A. Ribera Gomes, D. C. Salazar García, in *El Naiximent d'un Poble. Història i Arqueologia de la Font de la Figuera* (2013), pp. 47–59.
  104. O. García-Puchol, S. B. McClure, J. Juan-Cabanilles, A. A. Díez-Castillo, J. Bernabeu-Aubán, B. Martí-Oliver, S. Pardo-Gordó, J. L. Pascual-Benito, M. Pérez-Ripoll, L. Molina-Balaguer, Cocina cave revisited: Bayesian radiocarbon chronology for the last hunter-gatherers and first farmers in Eastern Iberia. *Quat. Int.* **472**, 259–271 (2018).
  105. L. Pericot, La Cueva de la Cocina (Dos Aguas). Nota preliminar. *Arch. Prehist. Levantina, Mus. Prehist.* (1945), pp. 39–71.
  106. J. Fortea Pérez, *Los complejos microlaminares y geométricos del Epipaleolítico mediterráneo español* (Universidad de Salamanca, Salamanca, 1973), *Memorias del Seminario de Prehistoria y Arqueología*.
  107. J. Fortea, B. Martí, P. Fumanal, M. Dupré, M. Pérez Ripoll, Epipaleolítico y neolitización en la zona oriental de la Península Ibérica. *Premières communautés paysannes en Méditerranée Occident. Actes du Colloq. Int. du CNRS (Montpellier, 1983), éditions du CNRS, Paris* (1987), pp. 599–606.
  108. A. Díez Castillo, A. Cortell Nicolau, O. García Puchol, P. Escribá Ruiz, Entorno 3d para el análisis y la recreación virtual de las actuaciones arqueológicas en cueva de la cocina (Dos Aguas, Valencia, España). *Virtual Archaeol. Rev.* **8**, 75–83 (2017).
  109. O. García Puchol, J. Juan Cabanilles, S. B. McClure, A. Díez Castillo, S. Pardo Gordó, Avance de resultados de los nuevos trabajos arqueológicos en Cueva de la



- Cocina (Dos Aguas, Valencia): campaña de 2015. *Saguntum. Papeles del Lab. Arqueol. Val.* **47**, 251–255 (2015).
110. S. Pardo-gordó, S. Pardo-gordó, O. García, A. A. Diez, S. B. McClure, Taphonomic processes inconsistent with indigenous Mesolithic acculturation during the transition to the Neolithic in the Western Mediterranean Taphonomic processes inconsistent with indigenous Mesolithic acculturation during the transition to the Neolithi. *Quat. Int.* **483**, 136–147 (2018).
  111. M. J. de Pedro Michó, L. Fortea Cervera, E. Ripollés Adelantado, *Vivir junto al Turia hace 4.000 años: la Lloma de Betxi* (Museu de Prehistòria de València, 2015).
  112. A. Ribera Gomes, J. Pascual Beneyto, M. Barberá, J. M. Belda, El poblament de l'Edat del Bronze a la Font de la Figuera (València). *Recer. del Mus. d'Alcoi*, 27–78 (2005).
  113. P. García Borja, D. C. Salazar García, I. Collado Beneyto, E. Cortell Pérez, Los restos humanos de la Coveta Emparetà: Contexto cronológico y cultural. *Recer. del Mus. d'Alcoi*. **1**, 31–46 (2016).
  114. G. Pérez Jordà, J. Bernabeu Aubán, Y. Carrión Marco, O. García Puchol, L. Molina Balaguer, M. Gómez Puche, La Vital.Vida y muerte en la desembocadura del Serpis entre el III y el II Milenio cal AC. *Ser. Trab. Var. del S.I.P.* **113** (2011).
  115. G. Aguilera Arzo, B. Agustí i Farjas, R. Gómez, N. Arquer Gasch, J. Luján, Un túmul funerari de l'edat del bronze al Tossal del Mortórum (Cabanes, Plana Alta, Castelló). *Quad. prehistòria i Arqueol. Castelló* (2009), pp. 29–39.
  116. G. Aguilera Arzo, D. Román Monroig, P. García Borja, *La Cova dels Diablets (Alcalà de Xivert, Castelló)*. *Prehistòria a la Serra d'Irta* (Diputació de Castelló, 2014).
  117. P. A. A. Gil, Necrópoles de Cistas na realidade do Sudoeste Peninsular durante o II milénio aC: praticas funerárias e análise antropológica dos restos ósseos humanos exumados das Necrópoles de Casas Velhas e Monte da Cabida 3. *Master's thesis. Coimbra, Dep. Ciências da Vida, Univ. Coimbra.* (2014).
  118. A. C. Valera, Recinto Calcolítico dos Perdigões: fossos e fossas do Sector I. *Apointamentos Arqueol. e Património*. **3** (2008), p. NIA-ERA 19-27.
  119. A. Silva, I. Leandro, A. Valera, D. Pereira, C. Afonso, in *Death as Archaeology of Transition: Thoughts and Materials Papers from the II International Conference of Transition Archaeology: Death Archaeology*, L. Rocha, P. Bueno-Ramirez, G. Branco, Eds. (2015), p. BAR –S2708 245-250.
  120. H. Schubart, Die Kultur der Bronzezeit im Südwesten der Iberischen Halbinsel. *Madriider Forschungen*, **9**. **1** (1975).
  121. C. Tavares da Silva, J. Soares, Pré-História da área de Sines. *Gab. da Área Sines, Lisboa* (1981).
  122. A. M. Silva, P. Gil, J. Soares, C. T. da Silva, Evidence of non-masticatory dental use in Bronze Age individuals exhumed from the Necropolis of Casas Velhas (Portugal). *Bull. Int. Assoc. Paleodont.* **10** (2016), pp. 31–38.
  123. A. M. Silva, P. Gil, J. Soares, C. T. da Silva, Evidence of Trepanation on a Female Individual from the Middle Bronze Age Necropolis of Casas Velhas (Melides, Portugal). *Int. J. Osteoarchaeol.* **27** (2017), pp. 515–521.
  124. J. Soares, C. Tavares da Silva, in *Existe uma Idade do Bronze Atlântico? (Trabalhos de Arqueologia, 10)* (Instituto Português de Arqueologia, 1998), pp. 231–245.
  125. C. Tavares da Silva, J. Soares, Práticas funerárias no Bronze Pleno do litoral alentejano: o Monumento II do Pessegueiro. *Estud. Arqueol. Oeiras*. **17**, 389–420 (2009).

- 797 126. G. Gally, K. Spindler, L. Trindade, O. Veiga Ferreira, O monumento pré-  
798 histórico de Pai Mogo (Lourinhã). *Lisboa, Assoc. Arqueólogos Port.* (1973).
- 799 127. K. Spindler, G. Gally, Kupferzeitliche Siedlung und Begräbnisstätten von  
800 Matações in Portugal. *Mainz am Rhein, Verlag Philipp von Zabern.* **1** (1973).
- 801 128. A. Silva, Antropologia funerária e Paleobiologia das populações portuguesas  
802 (litorais) do Neolítico final/Calcolítico. *PhD Diss. Anthropol. Dep. Anthropol.*  
803 *Fac. Sci. Technol. Univ. Coimbra* (2002).
- 804 129. A. M. Silva, Portuguese Populations of the Late Neolithic and Chalcolithic  
805 Periods exhumed from Collective burials: an overview. *Anthropologie.* **XLI/1-2**,  
806 55–64 (2003).
- 807 130. E. J. Guiry, M. Hillier, R. Boaventura, A. M. Silva, L. Oosterbeek, T. Tomé, A.  
808 Valera, J. L. Cardoso, J. C. Hepburn, M. P. Richards, The transition to  
809 agriculture in south-western Europe: new isotopic insights from Portugal's  
810 Atlantic coast. *Antiquity.* **90**, 604–616 (2016).
- 811 131. A. Waterman, R. Tykot, A. M. Silva, Stable Isotope Analysis of diet-based social  
812 differentiation at Late Prehistoric Collective burials in southwestern Portugal.  
813 *Archaeometry.* **58**, 131 – 151 (2016).
- 814 132. A. M. Silva, in *Antropología y biodiversidad actas do XII congreso de la*  
815 *sociedad española de antropología biológica.* Bellaterra ed., Barcelona (2003),  
816 pp. 506–512.
- 817 133. R. Longin, New method of collagen extraction for radiocarbon dating. *Nature.*  
818 **230**, 241–242 (1971).
- 819 134. J. C. Lohse, D. B. Madsen, B. J. Culleton, D. J. Kennett, Isotope paleoecology of  
820 episodic mid-to-late Holocene bison population expansions in the Southern  
821 Plains, U.S.A. *Quat. Sci. Rev.* **102**, 14–26 (2014).
- 822 135. G. J. Van Klinken, Bone collagen quality indicators for palaeodietary and  
823 radiocarbon measurements. *J. Archaeol. Sci.* **26**, 687–695 (1999).
- 824 136. J. C. Vogel, A. Fuls, E. Visser, B. Becker, Radiocarbon Fluctuations During the  
825 Third Millennium BC. *Radiocarbon.* **28**, 935–938 (1986).
- 826 137. G. M. Santos, J. R. Southon, K. C. Druffel-Rodriguez, S. Griffin, M. Mazon,  
827 Magnesium Perchlorate as an Alternative Water Trap in AMS Graphite Sample  
828 Preparation: A Report On Sample Preparation at Kccams at the University of  
829 California, Irvine. *Radiocarbon.* **46**, 165–173 (2004).
- 830 138. M. Stuiver, H. A. Polach, Reporting of <sup>14</sup>C Data. *Radiocarbon.* **19**, 355–363  
831 (1977).
- 832 139. J. Dabney, M. Knapp, I. Glocke, M.-T. Gansauge, A. Weihmann, B. Nickel, C.  
833 Valdiosera, N. García, S. Pääbo, J.-L. Arsuaga, M. Meyer, Complete  
834 mitochondrial genome sequence of a Middle Pleistocene cave bear reconstructed  
835 from ultrashort DNA fragments. *Proc. Natl. Acad. Sci. U.S.A.* **110**, 15758–63  
836 (2013).
- 837 140. N. Rohland, I. Glocke, A. Aximu-Petri, M. Meyer, Extraction of highly degraded  
838 DNA from ancient bones, teeth and sediments for high-throughput sequencing.  
839 *Nat. Protoc.* **13**, 2447–2461 (2018).
- 840 141. P. Korlević, T. Gerber, M. T. Gansauge, M. Hajdinjak, S. Nagel, A. Aximu-Petri,  
841 M. Meyer, Reducing microbial and human contamination in dna extractions from  
842 ancient bones and teeth. *Biotechniques.* **59**, 87–93 (2015).
- 843 142. A. W. Briggs, U. Stenzel, M. Meyer, J. Krause, M. Kircher, S. Pääbo, Removal  
844 of deaminated cytosines and detection of in vivo methylation in ancient DNA.  
845 *Nucleic Acids Res.* **38**, e87 (2010).
- 846 143. M. T. Gansauge, T. Gerber, I. Glocke, P. Korlević, L. Lippik, S. Nagel, L. M.  
847 Riehl, A. Schmidt, M. Meyer, Single-stranded DNA library preparation from  
848 highly degraded DNA using T4 DNA ligase. *Nucleic Acids Res.* **45**, e79 (2017).

144. M.-T. Gansauge, M. Meyer, Single-stranded DNA library preparation for the sequencing of ancient or damaged DNA. *Nat. Protoc.* **8**, 737–48 (2013).
145. M. Kircher, S. Sawyer, M. Meyer, Double indexing overcomes inaccuracies in multiplex sequencing on the Illumina platform. *Nucleic Acids Res.* **40**, 1–8 (2012).
146. Yang D.Y, Wayne J.S, Dудар J.C, Saunders S.R, Technical note : improved DNA extraction from ancient bone using silica-based spin columns. *Am J Phys Anthr.* **105**, 539–543 (1998).
147. D. E. MacHugh, C. J. Edwards, J. F. Bailey, D. R. Bancroft, D. G. Bradley, The Extraction and Analysis of Ancient DNA From Bone and Teeth: a Survey of Current Methodologies. *Anc. Biomol.* **3**, 81 (2000).
148. D. M. Behar, M. van Oven, S. Rosset, M. Metspalu, E.-L. Loogväli, N. M. Silva, T. Kivisild, A. Torroni, R. Villems, A “Copernican” reassessment of the human mitochondrial DNA tree from its root. *Am. J. Hum. Genet.* **90**, 675–84 (2012).
149. H. Li, R. Durbin, Fast and accurate short read alignment with Burrows–Wheeler transform. *Bioinformatics.* **25**, 1754–1760 (2009).
150. T. Daley, A. D. Smith, Predicting the molecular complexity of sequencing libraries. *Nat. Methods.* **10**, 325–7 (2013).
151. Q. Fu, A. Mitnik, P. L. F. Johnson, K. Bos, M. Lari, R. Bollongino, C. Sun, L. Giemsch, R. Schmitz, J. Burger, A. M. Ronchitelli, F. Martini, R. G. Cremonesi, J. Svoboda, P. Bauer, D. Caramelli, S. Castellano, D. Reich, S. Pääbo, J. Krause, A revised timescale for human evolution based on ancient mitochondrial genomes. *Curr. Biol.* **23**, 553–9 (2013).
152. T. S. Korneliussen, A. Albrechtsen, R. Nielsen, ANGSD : Analysis of Next Generation Sequencing Data. *BMC Bioinformatics.* **15**, 1–13 (2014).
153. H. Weissensteiner, D. Pacher, A. Kloss-Brandstätter, L. Forer, G. Specht, H.-J. Bandelt, F. Kronenberg, A. Salas, S. Schönherr, HaploGrep 2: mitochondrial haplogroup classification in the era of high-throughput sequencing. *Nucleic Acids Res.* **44**, W58-63 (2016).
154. N. Solé-Morata, P. Villaescusa, C. García-Fernández, N. Font-Porterias, M. J. Illescas, L. Valverde, F. Tassi, S. Ghirotto, C. Férec, K. Rouault, S. Jiménez-Moreno, B. Martínez-Jarreta, M. F. Pinheiro, M. T. Zarrabeitia, Á. Carracedo, M. M. De Pancorbo, F. Calafell, Analysis of the R1b-DF27 haplogroup shows that a large fraction of Iberian Y-chromosome lineages originated recently in situ. *Sci. Rep.* **7**, 1–13 (2017).
155. L. Valverde, M. J. Illescas, P. Villaescusa, A. M. Gotor, A. García, S. Cardoso, J. Algorta, S. Catarino, K. Rouault, C. Férec, O. Hardiman, M. Zarrabeitia, S. Jiménez, M. F. Pinheiro, B. M. Jarreta, J. Olofsson, N. Morling, M. M. de Pancorbo, New clues to the evolutionary history of the main European paternal lineage M269: dissection of the Y-SNP S116 in Atlantic Europe and Iberia. *Eur. J. Hum. Genet.* **24**, 437–441 (2016).
156. D. J. Kennett, S. Plog, R. J. George, B. J. Culleton, A. S. Watson, P. Skoglund, N. Rohland, S. Mallick, K. Stewardson, L. Kistler, S. A. LeBlanc, P. M. Whiteley, D. Reich, G. H. Perry, Archaeogenomic evidence reveals prehistoric matrilineal dynasty. *Nat. Commun.* **8**, 14115 (2017).
157. J. M. Monroy Kuhn, M. Jakobsson, T. Günther, Estimating genetic kin relationships in prehistoric populations. *PLoS One.* **13**, 1–21 (2018).
158. I. Lazaridis, D. Nadel, G. Rollefson, D. C. Merrett, N. Rohland, S. Mallick, D. Fernandes, M. Novak, B. Gamarra, K. Sirak, S. Connell, K. Stewardson, E. Harney, Q. Fu, G. Gonzalez-Fortes, E. R. Jones, S. A. Roodenberg, G. Lengyel, F. Bocquentin, B. Gasparian, J. M. Monge, M. Gregg, V. Eshed, A.-S. Mizrahi, C. Meiklejohn, F. Gerritsen, L. Bejenaru, M. Blüher, A. Campbell, G. Cavalleri,

- D. Comas, P. Froguel, E. Gilbert, S. M. Kerr, P. Kovacs, J. Krause, D. McGettigan, M. Merrigan, D. A. Merriwether, S. O'Reilly, M. B. Richards, O. Semino, M. Shamoon-Pour, G. Stefanescu, M. Stumvoll, A. Tönjes, A. Torroni, J. F. Wilson, L. Yengo, N. A. Hovhannisyan, N. Patterson, R. Pinhasi, D. Reich, Genomic insights into the origin of farming in the ancient Near East. *Nature*. **536**, 1–22 (2016).
159. F. Broushaki, M. G. Thomas, V. Link, S. López, L. Van Dorp, K. Kirsanow, Y. Diekmann, L. M. Cassidy, D. Díez-del-molino, A. Kousathanas, C. Sell, H. K. Robson, R. Martiniano, J. Blöcher, A. Scheu, S. Kreutzer, D. Bobo, H. Davudi, O. Munoz, M. Currat, K. Abdi, D. Wegmann, G. Hellenthal, J. Burger, Early Neolithic genomes from the eastern Fertile Crescent. *Science*. **7943**, 1–16 (2016).
160. L. M. Cassidy, R. Martiniano, E. M. Murphy, M. D. Teasdale, J. Mallory, B. Hartwell, D. G. Bradley, Neolithic and Bronze Age migration to Ireland and establishment of the insular Atlantic genome. *Proc. Natl. Acad. Sci. U.S.A.* **113**, 1–6 (2016).
161. Q. Fu, H. Li, P. Moorjani, F. Jay, S. M. Slepchenko, A. a. Bondarev, P. L. F. Johnson, A. Aximu-Petri, K. Prüfer, C. de Filippo, M. Meyer, N. Zwyns, D. C. Salazar-García, Y. V. Kuzmin, S. G. Keates, P. a. Kosintsev, D. I. Razhev, M. P. Richards, N. V. Peristov, M. Lachmann, K. Douka, T. F. G. Higham, M. Slatkin, J.-J. Hublin, D. Reich, J. Kelso, T. B. Viola, S. Pääbo, Genome sequence of a 45,000-year-old modern human from western Siberia. *Nature*. **514**, 445–449 (2014).
162. M. Haber, C. Doumet-Serhal, C. Scheib, Y. Xue, P. Danecek, M. Mezzavilla, S. Youhanna, R. Martiniano, J. Prado-Martinez, M. Szpak, E. Matisoo-Smith, H. Schutkowski, R. Mikulski, P. Zalloua, T. Kivisild, C. Tyler-Smith, Continuity and admixture in the last five millennia of Levantine history from ancient Canaanite and present-day Lebanese genome sequences. *Am. J. Hum. Genet.* **101**, 1–9 (2017).
163. Z. Hofmanová, S. Kreutzer, G. Hellenthal, C. Sell, Y. Diekmann, D. Díez-del-Molino, L. van Dorp, S. López, A. Kousathanas, V. Link, K. Kirsanow, L. M. Cassidy, R. Martiniano, M. Strobel, A. Scheu, K. Kotsakis, P. Halstead, S. Triantaphyllou, N. Kyparissi-Apostolika, D. Urem-Kotsou, C. Ziota, F. Adaktylou, S. Gopalan, D. M. Bobo, L. Winkelbach, J. Blöcher, M. Unterländer, C. Leuenberger, Ç. Çilingiroglu, B. Horejs, F. Gerritsen, S. J. Shennan, D. G. Bradley, M. Currat, K. R. Veeramah, D. Wegmann, M. G. Thomas, C. Papageorgopoulou, J. Burger, Early farmers from across Europe directly descended from Neolithic Aegeans. *Proc. Natl. Acad. Sci. U.S.A.* **113**, 6886–6891 (2016).
164. E. R. Jones, G. Gonzalez-Fortes, S. Connell, V. Siska, A. Eriksson, R. Martiniano, R. L. Mc Laughlin, M. G. Llorente, L. M. Cassidy, C. Gamba, T. Meshveliani, O. Bar-Yosef, W. Muller, A. Belfer-Cohen, Z. Matskevich, N. Jakeli, T. F. G. Higham, M. Currat, D. Lordkipanidze, M. Hofreiter, A. Manica, R. Pinhasi, D. G. Bradley, Upper palaeolithic genomes reveal deep roots of modern eurasians. *Nat. Comm.* **6**, 1–8 (2015).
165. A. Keller, A. Graefen, M. Ball, M. Matzas, V. Boisguerin, F. Maixner, P. Leidinger, C. Backes, R. Khairat, M. Forster, B. Stade, A. Franke, J. Mayer, J. Spangler, S. McLaughlin, M. Shah, C. Lee, T. T. Harkins, A. Sartori, A. Moreno-Estrada, B. Henn, M. Sikora, O. Semino, J. Chironi, S. Rootsi, N. M. Myres, V. M. Cabrera, P. a Underhill, C. D. Bustamante, E. E. Vigl, M. Samadelli, G. Cipollini, J. Haas, H. Katus, B. D. O'Connor, M. R. J. Carlson, B. Meder, N. Blin, E. Meese, C. M. Pusch, A. Zink, New insights into the Tyrolean Iceman's origin and phenotype as inferred by whole-genome sequencing. *Nat. Commun.* **3**,

- 698 (2012).
166. G. M. Kilinc, A. Omrak, F. Özer, J. Stora, T. Günther, A. M. Büyükkarakaya, E. Biçakçi, D. Baird, H. M. Dönertas, A. Ghalichi, R. Yaka, D. Koptekin, M. Jakobsson, A. Götherstrom, The Demographic Development of the First Farmers in Anatolia. *Curr. Biol.* **26**, 1–8 (2016).
167. I. Lazaridis, A. Mittnik, N. Patterson, S. Mallick, N. Rohland, S. Pfrengle, A. Furtwängler, A. Peltzer, C. Posth, A. Vasilakis, P. J. P. McGeorge, E. Konsolaki-Yannopoulou, G. Korres, H. Martlew, M. Michalodimitrakis, M. Özşait, N. Özşait, A. Papathanasiou, M. Richards, S. A. Roodenberg, Y. Tzedakis, R. Arnott, D. M. Fernandes, J. R. Hughey, D. M. Lotakis, P. A. Navas, Y. Maniatis, J. A. Stamatoyannopoulos, K. Stewardson, P. Stockhammer, R. Pinhasi, D. Reich, J. Krause, G. Stamatoyannopoulos, Genetic origins of the Minoans and Mycenaeans. *Nature*. **548**, 214–218 (2017).
168. M. Gallego Llorente, E. R. Jones, A. Eriksson, V. Siska, K. W. Arthur, J. W. Arthur, M. C. Curtis, J. T. Stock, M. Coltorti, P. Pieruccini, S. Stretton, F. Brock, T. Higham, Y. Park, M. Hofreiter, D. G. Bradley, J. Bhak, R. Pinhasi, A. Manica, Ancient Ethiopian genome reveals extensive Eurasian admixture in Eastern Africa. *Science*. **350**, 820–822 (2015).
169. I. Mathieson, S. Alpaslan-Roodenberg, C. Posth, A. Szécsényi-Nagy, N. Rohland, S. Mallick, I. Olalde, N. Broomandkhoshbacht, F. Candilio, O. Cheronet, D. Fernandes, M. Ferry, B. Gamarra, G. G. Fortes, W. Haak, E. Harney, E. Jones, D. Keating, B. Krause-Kyora, I. Kucukkalipci, M. Michel, A. Mittnik, K. Nägele, M. Novak, J. Oppenheimer, N. Patterson, S. Pfrengle, K. Sirak, K. Stewardson, S. Vai, S. Alexandrov, K. W. Alt, R. Andreescu, D. Antonovic, A. Ash, N. Atanassova, K. Bacvarov, M. B. Gusztáv, H. Bocherens, M. Bolus, A. Boroneant, Y. Boyadzhiev, A. Budnik, J. Burmaz, S. Chohadzhiev, N. J. Conard, R. Cottiaux, M. Čuka, C. Cupillard, D. G. Drucker, N. Elenski, M. Francken, B. Galabova, G. Ganetsovski, B. Gély, T. Hajdu, V. Handzhyiska, K. Harvati, T. Higham, S. Iliev, I. Jankovic, I. Karavanic, D. J. Kennett, D. Komšo, A. Kozak, D. Labuda, M. Lari, C. Lazar, M. Leppek, K. Leshtakov, D. Lo Vetro, D. Los, I. Lozanov, M. Malina, F. Martini, K. McSweeney, H. Meller, M. Mendišić, P. Mirea, V. Moiseyev, V. Petrova, T. D. Price, A. Simalcsik, L. Sineo, M. Šlaus, V. Slavchev, P. Stanev, A. Starovic, T. Szeniczey, S. Talamo, M. Teschler-Nicola, C. Thevenet, I. Valchev, F. Valentin, S. Vasilyev, F. Veljanovska, S. Venelinova, E. Veselovskaya, B. Viola, C. Virag, J. Zaninovic, S. Zäuner, P. W. Stockhammer, G. Catalano, R. Krauß, D. Caramelli, G. Zariņa, B. Gaydarska, M. Lillie, A. G. Nikitin, I. Potekhina, A. Papathanasiou, D. Borić, C. Bonsall, J. Krause, R. Pinhasi, D. Reich, The genomic history of southeastern Europe. *Nature*. **555**, 197–203 (2018).
170. I. Olalde, H. Schroeder, M. Sandoval-Velasco, L. Vinner, I. Lobón, O. Ramirez, S. Civit, P. García Borja, D. C. Salazar-García, S. Talamo, J. María Fullola, F. Xavier Oms, M. Pedro, P. Martínez, M. Sanz, J. Daura, J. Zilhão, T. Marquès-Bonet, M. T. P. Gilbert, C. Lalueza-Fox, A Common Genetic Origin for Early Farmers from Mediterranean Cardial and Central European LBK Cultures. *Mol. Biol. Evol.* **32**, 3132–3142 (2015).
171. A. Omrak, T. Günther, C. Valdiosera, E. M. Svensson, H. Malmström, H. Kiesewetter, W. Aylward, J. Storå, M. Jakobsson, A. Götherström, Genomic Evidence Establishes Anatolia as the Source of the European Neolithic Gene Pool. *Curr. Biol.* **26**, 270–275 (2016).
172. P. Skoglund, J. C. Thompson, M. E. Prendergast, A. Mittnik, K. Sirak, M. Hajdinjak, T. Salie, N. Rohland, S. Mallick, A. Peltzer, A. Heinze, I. Olalde, M. Ferry, E. Harney, M. Michel, K. Stewardson, J. I. Cerezo-Román, C. Chiumia, A.

- 1005 Crowther, E. Gomani-Chindebvu, A. O. Gidna, K. M. Grillo, I. T. Helenius, G.  
 1006 Hellenthal, R. Helm, M. Horton, S. López, A. Z. P. Mabulla, J. Parkington, C.  
 1007 Shipton, M. G. Thomas, R. Tibesasa, M. Welling, V. M. Hayes, D. J. Kennett, R.  
 1008 Ramesar, M. Meyer, S. Pääbo, N. Patterson, A. G. Morris, N. Boivin, R. Pinhasi,  
 1009 J. Krause, D. Reich, Reconstructing Prehistoric African Population Structure.  
 1010 *Cell*. **171**, 59–71.e21 (2017).
- 1011 173. M. Raghavan, P. Skoglund, K. E. Graf, M. Metspalu, A. Albrechtsen, I. Moltke,  
 1012 S. Rasmussen, T. W. Stafford, L. Orlando, E. Metspalu, M. Karmin, K. Tambets,  
 1013 S. Rootsi, R. Mägi, P. F. Campos, E. Balanovska, O. Balanovsky, E.  
 1014 Khusnutdinova, S. Litvinov, L. P. Osipova, S. a Fedorova, M. I. Voevoda, M.  
 1015 DeGiorgio, T. Sicheritz-Ponten, S. Brunak, S. Demeshchenko, T. Kivisild, R.  
 1016 Villems, R. Nielsen, M. Jakobsson, E. Willerslev, Upper Palaeolithic Siberian  
 1017 genome reveals dual ancestry of Native Americans. *Nature*. **505**, 87–91 (2014).
- 1018 174. S. Schiffels, W. Haak, P. Paajanen, B. Llamas, E. Popescu, L. Lou, R. Clarke, A.  
 1019 Lyons, R. Mortimer, D. Sayer, C. Tyler-Smith, A. Cooper, R. Durbin, Iron Age  
 1020 and Anglo-Saxon genomes from East England reveal British migration history.  
 1021 *Nat. Commun.* **7**, 10408 (2016).
- 1022 175. M. Sikora, A. Seguin-orlando, V. C. Sousa, A. Albrechtsen, A. Ko, S.  
 1023 Rasmussen, I. Dupanloup, P. R. Nigst, D. Marjolein, G. Renaud, M. E. Allentoft,  
 1024 A. Margaryan, S. V Vasilyev, V. Elizaveta, S. B. Borutskaya, T. Deviese, D.  
 1025 Comeskey, T. Higham, Ancient genomes show social and reproductive behavior  
 1026 of early Upper Paleolithic foragers. **1807**, 1–15 (2017).
- 1027 176. P. Skoglund, H. Malmström, A. Omrak, M. Raghavan, C. Valdiosera, T.  
 1028 Günther, P. Hall, K. Tambets, J. Parik, S. Karl-Göran, J. Apel, E. Willerslev, J.  
 1029 Storå, A. Götherström, M. Jakobsson, Genomic Diversity and Admixture Differs  
 1030 for Stone-Age Scandinavian Foragers and Farmers. *Science*. **201**, 786–792  
 1031 (2014).
- 1032 177. M. A. Yang, X. Gao, C. Theunert, H. Tong, A. Aximu-Petri, B. Nickel, M.  
 1033 Slatkin, M. Meyer, S. Pääbo, J. Kelso, Q. Fu, 40,000-Year-Old Individual from  
 1034 Asia Provides Insight into Early Population Structure in Eurasia. *Curr. Biol.* **27**,  
 1035 3202–3208 (2017).
- 1036 178. V. J. Schuenemann, A. Peltzer, B. Welte, W. P. van Pelt, M. Molak, C.-C. Wang,  
 1037 A. Furtwängler, C. Urban, E. Reiter, K. Nieselt, B. Teßmann, M. Francken, K.  
 1038 Harvati, W. Haak, S. Schiffels, J. Krause, Ancient Egyptian mummy genomes  
 1039 suggest an increase of Sub-Saharan African ancestry in post-Roman periods. *Nat.*  
 1040 *Commun.* **8** (2017), doi:10.1038/ncomms15694.
- 1041 179. R. Rodríguez-Varela, T. Günther, M. Krzewinska, J. Stora, T. H. Gillingwater,  
 1042 M. MacCallum, J. L. Arsuaga, K. Dobney, C. Valdiosera, M. Jakobsson, A.  
 1043 Götherström, L. Girdland-flink, Genomic analyses of Pre-European conquest  
 1044 human remains from the Canary Islands reveal close affinity to modern North  
 1045 Africans. *Curr. Biol.* **27**, 3396–3402 (2017).
- 1046 180. E. C. M. van den Brink, R. Beeri, D. Kirzner, E. Bron, A. Cohen-Weinberger, E.  
 1047 Kamaisky, T. Gonen, L. Gershuny, Y. Nagar, D. Ben-Tor, N. Sukenik, O.  
 1048 Shamir, E. F. Maher, D. Reich, A Late Bronze Age II clay coffin from Tel  
 1049 Shaddud in the Central Jezreel Valley, Israel: context and historical implications.  
 1050 *Levant*. **49**, 105–135 (2017).
- 1051 181. M. E. Allentoft, M. Sikora, K.-G. Sjögren, S. Rasmussen, M. Rasmussen, J.  
 1052 Stenderup, P. B. Damgaard, H. Schroeder, T. Ahlström, L. Vinner, A.-S.  
 1053 Malaspinas, A. Margaryan, T. Higham, D. Chivall, N. Lynnerup, L. Harvig, J.  
 1054 Baron, P. Della Casa, P. Dąbrowski, P. R. Duffy, A. V. Ebel, A. Epimakhov, K.  
 1055 Frei, M. Furmanek, T. Gralak, A. Gromov, S. Gronkiewicz, G. Grupe, T. Hajdu,  
 1056 R. Jarysz, V. Khartanovich, A. Khokhlov, V. Kiss, J. Kolář, A. Kriiska, I. Lasak,

- C. Longhi, G. McGlynn, A. Merkevicius, I. Merkyte, M. Metspalu, R. Mkrtychyan, V. Moiseyev, L. Paja, G. Pálfi, D. Pokutta, Ł. Pospieszny, T. D. Price, L. Saag, M. Sablin, N. Shishlina, V. Smrčka, V. I. Soenov, V. Szeverényi, G. Tóth, S. V. Trifanova, L. Varul, M. Vicze, L. Yepiskoposyan, V. Zhitenev, L. Orlando, T. Sicheritz-Pontén, S. Brunak, R. Nielsen, K. Kristiansen, E. Willerslev, Population genomics of Bronze Age Eurasia. *Nature*. **522**, 167–172 (2015).
182. S. Mallick, H. Li, M. Lipson, I. Mathieson, M. Gymrek, F. Racimo, M. Zhao, N. Chennagiri, S. Nordenfelt, A. Tandon, P. Skoglund, I. Lazaridis, S. Sankararaman, Q. Fu, N. Rohland, G. Renaud, Y. Erlich, T. Willems, C. Gallo, J. P. Spence, Y. S. Song, G. Poletti, F. Balloux, G. van Driem, P. de Knijff, I. G. Romero, A. R. Jha, D. M. Behar, C. M. Bravi, C. Capelli, T. Hervig, A. Moreno-Estrada, O. L. Posukh, E. Balanovska, O. Balanovsky, S. Karachanak-Yankova, H. Sahakyan, D. Toncheva, L. Yepiskoposyan, C. Tyler-Smith, Y. Xue, M. S. Abdullah, A. Ruiz-Linares, C. M. Beall, A. Di Rienzo, C. Jeong, E. B. Starikovskaya, E. Metspalu, J. Parik, R. Villems, B. M. Henn, U. Hodoglugil, R. Mahley, A. Sajantila, G. Stamatoyannopoulos, J. T. S. Wee, R. Khusainova, E. Khusnutdinova, S. Litvinov, G. Ayodo, D. Comas, M. F. Hammer, T. Kivisild, W. Klitz, C. A. Winkler, D. Labuda, M. Bamshad, L. B. Jorde, S. A. Tishkoff, W. S. Watkins, M. Metspalu, S. Dryomov, R. Sukernik, L. Singh†, K. Thangaraj, S. Pääbo, J. Kelso, N. Patterson, D. Reich, The Simons Genome Diversity Project: 300 genomes from 142 diverse populations. *Nature*. **538**, 201–206 (2016).
183. A. Auton *et al.*, A global reference for human genetic variation. *Nature*. **526**, 68–74 (2015).
184. N. Patterson, A. L. Price, D. Reich, Population structure and eigenanalysis. *PLoS Genet*. **2**, e190 (2006).
185. F. M. T. A. Busing, E. Meijer, R. Van Der Leeden, Delete- m Jackknife for Unequal m. *Stat. Comput.* **9**, 3–8 (1999).
186. C. Gamba, E. R. Jones, M. D. Teasdale, R. L. McLaughlin, G. Gonzalez-Fortes, V. Mattiangeli, L. Domboróczki, I. Kővári, I. Pap, A. Anders, A. Whittle, J. Dani, P. Raczky, T. F. G. Higham, M. Hofreiter, D. G. Bradley, R. Pinhasi, Genome flux and stasis in a five millennium transect of European prehistory. *Nat. Commun.* **5**, 5257 (2014).
187. A. Olivieri, A. Achilli, M. Pala, V. Battaglia, S. Fornarino, N. Al-zahery, R. Scozzari, F. Cruciani, D. M. Behar, J. Dugoujon, C. Coudray, A. S. Santachiara-benerecetti, O. Semino, H. Bandelt, V. Battag, The mtDNA Early Upper Legacy Palaeolithic of the Levantine in Africa. *Science*. **314**, 1767–1770 (2006).
188. B. Trombetta, E. D’Atanasio, A. Massaia, M. Ippoliti, A. Coppa, F. Candilio, V. Coia, G. Russo, J. M. Dugoujon, P. Moral, N. Akar, D. Sellitto, G. Valesini, A. Novelletto, R. Scozzari, F. Cruciani, Phylogeographic refinement and large scale genotyping of human Y chromosome haplogroup E provide new insights into the dispersal of early Pastoralists in the African continent. *Genome Biol. Evol.* **7**, 1940–1950 (2015).
189. C. Posth, G. Renaud, A. Mittnik, D. G. Drucker, H. Rougier, C. Cupillard, F. Valentin, C. Thevenet, A. Furtwängler, C. Wißing, M. Francken, M. Malina, M. Bolus, M. Lari, E. Gigli, G. Capecchi, I. Crevecoeur, C. Beauval, D. Flas, M. Germonpré, J. Van Der Plicht, R. Cottiaux, B. Gély, A. Ronchitelli, K. Wehrberger, D. Grigorescu, J. Svoboda, P. Semal, D. Caramelli, H. Bocherens, K. Harvati, N. J. Conard, W. Haak, A. Powell, J. Krause, Pleistocene mitochondrial genomes suggest a single major dispersal of non-africans and a late glacial population turnover in Europe. *Curr. Biol.* **26**, 827–833 (2016).

## Acknowledgements

We thank I. Mathieson, M. Lipson, I. Lazaridis, J. Sedig and K. Sirak for discussions, and M. E. Allentoft, K.-G. Sjögren, K. Kristiansen and E. Willerslev for facilitating sample collection. We thank M. Meyer for sharing the optimized oligo sequences for single-stranded library preparation. We thank the different museums for permission to study archaeological remains.

**Funding:** J.M.F., F.J.L.-C., J.I.M., X.O., J.D. and M.S.B. were supported by HAR2017-86509-P, HAR2017-87695-P and SGR2017-11 from the Generalitat de Catalunya, AGAUR agency. C.L.-F. was supported by Obra Social La Caixa and by FEDER-MINECO (BFU2015- 64699-P). C.L., P.R. and C.Bl. were supported by FEDER-MINECO (HAR2016-77600-P). D.J.K. and B.J.C. were supported by NSF BCS-1460367. K.T.L., A.W. and J.M. were supported by NSF BCS-1153568. We acknowledge support from the Portuguese foundation for science and technology (PTDC/EPH-ARQ/4164/2014) and the FEDER-COMPETE 2020 project 016899. P.S. was supported by the FCT Investigator Program (IF/01641/2013), FCT IP and ERDF (COMPETE2020 – POCI). M.S. and K.D. were supported by a Leverhulme Trust Doctoral Scholarship award. D.R. was supported by an Allen Discovery Center grant from the Paul Allen Foundation, NIH grant GM100233, and the Howard Hughes Medical Institute.

**Authors contributions:** N.R., N.A., N.B., O.C., B.J.C. D.F., A.M.L., M.M., J.O., K.S., Z.Z., M.Si., K.D., C.J.E., D.J.K. M.B.R., W.H., R.P. and D.R. performed or supervised laboratory work. J.M.J.A., I.J.T.M., D.C.S.G., P.C., M.Sa., J.T., M.L., J.F.-E., J.A.M.-A., C.Ba., F.J.B., J.B., N.C., E.V.M., D.V., A.C., J.M.F., O.G.-P., J.I.M., F.X.O., J.M.V., A.D.-C., I.O.-C., P.G.B., A.M.S., C.A.-F., J.J.E., A.M.-M., P.R.-G., J.R.M., E.V.V., K.T.L., J.M., A.W., G.D., B.A., F.C., A.Esp., G.d.P., A.Est., C.F., G.F., S.F., F.G.-G., T.M., A.R., J.V.-V., G.A.A., V.B.G., L.B.d.L.E., M.B.S., G.G.A., M.S.H.P., A.L., Y.C.M., I.C.B., A.F.F., D.L.-S., M.S.T., A.C.V., C.Bl., J.D., M.J.D.P.M., A.A.D.-C., R.F.F., J.F.F., R.G.-P., V.S.G., E.G.-D., A.M.H.-C., J.J.-C., C.L., F.J.L.-C., D.L.-R., S.B.M., M.M.P., A.O.F., G.P.B., P.R., M.S.B., A.C.S., J.M.V.E., M.Si., M.B.R., K.W.A., W.H., R.P., C.L.-F. and D.R. assembled archaeological material. I.O., S.M., N.P., M.F.B., V.V.-M., M.Si., C.J.E., F.G., M.P., P.S. and D.R. analyzed data. I.O., C.L.-F. and D.R. wrote the manuscript.

**Competing interests:** The authors declare no competing interests.

**Data and materials availability:** Sequencing data are available from the European Nucleotide Archive, accession PRJEB30874; genotype dataset is available as supplementary material.

## Supplementary Materials

Supplementary Text  
Table S1 – S22  
Fig S1 – S11  
Genotype dataset



# Supplementary Materials for

## The genomic history of the Iberian Peninsula over the past 8000 years

Iñigo Olalde, Swapan Mallick, Nick Patterson, Nadin Rohland, Vanessa Villalba-Mouco, Marina Silva, Katharina Dulias, Ceiridwen J. Edwards, Francesca Gandini, Maria Pala, Pedro Soares, Manuel Ferrando-Bernal, Nicole Adamski, Nasreen Broomandkhoshbacht, Olivia Cheronet, Brendan J. Culleton, Daniel Fernandes, Ann Marie Lawson, Matthew Mah, Jonas Oppenheimer, Kristin Stewardson, Zhao Zhang, Juan Manuel Jiménez Arenas, Isidro Jorge Toro Moyano, Domingo C. Salazar-García, Pere Castanyer, Marta Santos, Joaquim Tremoleda, Marina Lozano, Pablo García Borja, Javier Fernández-Eraso, José Antonio Mujika-Alustiza, Cecilio Barroso, Francisco J. Bermúdez, Enrique Viguera Mínguez, Josep Burch, Neus Coromina, David Vivó, Artur Cebrià, Josep Maria Fullola, Oretó García-Puchol, Juan Ignacio Morales, F. Xavier Oms, Tona Majó, Josep Maria Vergès, Antònia Díaz-Carvajal, Imma Ollich-Castanyer, F. Javier López-Cachero, Ana Maria Silva, Carmen Alonso-Fernández, Germán Delibes de Castro, Javier Jiménez Echevarría, Adolfo Moreno-Márquez, Guillermo Pascual Berlanga, Pablo Ramos-García, José Ramos Muñoz, Eduardo Vijande Vila, Gustau Aguilera Arzo, Angel Esparza Arroyo, Katina T. Lillios, Jennifer Mack, Javier Velasco-Vázquez, Anna Waterman, Luis Benítez de Lugo Enrich, María Benito Sánchez, Bibiana Agustí, Ferran Codina, Gabriel de Prado, Almudena Estalrich, Álvaro Fernández Flores, Clive Finlayson, Geraldine Finlayson, Stewart Finlayson, Francisco Giles-Guzmán, Antonio Rosas, Virginia Barciela González, Gabriel García Atiénzar, Mauro S. Hernández Pérez, Armando Llanos, Yolanda Carrión Marco, Isabel Collado Beneyto, David López-Serrano, Mario Sanz Tormo, António C. Valera, Concepción Blasco, Corina Liesau, Patricia Ríos, Joan Daura, María Jesús de Pedro Michó, Agustín A. Díez-Castillo, Raúl Flores Fernández, Joan Francès Farré, Rafael Garrido-Pena, Victor S. Gonçalves, Elisa Guerra-Doce, Ana Mercedes Herrero-Corral, Joaquim Juan-Cabanilles, Daniel López-Reyes, Sarah B. McClure, Marta Merino Pérez, Arturo Oliver Foix, Montserrat Sanz Borràs, Ana Catarina Sousa, Julio Manuel Vidal Encinas, Douglas J. Kennett, Martin B. Richards, Kurt Werner Alt, Wolfgang Haak, Ron Pinhasi, Carles Lalueza-Fox, David Reich

### **This PDF file includes:**

Supplementary Text  
Figs. S1 to S11  
Tables S6 to S22  
Caption for Tables S1, S2, S3, S4 and S5

### **Other Supplementary Material for this manuscript includes the following:**

Tables S1, S2, S3, S4 and S5 as excel files  
Genotype dataset

## Table of Contents

SI 1 -	Archaeological context of newly reported individuals.....	3
SI 2 -	Direct AMS <sup>14</sup> C Bone Dates.....	56
SI 3 -	Ancient DNA laboratory work .....	57
SI 4 -	Bioinformatics processing .....	58
SI 5 -	Mitochondrial and Y-chromosome haplogroup determination .....	58
SI 6 -	Kinship analysis.....	59
SI 7 -	Genome-wide analysis datasets .....	60
SI 8 -	Principal component analysis .....	61
SI 9 -	<i>f</i> -statistics.....	61
SI 10 -	Estimation of $F_{ST}$ coefficients .....	61
SI 11 -	<i>qpAdm</i> admixture modeling.....	61
SI 12 -	Allele frequency estimation of SNPs of phenotypic importance .....	72
SI 13 -	Date of the Carigüela pre-Neolithic individual .....	73

## SI 1 - Archaeological context of newly reported individuals

In this section we specify dates in one of two formats. If there is no direct radiocarbon date on the individual analyzed with aDNA, we give a date based on the archaeological context or on the genetic results, in a format like “2500–1700 BCE”. Alternatively, if there is a direct radiocarbon date on the bone being analyzed, we give a date in a format like “95.4% CI calibrated radiocarbon age (Conventional Radiocarbon Age, Lab number)” (an example is “365–204 cal BCE (2215±20 BP, PSUAMS-3466)”). All the dates were calibrated in OxCal 4.2.3 (27) using the IntCal13 calibration curve (28).

We thank the Dirección General de Bienes Culturales y Museos de la Consejería de Cultura de la Junta de Andalucía for authorizing the study of the samples held at the Museo Arqueológico y Etnológico de Granada. We thank the Museo de Arqueología de Alava, the Centro de Patrimonio Cultural Mueble GORDAILUA (Irun, Gipuzkoa), the Gobierno Vasco, the Direcció General de Cultura de la Generalitat Valenciana, the Ajuntament de València, the Ajuntament de Bocairent, the Ajuntament de la Font de la Figuera, the Museu de Prehistòria de València, the Museu de Castelló, the Museu de la Valltorta and the Museu d'Alcoi for granting permission to study archaeological remains

### Bray Cave (Gibraltar)

*Contact: Clive Finlayson, Francisco Giles, Geraldine Finlayson, Stewart Finlayson*

Bray's Cave is located about 330 m. a.s.l. on the western slope of the Rock. The cave formed along the bedding planes of the limestone layers which lie in a north-south orientation dipping to the west, and contains a number of types of speleothem formations, typical of closed cavities with gallery morphology. The current appearance of the cave, before the commencement of the first excavations (29), was caused by the regression of the hillside that led to the opening and collapse of its western wall, with subsequent sealing processes from hillside deposits.

A level associated with funerary use of the cave has been attributed to the Bronze Age. It is located in an area of gours (rimstone), soils, and walls of the cavity, forming an organized and hierarchical funerary space, with two separate burial areas (Burials 1 and 2). The fact that certain speleothems show signs of having continued in their development, as well as the stratigraphic position of the collapse of the walls of the cavity, indicate a closed cave environment, which would have only had a small entrance at the time of the burials. Both burials show anthropic adaptations of the karstic formations to

shape the tombs, and areas of re-interment of the bone remains. The latter are the product of the removal of soil and the reuse of the burial sites. Two dates have been obtained for these burials: 1664–1459 cal BCE (3290±40 BP, Beta-181890) (carbon) and 1900–1691 cal BCE (3480±40 BP, Beta-181891) (bone) (30, 31). We analyzed 3 individuals from this site:

- I10939/119: 1900–1400 BCE
- I10940/121: 1900–1400 BCE
- I10941/120: 1900–1400 BCE

## **Europa 1 (Gibraltar)**

*Contact: Clive Finlayson, Francisco Giles, Geraldine Finlayson, Stewart Finlayson*

The cave known as Europa 1 is located at the southernmost tip of Gibraltar, in the area known as Deadman's Beach. The cave formed along a fault gap in the limestone of the Rock, and its entrance is currently at approximately 5 m a.s.l., on the cliff below the marine platform known as Europa Point (15 -17 m a.s.l.), where there is a series of cavities located between 11 and 8.5 m a.s.l. which are all that remain after the erosion of a larger cave, and most are filled with marine conglomerate with remains of fauna and algal formations. Below these caves, filling a vertical karst channel, a marine conglomerate with fauna is located at 5.25 m a.s.l., and has been dated at  $92.5 \pm 1.5$  Ka. It is covered by a parietal, vadose zone and polycyclic stalagmite crust, which has been dated at 76 Ka at its base, and 41 Ka at its top. Above the marine deposit, and interspersed between the different stages of stalagmitic formation, there are karstic gaps with a reddish clay matrix, in which an erosive phase that affects both these materials and the marine ones can be observed. On top of this, new stalagmite growth is interspersed with karstic materials with a reddish clay matrix. Below the cave, there is a platform created by marine erosion at + 3 m a.s.l. and an undercut at + 1 m a.s.l. These stalagmitic crusts correspond to vadose speleothems which must have been formed inside a cave, showing that the deposits were formed inside a small cavity, elements of which are conserved in their innermost part (32).

Although no remains of these deposits are found in Europa 1, and given that they may remain below the archaeological levels, at +5 m a.s.l., evidence of borings by *Lithophaga* inside the cave, indicates that the sea level reached that height, and clearly related to the external marine deposit. The archaeological sediments are not sealed by any stalagmite

crust, with which it can be inferred that there were some major erosive conditions that formed this marine cave by breaking into an existing prehistoric karst system, which has subsequently been filled by archaeological deposits after 40 Ka.

The mouth of the cave had been blocked by 19th century masonry work until its discovery in 1996. After entering through a 1.40 m passageway, a small antechamber is accessed that extends across the general direction of the cave, and which via a narrow passage, opens into a small chamber which is filled almost entirely by marine deposits and a sedimentary accumulation containing archaeological and faunal remains that, due to its inclination, seems to originate from outside. The size of the cave precludes its use as a place of habitation.

Level 5 of the cave contained Black earth with limestone clasts, fauna (rabbit, deer, carnivores, birds, etc.), handmade ceramics (Neolithic), human bones (metatarsals, skull, phalanges) and lithic pieces of flint and jasper (33).

We analyzed one individual from this site:

- I10942/122: 5500–4500 BCE

### **Cabezo Redondo (Villena, Alacant/Alicante, Valencian Community, Spain)**

*Contact: Gabriel García Atienzar, Mauro Hernández, Virginia Barciela González, Domingo C. Salazar-García*

Cabezo Redondo is located about 2 km away from the town center of Villena on a circular hill whose summit is about 40 m above the surrounding land and 579 m a.s.l.. It is located in the center of the so-called "Villena basin", in which several natural corridors converge and connect the Mediterranean coast with the interior of the Iberian Peninsula and the highlands of Andalusia and Murcia with the interior of the Valencian region.

In 1949 J. M<sup>a</sup> Soler began excavations at Cabezo Redondo. These were interrupted by the exploitation of the hill for gypsum quarries. In 1987, the excavations at Cabezo Redondo were resumed, with field work on the western side (34).

This site has yielded 50 radiocarbon dates from domestic and funeral contexts. These dates and stratigraphic relationships define two moments of occupation. The first one is located at the top of the hill, where the first occupations date back to around 2100 BCE. This phase must have lasted until 1700 BCE, when this sector of the settlement was reorganized.

In a second phase, the region of habitation expanded to include the western slope. During this period (1700–1300 BCE; Late Bronze Age) an important architecture was developed on this slope; domestic structures built with mud. It also stands out for its urban complexity, which makes Cabezo Redondo one of the most important settlements in the east of the Iberian Peninsula. At this time, the funerary material was located under the floor of some houses, but also inside many of the cracks and small cavities of the hill. These burials follow different rituals and present different grave goods, always rare.

Among the archaeological materials associated with funerary and domestic contexts, there are gold objects, glass ornaments, ivory and bronze objects, and decorated ceramic vessels. These pieces connect the inhabitants of the village with the inhabitants of the Iberian Plateau, the Mediterranean and the European commercial circuits. The abandonment of the village must have taken place during the 13th century BCE, before the beginning of the Final Bronze Age.

A preliminary review of the human remains of the Cabezo Redondo shows the different conservation of the remains according to the burial space. The burials deposited in *pithos*, cists, and individual graves show a good state of conservation, while those found in caves are more disturbed. Demographically, at least 61 individuals are identified, with children being the best represented age range at the site. The number of juveniles is low, as is the number of adults, with a predominance of those who died between 30 and 39 years old. The abundance of children is interpreted as evidence of a high birth rate and a higher number of deaths in the early stages of life.

The identification of evidence of disease or injury to teeth and bones is skewed by partial bone preservation. Among the children remains there are some teeth with enamel hypoplasia. There are also some cases of orbital sieve related to anemia of different origin. In the adult population, there are signs that indicate intense physical activity in the arms and legs, typical of a population dedicated to cultivating the land and caring for animals. The microscopic dental analysis of Cabezo Redondo shows that the density of micro-striae is low. There are no differences between children or adults, indicating a similar consumption of food types. These data correspond to a type of diet with an important meat component and with refined cereal processing to obtain flour. Evidence of the use of teething for non-food activities is noteworthy. The presence of grooves in the anterior teeth of some individuals shows one of the few documented cases during recent prehistory related to textile activities (35).

The evidence related to social prestige in Cabezo Redondo is abundant and appears to be associated with habitation areas and funerary deposits. Interestingly, the presence of ornamental objects in only a few burials of adult individuals and, in particular, of a few children, reveals social differences between the inhabitants of the village and the hereditary nature of some privileges. Some ornaments are exceptional beyond their raw material. The gold and silver truncated cones, as well as the ivory combs and glass beads, reveals connections with the El Argar culture. We analyzed three individuals from this site:

- I3486/S-EVA 26078: 1700–1500 BCE [based on other dates in the second phase of occupation]
- I3488/S-EVA 22926: 1700–1500 BCE [based on other dates in the second phase of occupation]
- I3487/S-EVA 26688: 1734–1617 cal BCE (3365±20 BP, PSUAMS-2161)

### **Les Llometes (Alcoi, Alacant/Alicante, Valencian Community, Spain)**

*Contact: Domingo C. Salazar-García, Oreto García-Puchol*

Les Llometes includes two cavities, a cave and a crevice, situated within 15m of each other, and is located within the municipality of Alcoi, at the exit of the Barranc del Cinc ravine environment, towards the southeast of the Mariola Mountains in the province of Alacant/Alicante. A radiocarbon dataset has been recently produced on most of the skulls available to date, confirming a tight chronology of use of this site as a burial ground during the Late Neolithic and comprising the earliest evidence of cave collective burials in Eastern Iberia (36).

Les Llometes Cave has a stratigraphical sequence spanning at least two levels, reaching 1.8 m in depth from the surface. The first level included six skeletons (placed in prone position) and grave goods consisting mainly of pottery and metal weapons. The second level revealed 18 skeletons, positioned laterally and containing various remains including pottery, polished stone tools, large flint blades and flint arrowheads, as well as ornaments, although no metal artifacts were recorded (37). Most of the skeletal remains and grave goods recovered from Les Llometes Cave were dispersed among various private collections and later lost. However, five skulls were stored in the Archaeological Museum of Alcoi and the National Archaeological Museum of Madrid.

221 Les Llometes Crevice was narrow and difficult to access. The orientation of the human  
222 remains found in Les Llometes Crevice was not recorded, and the archaeologist described  
223 them as being completely commingled and desarticulated (37).

224 We analyzed three individuals from the cave:

- 225 • I7647/LL9: 4050–3340 cal BCE (5180±24 BP, MAMS-16335)
- 226 • I7601/LL10: 3660–3520 cal BCE (4810±22 BP, MAMS-16354)
- 227 • I7642/LL27: 2907–2761 cal BCE (4240±23 BP, MAMS-16338)

228 We analyzed nine individuals from the crevice:

- 229 • I7645/LL5: 3990–3550 cal BCE (5120±25 BP, MAMS-16340)
- 230 • I7646/LL7: 3710–3630 cal BCE (4880±28 BP, MAMS-16339)
- 231 • I7643/LL3: 3960–3710 cal BCE (5040±33 BP, MAMS-16344)
- 232 • I7600/LL12: 4100–2700 BCE [based on other dates in the same context]
- 233 • I7644/LL4: 3640–3380 cal BCE (4760±22 BP, MAMS-16353)
- 234 • I7594/LL2: 3519–3370 cal BCE (4670±22 BP, MAMS-16356)
- 235 • I7595/LL11: 3519–3370 cal BCE (4670±23 BP, MAMS-16332)
- 236 • I7597/LL24: 4100–2700 BCE [based on other dates in the same context]
- 237 • I7598/LL25: 3630–3370 cal BCE (4710±22 BP, MAMS-16346)

## 238 **Alto de la Huesera (Laguardia, Araba/Álava, Basque Country, Spain)**

239 *Contact: Javier Fernández-Eraso, José Antonio Mujika-Alustiza*

240 This site was described in Lipson et al. 2017 (13). We analyzed three new individuals:

- 241 • I1845/LHUE-Pet1, LHUE-2010, CUADRO KII, Sector 7, L-IV.: 3014–2877 BCE  
242 [3011–2877 cal BCE (4290±30 BP, Beta-301226), 3014–2891 cal BCE (4320±30 BP,  
243 Beta-301223), 3010–2970 cal BCE (4350±30 BP, Beta-301222)]
- 244 • I1846/LHUE-Pet3: LHUE-2010, CUADRO K12, Lecho 5: 3014–2877 BCE [3011–  
245 2877 cal BCE (4290±30 BP, Beta-301226), 3014–2891 cal BCE (4320±30 BP, Beta-  
246 301223), 3010–2970 cal BCE (4350±30 BP, Beta-301222)]



247 • I1978/LHUE-Pet2: LHUE-2010, CUADRO K10, Sector 5: 3014–2877 BCE [3011–  
248 2877 cal BCE (4290±30 BP, Beta-301226), 3014–2891 cal BCE (4320±30 BP, Beta-  
249 301223), 3010–2970 cal BCE (4350±30 BP, Beta-301222)]

250 **El Sotillo (Laguardia, Araba/Álava, Basque Country, Spain)**

251 *Contact: Javier Fernández-Eraso, José Antonio Mujika-Alustiza*

252 This site was described in Lipson et al. 2017 (13). It is a megalithic tomb used during the  
253 Late Chalcolithic, and after a hiatus of about 500 years it was reused during the Middle-  
254 Late Bronze Age. We analyzed six new individuals from the Bronze Age phase of the  
255 site:

- 256 • I2469/ES.2/4-3: 910–840 cal BCE (2740±30 BP, Beta-299308)
- 257 • I2471/ES.3/4-2: 1630–1497 cal BCE (3280±30 BP, Beta-299311)
- 258 • I1977/ES.2/4-4: 1660–1454 cal BCE (3260±30 BP, Beta-299312)
- 259 • I2472/ES.3/4-4: 1605–1425 cal BCE (3220±30 BP, Beta-299309)
- 260 • I2470/ES.3/4-1: 1411–1231 cal BCE (3060±30 BP, Beta-299307)
- 261 • I1840/ES.2/4-1: 1660–1454 cal BCE (3260±30 BP, Beta-299302)

262 **La Hoya (Laguardia, Araba/Álava, Basque Country, Spain)**

263 *Contact: Armando Llanos*

264 This site was described in Nuñez et al. 2016 (38). We analyzed three adult individuals  
265 from the Celtiberian period of the site.

- 266 • I3757/LHY 142-T: 400–300 BCE
- 267 • I3759/LHY073: 361–195 cal BCE (2195±25 BP, PSUAMS-2078)
- 268 • I3758/LHY136: 365–204 cal BCE (2215±20 BP, PSUAMS-3466)

269 **Las Yurdinas II (Peñacerrada-Urizaharra, Araba/Álava, Basque Country, Spain)**

270 *Contact: Javier Fernández-Eraso, José Antonio Mujika-Alustiza*

271 This site was described in Lipson et al. 2017 (13). We analyzed one new individual:

272 • I1842/LY.II.A.10.15064: 3350–2750 BCE [3022–2779 cal BCE (4290±40 BP, Beta-  
273 137895), 3090–2900 cal BCE (4360±40 BP, Beta-137896), 3310–2904 cal BCE  
274 (4390±40 BP, Beta-148054) three dates of the whole stratigraphy of the site]

275 **Cueva de la Paloma (Soto de las Regueras, Asturias, Spain)**

276 *Contact: Almudena Estalrrich, Antonio Rosas*

277 The cave site is situated approximately 16 km from the coastline and 12 km from Oviedo,  
278 the capital of the Asturias region. During the earliest Holocene, the northern Spanish  
279 coastline was situated around 6 km offshore (39).

280 The cave was discovered in 1912, and excavated between 1914 and 1915 by Eduardo  
281 Hernández Pacheco (40). The stratigraphic units of the cave contain archaeological  
282 materials, and the study of the lithic and bone artifacts classified the samples of La Paloma  
283 as belonging to the Magdalenian and Azilian cultures (40–42).

284 More than 5800 mammal bone remains have been recovered, with *Cervus elaphus* as the  
285 most dominant taxa (43, 44). Other species present included *Rupicapra rupicapra*,  
286 *Capreolus capreolus*, *Equus ferrus*, *Sus scrofa*, *Canis lupus*, *Panthera cf. leo*, *Vulpes*  
287 *vulpes*, and *Ursus arctos* (44, 45).

288 Bone samples from 4 adult right tibias are analyzed in this study, out of the 91  
289 anatomically modern human remains originally recovered at the site. The new dating of  
290 the analyzed human remains, however, does not correspond to an Azilian archeological  
291 and chronological context as originally published (40–42, 46), but instead to a Late  
292 Neolithic-Chalcolithic chronology. In fact, it was already noted that the superficial levels  
293 of the site were removed by looters (40), mixing the sediments and altering the  
294 stratigraphic units.

295 The analyzed individuals are:

- 296 • I3214/TDPAD-01: 3400–3100 BCE
- 297 • I3243/TDPAD-03: 2500–2200 BCE
- 298 • I3239/TDPAD-02: 2500–2200 BCE
- 299 • I3238/TDPAD-04: 2500–2200 BCE

300 **Cova de la Guineu (Font-rubí, Barcelona, Catalonia, Spain)**

301 *Contact: Marina Lozano, Artur Cebrià, Juan Ignacio Morales, Xavier Oms, Josep Maria*  
302 *Fullola*

303 The Cova de la Guineu site is in Font-Rubí (Barcelona, NE Iberian Peninsula), c. 730m  
304 amsl, excavated since the 1980's by the SERP group of the University of Barcelona (47,  
305 48). In this site, a long sequence covering the Late Upper Pleistocene and the Holocene  
306 has been uncovered, providing data on occupations from the Upper Paleolithic to the Late  
307 Bronze Age populations. In the Late Neolithic-Chalcolithic, the cave was used as an  
308 individual and successive burial place (47, 48). According to the dental data, a minimum  
309 number of 70 individuals of different age, including perinatal, subadults and adult  
310 individuals, were identified from a commingled funerary context. Some scarce grave-  
311 goods has been recovered (Bell-Beaker and plain vessels, lithics and shell-beads). Three  
312 dates on human bones are available for the Late Neolithic-Chalcolithic occupation: 2871–  
313 2505 cal BCE (4110±38 BP, OxA-16881); 3091–2916 cal BCE (4385±32 BP, OxA-  
314 16966); 3353–3099 cal BCE (4513±30 BP, OxA-29636).

315 We analyzed 13 individuals from this site:

- 316 • I10277/GN.08.Data:27/4; Nivell:Rx.Q:F3.n3: 3400–2500 BCE
- 317 • I10278/GN.88.E3.32: 3400–2500 BCE
- 318 • I10280/GN.89.E2.379a: 3400–2500 BCE
- 319 • I10282/GN.90.Remenat.General.n.5: 3400–2500 BCE
- 320 • I10283/Guineu.08.RemenatF3-4: 3400–2500 BCE
- 321 • I10284/Guineu.82.5.: 3400–2500 BCE
- 322 • I10285/Guineu.88.Rem.Cala123a: 3400–2500 BCE
- 323 • I10286/Guineu.89.Rem.Ext.3611a: 3400–2500 BCE
- 324 • I10287/Guineu.90.Rem.Ext.4001/Guineu.M.56.: 3400–2500 BCE
- 325 • I11303/Guineu.90.Rem.Ext.4002: 3400–2500 BCE
- 326 • I11304/Guineu.94.C5.125: 3400–2500 BCE
- 327 • I11305/Guineu.95.B7.424.: 3400–2500 BCE

328 • I11306/Guineu.95.Rem.Ext.4000: 3400–2500 BCE

329 **Turó de Ca n'Oliver (Cerdanyola, Barcelona, Catalonia, Spain)**

330 *Contact: Joan Francès Farré*

331 The Iberian settlement of Turó de Ca n'Oliver is located on the mountain ranges of the  
332 Collserola's slope in Cerdanyola del Vallès. Excavations in 2017 revealed the urban  
333 evolution and the chronology of the settlement on the hill, believed to have occupied 2  
334 hectares. Settlement evolution can be summarized as spanning 4 phases:

335 The first occupation of the hill (phase 0) is represented by a previous initial phase to the  
336 urban one formed by an aggrupation of huts situated on the natural rock, for which only  
337 some rock cut-outs and stick holes are preserved. Generally, the patterns of the post-holes  
338 suggest rectangular or subrectangular constructions without specific typology. Because  
339 of the lack of associated materials clearly differentiated from Phase 1, it is very difficult  
340 to date them. Despite this, Phase 0 can roughly be dated to the last quarter of 6th century  
341 BCE.

342 The first main urban phase of the settlement (Phase 1) is dated to between the last quarter  
343 of 6th century BCE and middle 5th century BCE, in an unequivocally Iberian cultural  
344 context. This phase is characterized by ceramics painted with bands and circle motifs,  
345 and reduced firing ceramics characterized by indigenous forms and other Mediterranean  
346 influence, along with handmade artifacts of an early Iberian culture attribution. The layout  
347 was characterized by techniques of the early Iberian period, with houses built into deep  
348 rock cut-outs, rectangular houses, modest dimensions and a great simplicity  
349 compartmentalized with walls made of stone sockets and adobe.

350 In the middle of the 5th century BCE the settlement was widely reformed and experienced  
351 a radical change in the conception of the habitation space (Phase 2). In this period the  
352 ancient cutout in the natural rock occupied by the chambers of the previous phase was  
353 filled. The filling of the cut allowed for larger houses that rested on a prominent wall that  
354 enclosed the village. The first human skull remains were found under this wall connected  
355 with horse remains in what seems like a ritual offering.

356 During Phase 3, dated to between the end of 4th century BCE or early 3rd century BCE  
357 and the end of the 3rd century BCE, new reformations of the town took place. Those  
358 changes must be related to the consolidation of the settlement as the main center of an  
359 extensive territory and with an important storage capacity as evidenced by new field of

silos. Ca n'Oliver was refortified with the construction of new accesses and possibly with a set of outer defences as reflected in excavated sections of the settlement moat. A fundamental element of this town is the silos field. It extends from the west side of the south gate to south, although only a small portion has been excavated. These are deposits of considerable volume and about three meters deep, which in some cases can reach 5.25 meters (ST-738). As regards the chronology, the oldest deposit must be dated to the end of the 4th century or the beginning of the 3rd century BCE and the date of abandonment of the silos field to 50 BCE. The structures appear on each side of the pit although they are more abundant outside its limits. Several of these moats contained human remains (skulls, mandibles) that must be linked to the so-called "cult of the skull" documented at this time in the Celtic world as well as in the Iberian.

We analyzed one individual from Phase 3 of the site:

- I3496/MC-1573: 300–200 BCE

A last phase, already reflecting Roman influence (Phase 4), dated from the first decades of the 2nd century BCE, and was characterized by a new urban reorganization affected by the events of the Second Punic War. This includes the construction of a new wall that did not exactly follow the layout of the previous one, and the expansion and continuity of the silos field as well as the construction of new houses, now extending beyond the perimeter of the settlement. The settlement was abandoned definitively around 50 BCE.

### **Mas d'en Boixos-1 (Pacs del Penedès, Barcelona, Catalonia, Spain)**

*Contact: Tona Majó, F. Javier López-Cachero*

Mas d'en Boixos is a site located in the Catalan Prelitoral depression in the Penedès region (Barcelona). Several excavation seasons have been undertaken since 1997 with more than 450 structures uncovered, most of them storage silos. There are stratigraphic layers ranging from the Early Neolithic until modern times with an especially intense occupation period during the Early Iron Age. The human remains retrieved from that period are scarce -two sub-adults, two adults and one infantile- although they are quite exceptional due to the fact they are inhumation burials. In addition, there are cremation remains belonging to one additional adult individual in a nearby silo structure. We analyzed three individuals from this site, two from structure E-448 and one from structure E-449:

- I12410/MB1 '08 E-448 Ind 1: 515–375 cal BCE (2350±30 BP, Beta-495153)
- I12877/MB1 '08 E-448 Ind 2: 515–375 BCE

- 392 • I12878/MB1 '08 E-449 Ind 1: 507–366 cal BCE (2340±30 BP, Beta-495155)
- 393 **Hort d'en Grimau (Castellví de la Marca, Barcelona, Catalonia, Spain)**
- 394 *Contact: Tona Majó, F. Javier López-Cachero*
- 395 Hort d'en Grimau site is located in the Alt Penedés region (Barcelona). During the 1980s,  
 396 different archaeological structures were excavated, most of them dated from the Middle  
 397 Neolithic. Only two features date from the Early Iron Age: a hut floor and a storage silo  
 398 containing the partially cremated remains of an adult woman and a complete male horse  
 399 skeleton, still in anatomical connection. The finding of the horse is exceptional in the  
 400 Iberian context during this period. We analyzed a tooth from the adult woman:
- 401 • I12879/HG-E10: 728–397 cal BCE (2390±30 BP, Beta-495156)
- 402 **Can Roqueta-Can Revella and Can Roqueta II (Sabadell, Barcelona, Catalonia,**  
 403 **Spain)**
- 404 *Contact: Tona Majó, F. Javier López-Cachero*
- 405 Can Roqueta is an excavation area within a large archaeological complex that covers 2.5  
 406 km<sup>2</sup> outside the town of Sabadell, 30 km away from Barcelona. This settlement area  
 407 occupied from the Neolithic to the Middle Ages presents structures of different functions  
 408 and typologies.
- 409 In the sector Can Roqueta II, The Early Bronze Age structures are dated between 2300–  
 410 1300 cal BCE, with several radiocarbon dates pointing to the primary occupational  
 411 period, between 2153–1734 cal BCE and 1638–1435 cal BCE (49, 50). Archaeological  
 412 work between 1999 and 2000 documented 121 graves in a landscape of 11 hectares. The  
 413 site was occupied by farming groups that used a sophisticated bronze technology; there  
 414 is evidence of crucibles, metal casts and cooper smelting. The pottery is diverse, with  
 415 Epi-Bell Beaker traits. There are numerous funerary structures that were sometimes re-  
 416 used with several, successive burials, sometimes accompanied by dog skeletons. There  
 417 are also functionally complex, semi-excavated structures where human bones have been  
 418 found in fillings as well as in places deliberately designed as graves (51, 52).
- 419 We analyzed four individuals from the Bronze Age period of the Can Roqueta II sector:
- 420 • I1311/E-498; N°617: 2000–1400 BCE [1930–1634 cal BCE (3465±60 BP, UBAR-  
 421 697), 1867–1526 cal BCE (3370±50 BP, UBAR-670), 1736–1453 cal BCE (3305±55 BP,

422 UBAR-671), 1877–1526 cal BCE (3380±60 BP, UBAR-672), four dates of the whole  
423 stratigraphy of the site]

424 • I1312\_d/E-459\_No6: 2000–1400 BCE [1930–1634 cal BCE (3465±60 BP, UBAR-  
425 697), 1867–1526 cal BCE (3370±50 BP, UBAR-670), 1736–1453 cal BCE (3305±55 BP,  
426 UBAR-671), 1877–1526 cal BCE (3380±60 BP, UBAR-672), four dates of the whole  
427 stratigraphy of the site]

428 • I1313\_d/E-459\_No147: 2000–1400 BCE [1930–1634 cal BCE (3465±60 BP, UBAR-  
429 697), 1867–1526 cal BCE (3370±50 BP, UBAR-670), 1736–1453 cal BCE (3305±55 BP,  
430 UBAR-671), 1877–1526 cal BCE (3380±60 BP, UBAR-672), four dates of the whole  
431 stratigraphy of the site]

432 • I1310/E-459\_No148: 2000–1400 BCE [1930–1634 cal BCE (3465±60 BP, UBAR-  
433 697), 1867–1526 cal BCE (3370±50 BP, UBAR-670), 1736–1453 cal BCE (3305±55 BP,  
434 UBAR-671), 1877–1526 cal BCE (3380±60 BP, UBAR-672), four dates of the whole  
435 stratigraphy of the site]

436 In the sectors of Can Roqueta II and Can Revella we also sampled four Iron Age  
437 inhumations, contemporaneous to the nearby necropolis of Can Piteu-Can Roqueta with  
438 more than a thousand cremation burials (49). In this context, the Iron Age inhumations  
439 from Can Roqueta II and Can Revella represent exceptions to the dominant funerary rite.

440 Can Revella:

441 • I12640/CRCRV285-ADNUB50: 696–540 BCE (dating on Equus bones buried  
442 alongside the human skeleton)

443 • I12641/CRCRV110-ADNUB52: 791–540 cal BCE (2510±30 BP, Beta 449093)

444 Can Roqueta II:

445 • I12642/CRII-193-ADNUB54: 731–399 cal BCE (2400±30 BP, Beta 463858)

446 • I12643/CRII-107-ADNUB55: 758–429 cal BCE (2460±30 BP, Beta 449091)

#### 447 **Cova del Gegant (Sitges, Barcelona, Catalonia, Spain)**

448 *Contact: Joan Daura, Montserrat Sanz Borràs*

449 Cova del Gegant is a cave located in the northeast of the Iberian Peninsula, ~40 km south  
450 of Barcelona. It consists of a principal chamber (GP), now eroded by wave action, and its  
451 inner part (GP1 and GP2), where a small conduit (GLT) leads to the adjacent Cova Llargà.

Two galleries branch off of the right side of GP, one more interiorly (GL2) and another near to the sea (GL1). At least eight site formation episodes from the Upper Pleistocene (Episodes 0-3) to the Holocene (Episodes 4-7) have been recognized in the Cova del Gegant stratigraphic sequence, alternating between continental sediment deposition and periods of marine erosion followed by the accumulation of beach deposits (53). The first Holocene deposition in GP2 corresponds to layer XXV (Episode 4). This archaeological layer is ascribed to the Bronze Age and mainly corresponds to a collective burial radiocarbon dated to the Middle Bronze Age, 1600-1400 cal BCE. The funerary context that also yielded numerous fragments of Late Bell Beaker pottery, gold and amber ornaments and human remains (MNI=19). This layer has been dated on the basis of three human teeth yielding an age of 1622–1460 (3270±30 BP, Beta-312860), 1521–1417 (3200±30 BP; Beta-312861) and 1604–1430 (3225±27 BP; OxA-29612) (54). One human remain, corresponding to an isolated lower left permanent incisor (I<sub>1</sub>) from a Bronze Age individual was successfully analyzed for ancient DNA and radiocarbon dated:

- I1836/CG13-5135: 1682–1505 cal BCE (3310±35 BP, Poz-83482)

#### **Font de la Canya (Avinyonet del Penedés, Barcelona, Catalonia, Spain)**

*Contact: Marta Merino Pérez, Daniel López-Reyes*

The prehistoric site of Font de la Canya is an emblematic site for archaeological research in Catalonia. With a sequence of more than 15 years of consecutive archaeological campaigns (1999–2017), the volume of data is exceptional both in quality and quantity and represents an important contribution to the knowledge of the early Iron Age and of the Iberian culture

Font de la Canya was a trading center belonging to the Iron Age Iberian culture and located in the middle of the Penedés region. It was inhabited between the 7th-1st centuries BCE. The storage and distribution of cereals, extremely important for the agriculture and diet of the time, was the main economic activity at the site. This is demonstrated by the finding of hundreds of “silos” or cereal deposits, as well as several working spaces dedicated to the managing of cereals and other goods.

The rich archaeological materials recovered inform us about the economy of the Iberian culture and trading with other Mediterranean civilizations such as the Phoenicians, Greeks, Carthaginians and Romans. The exchanges highlight the cosmopolitan and commercial orientation of the people who lived at the site. For instance, archaeological



excavations have identified evidence of the earliest wine production in the territory during the 7th century BCE, associated with contacts with the Phoenicians.

We analyzed one individual from this site:

- I4556/TFC-16.SI.204.Ind 2 (tooth 31 + 32): 700–500 BCE

### **L'Esquerda (Roda de Ter, Barcelona, Catalonia, Spain)**

*Contact: Imma Ollich-Castanyer, Antònia Díaz-Carvajal*

L'Esquerda is an archaeological site located in a peninsula created by the river Ter in Roda de Ter. This location creates strategic features that explain the continuity of settlement from the end of the Bronze Age to the 14th century CE. From the oppidum of the Ausetani tribe to the Roda Civitas of the Visigoths and Carolingians, its walls demonstrate the importance of the site as a fortress that witnessed the establishment of different peoples (55).

With the establishment of the Carolingians at the end of the 8th century CE over the ruins of the old Iron Age Iberian fortress and making use of the Visigoth wall, an initial settlement was formed. It was consolidated during the 9th and 10th centuries CE around a church called Sant Pere de Roda. During the first half of the 11th century CE, a new church was built in the same location, whose remains can still be seen. A necropolis was created around the church with burials in three different levels. The lowest level was characterized by anthropomorphic tombs excavated in the rock and dated to the end of the 8th century CE and the beginning of the 10th century CE. We analyzed five individuals from this level:

- I7674/T-143: 785–801 CE [between conquest of Girona and conquest of Barcelona]
- I7672/T-120-1: 785–801 CE [between conquest of Girona and conquest of Barcelona]
- I7676/T-191: 785–801 CE [between conquest of Girona and conquest of Barcelona]
- I7675/T-194: 785–801 CE [between conquest of Girona and conquest of Barcelona]
- I7673/T-120-2: 785–801 CE [between conquest of Girona and conquest of Barcelona]

The second level was characterized by slab tombs corresponding to the 11th–13th centuries CE when the Romanic church was in use.

The third and more superficial level dated between the end of the 13th century CE to the end of the 14th century CE, with burials in a simple or complex pit (56).

515 Beside the already mentioned necropolis, a different burial place was found outside the  
516 wall, radiocarbon dated to the second half of the 7th century CE (57). A total of 13 simple  
517 pit and slab tombs have been identified, with male adults and male and female infants.  
518 We analyzed five individuals from this burial place:

- 519 • I3778/T-269: 600–700 CE
- 520 • I3776/T-267: 600–700 CE
- 521 • I3866/T-264: 600–700 CE
- 522 • I3775/T-266: 600–700 CE
- 523 • I3777/T-268: 600–700 CE

524 **El Hundido (Monasterio de Rodilla, Burgos, Castilla y León, Spain)**

525 *Contact: Javier Jiménez Echevarría, Carmen Alonso*

526 This site was described in Szécsényi-Nagy et al (58). We analyzed two individuals from  
527 this site:

- 528 • EHU001/UE 750: 2287–2044 cal BCE (3760±30 BP, Beta-492280)
- 529 • EHU002/UE 450: 2562–2306 cal BCE (3933±32 BP, CSIC-1896)

530 **El Cerro (La Horra, Burgos, Castilla y León, Spain)**

531 *Contact: Domingo C. Salazar-García, Ángel Esparza Arroyo, Javier Velasco Vázquez,*  
532 *Germán Delibes de Castro*

533 The site of El Cerro, like other “Campos de hoyos” of the archaeological culture Cogotas  
534 I (Central Iberian Meseta Middle-Late Bronze Age, ca. 1850–1150 cal BCE), presents  
535 some remains of some shacks as well as numerous dug structures filled with waste  
536 material (potsherds, animal bones, ashes) that were originally grain storage pits. A triple  
537 burial was excavated and contained three subadults, whose death must have resulted in  
538 the ritualized abandonment of the site (59–61).

539 We analyzed one individual from this site:

- 540 • I3490/S-EVA 9674: 1850–1150 BCE

541 **Virgazel (Tablada de Rudrón, Burgos, Castilla y León, Spain)**

542 *Contact: Germán Delibes de Castro, Elisa Guerra*

543 This site was described in Olalde et al. 2018 (9). We analyzed one new individual dated  
544 to the Bronze Age:

- 545 • I6470/RISE912: 1753–1549 cal BCE (3375±35 BP, Poz-49177)

546 **Valdescusa (Hervías, La Rioja, Spain)**

547 *Contact: Javier Jiménez Echevarría, Carmen Alonso*

548 This site was described in Szécsényi-Nagy et al (58). We analyzed five individuals from  
549 this site:

- 550 • VAD001/E45: 1867–1616 cal BCE (3400±35 BP, Ua-36345)  
551 • VAD002/E47: 1689–1528 cal BCE (3330±30 BP, Beta-479536)  
552 • VAD003/E69: 1689–1528 cal BCE (3330±30 BP, Beta-479534)  
553 • VAD004/E74: 1673–1255 BCE  
554 • VAD005/E77: 1742–1546 cal BCE (3360±30 BP, Beta-479535)

555 **Campo de Hockey (San Fernando, Cádiz, Andalusia, Spain)**

556 *Contact: Eduardo Vijande Vila, José Ramos Muñoz, Pablo Ramos-García, Adolfo*  
557 *Moreno-Márquez*

558 The Campo de Hockey site is located in the Bay of Cádiz, the southernmost region of the  
559 Iberian Peninsula. Geo-archaeological studies have confirmed that, during the Neolithic,  
560 this marshy area was mostly under the sea, with the most elevated areas both in the city  
561 and its immediate hinterland forming small islets (62).

562 In 2007, the construction of a hockey stadium exposed the remains of this late Neolithic  
563 settlement, dated to the turn of the 4<sup>th</sup> millennium BCE (63).

564 The excavation revealed the existence of three areas of activity. The highest, westernmost  
565 sector was the domestic area. The middle sector contained five features cut into the  
566 tertiary marl soil which, based on typology, have been interpreted as ‘pits’. The size of  
567 these structures suggests their use for storage, for example as grain silos. Finally, the  
568 necropolis was found in the lowest area. The funerary ritual attested in this necropolis has

characteristics that have not been described elsewhere in the region during this period. Most graves contain only one individual, which allows us to infer social differences, also reflected on the typology of the tomb and the grave offerings, as well as to collect data concerning gender and age distribution (64) (often an impossible task with collective tombs in which bones are mixed).

Different types of grave exist, from simple burial pits to burial mounds or more elaborate graves (63, 64). A total of 60 graves have been excavated to date, including 49 (82%) individual graves, eight double graves and 2 quadruple graves, amounting to a total of 73 individuals. The presence of rich grave offerings (beads made of amber, variscite and turquoise, and imported polished axes) in the most elaborate graves is a clear indication of social inequality.

We sampled six individuals from this site:

- I7160/CH-08-C15-UE1514-E16: 4039–3804 cal BCE (5140±35 BP, CNA4579.1.1)
- I7679/CH-08-C14A-UE1402-E21: 4300–3700 BCE [from layer dates on different skeletons: 3948–3708 cal BCE (5020±50 BP, CNA360); 4221–3990 cal BCE (5650±40 BP, CNA664); 4244–3983 cal BCE [5665±50 BP, CNA833]]
- I7547/CH-08-C12-UE1210-E2: 4300–3700 BCE [from layer dates on different skeletons: 3948–3708 cal BCE (5020±50 BP, CNA360); 4221–3990 cal BCE (5650±40 BP, CNA664); 4244–3983 cal BCE [5665±50 BP, CNA833]]
- I7549/CH-08-C12-UE1214-E6: 4300–3700 BCE [from layer dates on different skeletons: 3948–3708 cal BCE (5020±50 BP, CNA360); 4221–3990 cal BCE (5650±40 BP, CNA664); 4244–3983 cal BCE [5665±50 BP, CNA833]]
- I7550/CH-08-C15-UE1502-E4: 4300–3700 BCE [from layer dates on different skeletons: 3948–3708 cal BCE (5020±50 BP, CNA360); 4221–3990 cal BCE (5650±40 BP, CNA664); 4244–3983 cal BCE [5665±50 BP, CNA833]]
- I8134/CH-08-C17A-UE1709-E4: 4300–3700 BCE [from layer dates on different skeletons: 3948–3708 cal BCE (5020±50 BP, CNA360); 4221–3990 cal BCE (5650±40 BP, CNA664); 4244–3983 cal BCE [5665±50 BP, CNA833]]

597 **Loma del Puerco (Chiclana de la Frontera, Cádiz, Andalusia, Spain)**

598 *Contact: Eduardo Vijande Vila, José Ramos Muñoz, Pablo Ramos-García, Adolfo*  
599 *Moreno-Márquez*

600 The necropolis of Loma del Puerco is 8 km away from the town of Chiclana de la  
601 Frontera, in the Bay of Cádiz. The funerary structures are 400 m from the coastline, in a  
602 gentle southwest-facing slope.

603 The first excavation season took place in 1991, when four graves were excavated. These  
604 are collective graves, circular or oval in shape, cut into the tertiary marl soil and lined by  
605 large vertical slabs of sandstone, fit in with small and middle-sized stones (65). These  
606 four graves contained a total of 14 individuals and very poor grave offerings.

607 A second excavation season was undertaken in 2016. Two more graves were identified.  
608 The most interesting of these features (UE 1038) was a rectangular pit, 2 x 1.20 m in size,  
609 cut into the tertiary marl soil and lined by large vertical slabs. Inside this grave, three  
610 anatomically articulated adult individuals were found, along with the scattered remains  
611 of a sub-adult individual. Individual number 1 (who was sampled for this study)  
612 corresponds to a woman, and was the only one to carry any kind of grave goods (two  
613 gypsum beads and a shell fragment):

- 614 • I7162/LM-16-Sep1: 1932-1697 cal BCE [1932–1756 cal BCE (3524±30 BP,  
615 CNA4237.1.1), 1880-1697 cal BCE (3465±20 BP, PSUAMS-4262)]

616 **Els Estrets de la Rata (Vilafamés, Castelló/Castellón, Valencian Community, Spain)**

617 *Contact: Domingo C. Salazar-García*

618 This site is located in the pre-coastal mountain ranges in the province of  
619 Castelló/Castellón, overlooking the plain of Vilafamés and the pass of “la rambla de la  
620 viuda”.

621 The settlement is delimited by a wall with a circular tower at its most accessible corner.  
622 It is dated to the “Iberian” period between 3rd-2nd centuries BCE by the different type of  
623 ceramics: Roman, local Iberian and importation ceramics. The defensive structure  
624 encloses a space with several rectangular compartments built with masonry that could  
625 have served as storage spaces. Under the rooms, two newborn burials were found (66).  
626 We analyzed both individuals:

- 627 • I3321/S-EVA 9303; Ind 2: 300–100 BCE

628 • I3320/S-EVA 9305; Ind 1: 300–100 BCE

629 **Puig de la Misericordia (Vinarós, Castelló/Castellón, Valencian Community, Spain)**

630 *Contact: Domingo C. Salazar-García, Arturo Oliver Foix*

631 This site is located at the top of a hill in the middle of the coastal plain of Vinarós,  
632 controlling the coast and the access to the plain delimited by the foothills of “Serra d'Irta”,  
633 “Montsià”, “Maestrazgo” and “Tinença de Benifassar”.

634 The site contains four occupations from Late Bronze Age to the Late Iron Age. Between  
635 700 and 400 BCE the settlement was used as a fortified residence, with evidence of  
636 trading with Phoenicians and Greeks (67). Newborn burials were located under one of  
637 the settlement rooms and dated to the early stage of the “Iberian culture” around the 6th  
638 century BCE. The latest phase of the site corresponds to the second half of the 2nd century  
639 BCE during the Roman Republic, during which a building related to the agricultural  
640 colonization was built, beginning the Roman domination in the area. We sampled one  
641 individual from this site:

642 • I3322/S-EVA 9307: 600–500 BCE

643 **Cingle del Mas Nou (Ares del Maestre, Castelló/Castellón, Valencian Community,**  
644 **Spain)**

645 *Contact: Domingo C. Salazar-García*

646 Cingle del Mas Nou is an open-air site close to a rock shelter situated in the town of Ares  
647 del Maestre. It is on the southern side of Serra d'En Seller, close to the valleys of Cirerals  
648 and Molero, at 940 m above sea level. The site was discovered in 1975, and excavations  
649 ran from 1986 to 1999. The stratigraphic sequence of the site is divided into five levels,  
650 grouped in two occupation phases: Levels I and II are associated with the Early Neolithic,  
651 Levels III and IV to the Geometric Mesolithic, and Level 5 is sterile. The analysis of the  
652 excavated remains is ongoing (68). Nine human individuals dating to the Mesolithic have  
653 been described: 2 adults and 7 children of different ages (69).

654 We analyzed one Mesolithic individual:

655 • I3209/Q4[-125/-144]: 5976-5783 cal BCE (6980±25 BP, PSUAMS-4414)

**Castillejo del Bonete (Terrinches, Ciudad Real, Castilla-La Mancha, Spain)**

*Contact: Domingo C. Salazar-García, Luis Benítez de Lugo Enrich, María Benito Sánchez*

Castillejo del Bonete was a ceremonial site used for more than one thousand years during the Copper and Bronze Ages. It is located in the interior of the Iberian Peninsula, on the southern edge of the Castilian Meseta, on top of a hill with great visibility controlling a natural pass along the southeast of Ciudad Real province. It holds a strategic position between the river basins of the Guadiana and the Guadalquivir. Excavations at this site began in 2003 and are still ongoing. Rites performed at this site were related to death and resurrection of the sun, human death, and veneration of ancestors. Some examples are feasting rites, offerings to the dead, and architecture oriented towards the winter solstice (70, 71). A natural cave was monumentalized and used as funerary chamber, building a large tumulus and creating cave art. This main tumulus is connected with others through several corridors.

Several radiocarbon dates have been obtained on human and non-human material, all yielding dates between 2465–1565 cal BCE (72, 73).

Burials have been found in the tumulus and its surroundings, both primary (in fetal position and lateral decubitus position on the right side) and secondary deposits, which indicates the reuse of the funerary space. A good example of this pattern is Tumba 1 which, although altered, still preserved the remains of a 30-35-year-old male individual that was sampled for DNA analysis:

- I3756/TEBO'03, D8 UE12; Tumba 1: 2014–1781 cal BCE (3565±25 BP, PSUAMS-2077)

Another good example is Tumba 4, the only multiple burial in this site with a 40-50-year-old male and a 30-40-year-old female who was buried with two ivory buttons and who had a marine diet, suggesting a non-local origin (74). We sampled both individuals from Tumba 4:

- I3484/TEBO'04 Tumba 4 Ind 2: 2271–1984 cal BCE (3720±70 BP, Rome-1687)
- I3485/TEBO'04 Tumba 4 Ind 1: 2300–1900 BCE

Tumba 5, also located in the main tumulus, belonged to a 40-50-year-old male with degenerative signs such as osteoarthritis and dorsal Kyphoscoliosis. This individual also

687 presented muscle stress signs on the upper limbs and shoulder girdle suggesting activities  
688 related to archery:

- 689 • I12809/TE'15 BO 1257-56, Tumba 5: 1880–1770 BCE

690 The last individual analyzed here was a young male found inside the monumentalized  
691 sepulchral cave with a large burial mound; specifically, in Gallery 3 (subsector 3.1.7).  
692 This is an area that remained closed and sealed from Prehistory to the present-day. Human  
693 bones from a minimum of two individuals were found, but most of the remains belonged  
694 to one of them (Individual 1), who was analyzed here:

- 695 • I12855/TE'17 BO UF73: 1880–1770 BCE

696 This burial appeared without strict anatomical connection, except for some bones that  
697 were found articulated (spine and some ribs). The bones that had lost the strict articulation  
698 were in their anatomical place, which implies a primary burial in fetal position and a later  
699 anthropic removal. In this tomb, a limestone funerary stele with 15 bivalve fossils  
700 (Pectinidae) has been found. The rock was moved inside this cave from a distance of 40  
701 km (75). The two individuals were likely deposited on the bottom of the cave in this  
702 closed place, without being buried in a pit; as no excavation of any pit has been detected.  
703 Gallery 3 is a rocky cavity where there is no soil with sufficient land to house a burial.

704 Castillejo del Bonete acts as a karstic system of funerary galleries (72) that were  
705 artificially sealed, suggesting sociocultural stratification. Outside the main tumulus 6  
706 individuals were found in 5 graves, whereas inside the funerary cave there was a  
707 minimum of 11 individuals (6 adults and 5 subadults). Although anthropological analyses  
708 are still ongoing, we can conclude that this is a small number of individuals given the  
709 long period of use of this monument. This could be explained by cultural hierarchy or by  
710 the social role played by the buried individuals.

### 711 **Sima del Ángel (Lucena, Córdoba, Andalusia, Spain)**

712 *Contact: Enrique Viguera, Cecilio Barroso, Francisco J. Bermúdez*

713 Ángel Cave (Lucena, Córdoba, Spain. 37° 22' 11" N; 4° 28' 44" W; 608 m.a.s.l.) is an  
714 important Middle Pleistocene site located in the south of Iberian Peninsula. It is a karst  
715 system made up of several units (76). The main site, excavated beginning in 1995, is  
716 open-air, the remainder of a former cave that collapsed. The most striking feature of the  
717 site is the presence of one of the largest hearths in Europe, which covers the entire  
718 stratigraphic sequence, without a single hiatus, at a depth of 5 m. The assemblage is



composed of more than 5000 tools (mainly flake and retouched tools, in addition to nearly 50 handaxes), conforms to Final Acheulean, with the special presence of bone retouchers (77). The vast majority of the *ca.* 9,000 fossil remains (mainly equids, large bovids and cervids) are burnt and highly fragmented due to marrow extraction activities, and a good number of them displayed cut marks (76, 77). Stratigraphic and archaeological data, along with new radiometric dating, indicate an uninterrupted occupation of the site between 320 and 180 ka BP (78).

Close to the main site there is a small cave. In order to relate its archaeology to that of the Paleolithic cave, it was cleared between 2013 and 2016 and an extraordinary number of human remains and archaeological materials were discovered. That record was out of stratigraphic context but it denotes the use of the cave as a burial place in recent Prehistory. From this cave, two narrow holes lead to a larger cavity, the ‘Sima’, where the sample for the present study was recovered. It is a 60 m deep vertical fracture that hosts a pyramidal sedimentary package made up by materials brought from outside the site. An area on the southeastern slope of this deposit, with an inclination of *ca.* 40°, has been excavated since 2013. The profuse archaeological record recovered at ‘Sima del Ángel’ reveals a continuous use of the karst system for burials for a long period of recent prehistory between the VI and II millennia BCE. Even though it is difficult to arrange the deposits in a precise chronostratigraphic sequence, it can be deduced from the archaeological record and available dating that the ‘Sima’ was used as an immense natural ossuary, into which human remains and grave goods placed in the upper cave were gradually thrown down, with an especially intense use in Neolithic and Chalcolithic times.

The Neolithic pottery record from ‘Sima del Ángel’ ranges from the VI to V millennia BCE. It is mainly composed of fragments of bowls and globular vessels decorated with incisions and/or impressions and red ochre *engobe*, while *Cardium* pottery has also been collected. Chalcolithic ceramics are well exemplified by fragments of plates and dishes with incised and impressed decoration. Thickened rim plates are characteristic of this period and are datable to between 2800 and 2200 BCE. In addition, there are some Bell Beaker pottery fragments. The stone tool assemblage is primarily composed of flint blades, but there are also ground stone axe heads and gouges. Finally, many personal ornaments, such as stone bracelets, plenty of beads (made of shell, stone and bone) and shell pendants, have been recovered.

Up to now around 2,500 human remains (bones, bone fragments and isolated teeth) have been exhumed. Due to environmental conditions and geologic dynamics within the site, the state of preservation of anthropological remains is poor. Anatomical connections have not been reported and, for the moment, a minimal number of more than 40 individuals has been estimated (among which 1/3 are subadults). Traces of deliberate manipulation have been detected in minority of the human remains, and they include cut marks, scratches and heat induced changes, which may result from a secondary funerary rite. However, the evidence of some bone fractures and marrow extraction on human bones agrees with a cannibalistic practice.

The samples analyzed in this paper were recovered in the 2016 excavation. Environmental conditions within the cave are favorable for ancient DNA preservation, and human remains were collected and handled following an anti-contamination process and then stored at 4°C. The current sample comes from the Chalcolithic horizon in ‘Sima del Ángel’, radiocarbon dated with ages of 2862–2500 cal BCE (4096±31 BP, OxA-32885) and 2831–2474 cal BCE (4040±28 BP, OxA-35790). It consists of teeth and petrous portions of the temporal bone belonging to 16 individuals. There are at least 6 males and 5 females among them. Some of the remains are those of subadult individuals: I8154 is the maxillary first deciduous molar of a ~7-year-old girl; I8158 is the shovel shaped lateral deciduous incisor of a ~4-year-old boy; I8198 is the left temporal bone of a ~5-year-old girl. Generally, the teeth from adult individuals are highly worn and some of them have slight cervical carious lesions. Analyzed individuals are listed below:

- I7588/SIMA107: 2900–2500 BCE
- I7587/SIMA10,181: 2900–2500 BCE
- I8148/11801: 2900–2500 BCE
- I8149/11813: 2900–2500 BCE
- I8150/11849: 2900–2500 BCE
- I8153/11802: 2900–2500 BCE
- I8154/11831: 2900–2500 BCE
- I8155/11832: 2900–2500 BCE
- I8156/11807: 2900–2500 BCE

- 782 • I8157/11800: 2900–2500 BCE
- 783 • I8158/11803: 2900–2500 BCE
- 784 • I8197/11834: 2900–2500 BCE
- 785 • I8198/11838: 2900–2500 BCE
- 786 • I8199/11853: 2900–2500 BCE
- 787 • I8364/11836: 2706–2569 BCE
- 788 • I8365/11837: 2706–2569 BCE

## 789 **Empúries (Girona, Catalonia, Spain)**

790 *Contact: Marta Santos, Pere Castanyer, Joaquim Tremoleda*

791 The archaeological site of Empúries is composed by the remains of the ancient Greek  
 792 colony of Emporion—founded by the Phocaeans in the first half of the 6th century BCE  
 793 (19)—and by the remains of a Roman city created at the beginning of the 1st century BCE  
 794 on an area previously occupied by a fortified camp built after the earliest Roman presence  
 795 in the area. Both town were later integrated into the *municipium Emporiae*, which was  
 796 founded at the beginning of the Roman imperial period.

797 Several sites in the vicinity of Empúries attest the previous occupation of the area—  
 798 located in the southern of the Gulf of Rosas—from the Neolithic and specially during the  
 799 Final Bronze Age and the Early Iron Age. Other sites demonstrate the habitation of the  
 800 area during de Late Antiquity and Medieval Period, after the abandonment of the Roman  
 801 city in the 3rd century CE.

802 The Greek and Roman towns were surrounded by several funerary areas, some of which  
 803 suffered from intense pillage before the beginning of excavations under the initiative of  
 804 the “Junta de Museus de Barcelona” in 1908. In other cases it was possible to carry out  
 805 excavations documenting the numerous tombs—both inhumations and cremations—  
 806 published by Martín Almagro in two volumes in 1953 and 1955. However, besides the  
 807 study of the funerary materials associated with those tombs and general descriptions of  
 808 the characteristics of the burials, until very recently the anthropological information has  
 809 been extremely incomplete because in most of the cases the remains have not been  
 810 preserved.

811 Together with the new burials documented in the 80s in the parking area of the site, other  
812 more recent interventions in specific areas located south of the Greek town have  
813 recovered a group of funerary structures that increase our knowledge of the necropolises  
814 on the eastern slope of Empúries hill, next to the tracks leading to the town. We have  
815 analyzed a total of 24 individuals from these latest excavations.

816 A first group of burials correspond to an area of the necropolis excavated in 2010 due to  
817 the construction of a new reception building of the MAC- Empúries. This area, south of  
818 the Greek town, was identified as 10-SU-28-D1. The southern part of this area was  
819 occupied by tombs associated to the Greek town, mainly inhumations on the rock or  
820 taking advantage of the substrate depressions. Although some of these tombs lacked grave  
821 goods, the recovered materials in other tombs date the use of this necropolis during the  
822 5th and 4th centuries BCE. We have analyzed 10 individuals from this area:

- 823 • I8211/10-SU-28-D1-E-96: 500-450 BCE
- 824 • I8213/10-SU-28-D1-E-60: 500-400 BCE
- 825 • I8344/10-SU-28-D1-E-74: 500-400 BCE
- 826 • I8209/10-SU-28-D1-E-99: 450-400 BCE
- 827 • I8214/10-SU-28-D1-E-82: 400-350 BCE
- 828 • I8215/10-SU-28-D1-E-76: 400-350 BCE
- 829 • I8210/10-SU-28-D1-E-91: 500-350 BCE
- 830 • I8212/10-SU-28-D1-E-46: 500-350 BCE
- 831 • I8340/10-SU-28-D1-E-63: 500-350 BCE
- 832 • I8341/10-SU-28-D1-E-62: 500-350 BCE

833 Further south, and without disturbing the old cemetery, this area was used again as  
834 necropolis during the Roman Period, specially during the 2nd century CE, with pit burials  
835 and tombs with *tegulae* cover. We analyzed 7 individuals from this group of tombs:

- 836 • I8216/10-SU-28-D1-E-35: 57–208 cal CE (1895±20 BP, PSUAMS-4212)
- 837 • I8474/10-SU-28-D1-E-47: 100-200 CE
- 838 • I8475/10-SU-28-D1-E-16: 100-200 CE

839 • I8338/10-SU-28-D1-E-15: 100-200 CE

840 • I8339/10-SU-28-D1-E-8: 100-200 CE

841 • I10865/10-SU-28-D1-E-37: 100-200 CE

842 • I10866/10-SU-28-D1-E-20: 43 cal BCE–51 cal CE (2005±15 BP, PSUAMS-5281)

843 The second area, located quite far south from the limits of the Greek city, corresponds to  
844 the so-called Granada Necropolis, partially excavated and published by Martín Almagro.  
845 More recently, due to the urbanization of this area identified as SU-33-A4, preventive  
846 archaeological excavations have described the sequence of use of this cemetery. Although  
847 this space was used since the 5th century BCE, the burials analyzed here date to a period  
848 between the 3rd and 2nd centuries BCE, which is well documented in the new  
849 excavations. They correspond to inhumations excavated in the rock or in the sand layer  
850 above the rock, oriented west-east, often marked by a simple stone mound and containing  
851 only ointment cases deposited next to the bodies. We analyzed five individuals from this  
852 area:

853 • I8203/02-SU-33-A4-T1058: 300–100 BCE

854 • I8204/12-SU-33-A4-600: 300–100 BCE

855 • I8205/12-SU-33-A4-T180: 300–100 BCE

856 • I8206/12-SU-33-A4-T680: 300–100 BCE

857 • I8208/12-SU-33-A4-T510: 370-204 cal BCE (2220±20 BP, PSUAMS-4277)

858 A new phase of this necropolis, associated with the cremation rite and dated between the  
859 1st century BCE and the 1st century CE, has been documented. Finally, the most recent  
860 phase of the necropolis involved the return to the inhumation rite, although within the  
861 excavated part only one burial was found. The tomb was south-north oriented and dates  
862 to the 2nd century CE or later. The analyzed individual is:

863 • I8202/02-SU-33-A4-T1077: 100–300 CE

864 The last individual belonged to one of the Late Roman cemeteries located in the lower  
865 part of the western side of the Empúries hill, related to funerary or worship buildings.  
866 Specifically, the tomb was excavated in 2005 together with other tombs in the area called  
867 Santa Magdalena, which belongs to the necropolis created next to an old mausoleum  
868 transformed into a church. This necropolis was also used during the Medieval period. The

869 tomb corresponds to an individual inhumation inside a pit delimited by stones and without  
870 a preserved cover, dated to the 6th century CE:

- 871 • I8343/05-SMG-8075: 500–600 CE

## 872 **Puig de Sant Andreu (Ullastret, Girona, Catalonia, Spain)**

873 *Contact: Gabriel de Prado, Bibiana Agustí, Ferran Codina*

874 The Iberian culture town of Ullastret (6th-2nd centuries BCE) is located in the Ampurdán  
875 (Girona) plain and constitutes one of the most important archaeological sites of the Iron  
876 Age in the northwest Mediterranean. This large urban area was formed by two inhabited  
877 sites, Puig de Sant Andreu and la Illa d'en Reixac, separated by 300 meters and  
878 representing a true *dipolis*. The combined sites occupied more than 15 hectares after the  
879 4th century BCE and were the capital of the Iberian culture Indigetes (or Indiketes) tribe,  
880 which is cited in classical sources including Avienus, Ptolemy and Strabo

881 The Iberian culture practiced the funerary ritual of body cremation, which resulted in a  
882 very small number of human remains for study. In this sense, the site of Ullastret is unique  
883 because excavations have identified remains from more than 40 individuals, mostly  
884 mandibles, skulls and isolated teeth. In most of the cases, these remains present evidence  
885 of violence and could correspond to the heads of enemies beheaded in combat that were  
886 exhibited as war trophies in public spaces. This ritual is archaeologically documented in  
887 the northeast corner of Iberia and in southern Gaul where archaeological evidence,  
888 iconography and classic sources are available.

889 The remains analyzed in this study correspond to a group of 34 isolated fragments from  
890 a minimum of 8 individuals. They were found on the floor of the main street (zone 13)  
891 near a large aristocratic building (zone 14). They were directly covered by the ruins of  
892 the building and the city which was abandoned around 200 BCE. Their location and  
893 characteristics suggest that they represented enemies' heads exhibited at the building's  
894 entrance together with their weapons. After being exposed for some time, maybe years,  
895 they finally dropped to the street floor before the abandonment of the city, by which time  
896 they likely had already lost their significance.

897 We analyzed five samples from this site that corresponded to four different individuals:

- 898 • I3326/4979: 250–200 BCE
- 899 • I3327/4980: 250–200 BCE

- 900 • I3324/4976: 360–193 cal BCE (2190±20 BP, PSUAMS-2159)
- 901 • I3323/4975+4977: 365–204 cal BCE (2215±20 BP, PSUAMS-2158)

## 902 **Sant Julià de Ramis (Girona, Catalonia, Spain)**

903 *Contact: Neus Coromina, Josep Burch, David Vivó*

904 The necropolis of Sant Julià de Ramis is located on the top of the mountain of the same  
 905 name (79). The first stable habitat established in this place was an Iberian Iron Age  
 906 settlement in the mid/second half of the 6th century BCE. When it was abandoned, a small  
 907 rural establishment was constructed at the bottom of the mountain that survived, with  
 908 successive alterations, until the mid-4th century CE. This period coincided with the  
 909 building of a large fort on the top of the mountain, whose strategic situation should be  
 910 considered in light of the fact that it was adjacent to the Via Augusta and close to the city  
 911 of *Gerunda*. Even when the Western Roman Empire fell, the fort was not deserted.  
 912 Instead, it underwent extensive remodeling. Subsequently, in association with the fort, a  
 913 group of houses were built on top of the mountain and over time were organized around  
 914 a chapel built in the same period.

915 The Muslim conquest of the area at the beginning of the 8th century led to the  
 916 abandonment of the fort which rapidly became a ruin, as described in documentary  
 917 sources from the 9th century CE. However, the archaeological excavations completed to  
 918 date have revealed that in the second half/end of the 8th century, a cemetery developed  
 919 around the chapel that would be in use until the start of the 21st century. The vitality of  
 920 the place, which became the center of a parish in the medieval period, is further reflected  
 921 in the construction of a new church at the end of the 10th century-start of the 11th century,  
 922 dedicated to Sant Julià.

923 We analyzed seven individuals from this site:

- 924 • I10851/SJR'15-1669: 887–1013 cal CE (1100±30 BP, Beta-458691)
- 925 • I10852/SJR'14-1670: 973–1150 cal CE (1010±30 BP, Beta-458692)
- 926 • I10853/SJR'15-1796: 989–1153 cal CE (990±30 BP, Beta-448950)
- 927 • I10854/SJR'15-1820: 973–1150 cal CE (1010±30 BP, Beta-448952)
- 928 • I10892/SJR'15-1846: 770–1200 CE (based on dates in the same context)
- 929 • I10895/SJR'15-1828: 777–981 cal CE (1140±30 BP, Beta-448953)

930 • I10897/SJR'17-2099: 1033–1204 cal CE (910±30 BP, Beta-477258)

931 **Pla de l'Horta (Sarrià de Ter, Girona, Catalonia, Spain)**

932 *Contact: Neus Coromina, Josep Burch, David Vivó*

933 The Pla de l'Horta villa is located in Sarrià de Ter, around four kilometers from the city  
934 of Girona, and therefore it should be considered a *fundus* that belonged to the *suburbium*  
935 of *Gerunda* (80). It was constructed in the middle of the 1st century BCE. The residential  
936 part underwent substantial alterations in the Flavian and Severan periods, on both  
937 occasions with notable use of mosaic floors. In the industrial district of this settlement  
938 we can identify the area of the wine presses, especially from the 4th century CE, which  
939 is the last phase for which there is evidence on the villa. However, due to the villa's  
940 considerable size, we can deduce that it probably had a large industrial area that has not  
941 yet been excavated to the north of the structures that have been discovered.

942 Immediately to the north of this area, a necropolis associated with the villa has been  
943 found, with a funerary building and a series of tombs. This site clearly belongs to the  
944 villa, which would subsequently be extended in the Visigoth period. The samples that  
945 have been analyzed correspond to this Visigothic phase. Several types of burials can be  
946 seen, from a simple grave to a cist. The number of burials identified (58), as well as the  
947 results of the analysis, demonstrate the persistence and importance of the habitat, even  
948 though it has not yet been identified archaeologically. The grave goods and the typology  
949 of the tombs point to a Visigothic origin of the individuals.

950 We analyzed nine individuals from this site:

951 • I12029/PH'06-1144: 500–600 CE

952 • I12030/PH'06-1169: 500–600 CE

953 • I12031/PH'06-1172: 500–600 CE

954 • I12032/PH'06-1183: 500–600 CE

955 • I12033/PH'06-1192: 500–600 CE

956 • I12034/PH'06-1207: 500–600 CE

957 • I12162/PH'06-1163: 500–600 CE

958 • I12163/PH'06-1166: 500–600 CE



959 • I12164/PH'06-1157: 500–600 CE. First degree relative of I12032.

960 **Cueva de la Carigüela (Piñar, Granada, Andalusia, Spain)**

961 *Contact: Juan Manuel Jiménez Arenas, Isidro Jorge Toro Moyano*

962 The anatomically modern human mandible of Carigüela (Car1) was found during the field  
963 seasons led by J.P. Spahni during the 50s of the last century. Initially, it was almost  
964 complete although at present only the right half mandible with three molars is conserved.  
965 The stratigraphic position is level III, associated with pre-neolithic lithic industry and a  
966 fragment of parietal bone. Car1 was described and measured by García Sánchez (81) who  
967 focused on the presence of ancestral features. In that paper, a close affinity of Car1 with  
968 the male mandible from Combe Capelle was concluded.

969 Relevant features of Car1 include the presence of a retromolar space, a well-defined  
970 mylohyoid line and deep submandibular fossa, and the presence of a goniac extroversion.

971 We analyzed a tooth from this mandible:

972 • I10899/Car1: 9700–5500 BCE (see SI 13)

973 **Cerro de la Virgen (Orce, Granada, Andalusia, Spain)**

974 *Contact: Juan Manuel Jiménez Arenas, Isidro Jorge Toro Moyano*

975 The site of Cerro de la Virgen is located in Orce (northeast Granada province), in a  
976 flattened spur that was subsequently affected by agricultural activities, a building  
977 construction now demolished, and a small church at the highest point of the hill. The site  
978 is delimited by the river Orce in the north and by two gullies in the east and west. All the  
979 recovered materials are attributed to the Bronze Age and show connections to the El Argar  
980 culture (82). This site includes 36 individual and double cist burials inside the habitational  
981 units.

982 We analyzed two individuals from this site:

983 • I8144/8: 1877–1636 cal BCE (3426±34 BP, Ua-39403)

984 • I8136/19: 1606–1418 cal BCE (3216±33 BP, Ua-39408)

985 **Cerro de la Encina (Monachil, Granada, Andalusia, Spain)**

986 *Contact: Juan Manuel Jiménez Arenas, Isidro Jorge Toro Moyano*

987 Cerro de la Encina is a site located 7 kilometers from the city of Granada, on the right  
988 bank of the Monachil river, in one of the valleys leading to Sierra Nevada. The settlement  
989 spread over a wide hill that clearly stands out from its surroundings. It has a strategic  
990 location due to its natural defenses that limit access to the settlement, and due to its control  
991 of La Vega de Granada and the access to Sierra Nevada.

992 The habitation spaces are located on the hillsides and adjacent plateaus, with the  
993 fortification as the central element around which the settlement is articulated. The burials  
994 are located under the house floors.

995 We analyzed one individual from this site:

- 996 • I8140\_d/13: 2117–1779 cal BCE (3590±40 BP, Beta-230003)

997 **La Navilla (Arenas del Rey, Granada, Andalusia, Spain)**

998 *Contact: Juan Manuel Jiménez Arenas, Isidro Jorge Toro Moyano*

999 La Navilla is part of a group of collective burials (megaliths) located in the Alhama region  
1000 in the southwest of the Granada province (83). It is a corridor tomb with a trapezoidal  
1001 chamber located in the right bank of the Cacin river and containing 34 burials. It is  
1002 surrounded by a group of orthostats.

1003 We analyzed three individuals from this site:

- 1004 • I8048/13: 2200–2000 BCE

- 1005 • I8141/7: 2200–2000 BCE

- 1006 • I8142/8: 2200–2000 BCE

1007 **Necrópolis de Cobertizo Viejo (La Zubia, Granada, Andalusia, Spain)**

1008 *Contact: Juan Manuel Jiménez Arenas, Isidro Jorge Toro Moyano*

1009 Cobertizo Viejo is a singular building located along the road from Granada to La Zubia.  
1010 The first two phases of the building are dated to the Nazari period (14th-15th centuries  
1011 CE) by the associated ceramic material (84). The building originally had a religious

1012 purpose, acting as the tomb of a Marabout, and was later enlarged with other constructions  
1013 (including a cemetery) as the main tomb became increasingly important.

1014 The three analyzed tombs were excavated from the cemetery north of the main building:

- 1015 • I8145/sepultura 1: 1300–1500 CE
- 1016 • I8146/sepultura 4: 1300–1500 CE
- 1017 • I8147/sepultura 18: 1300–1500 CE

#### 1018 **Calle Panaderos 21-23 (Granada, Andalusia, Spain)**

1019 *Contact: Juan Manuel Jiménez Arenas, Isidro Jorge Toro Moyano*

1020 This site is located in the city of Granada and was excavated in 2005 (85). The level of  
1021 the Islamic necropolis is marked by a stratum of loose reddish-brown soil that appeared  
1022 in the central part of the site, south of the jar E-17 and near the southwest limit. This  
1023 stratum was irregularly distributed and covered burials CEF-20, CEF-43, CEF-36, CEF-  
1024 37, CEF-40, CEF-25, CEF-47, CEF-28, CEF-29, CEF-23, CEF-24 and CEF-56. The  
1025 bodies were oriented towards the southeast and in lateral decubitus position on the right  
1026 side, following the Islamic tradition, with various degrees of limb flexion. Radiocarbon  
1027 dating at the “Centro de Instrumentación Científica de la Universidad de Granada”  
1028 confirmed that these burials belonged to the period of Muslim rule, more specifically to  
1029 period of the Caliphate of Cordoba during the 10th century CE.

1030 We analyzed one individual from this site:

- 1031 • I7427/CEF-43: 900–1000 CE

#### 1032 **Casa Cuartel Guardia Civil (Alhama de Granada, Granada, Andalusia, Spain)**

1033 *Contact: Juan Manuel Jiménez Arenas, Isidro Jorge Toro Moyano*

1034 In 2009, during construction works for the new headquarters of the “Guardia Civil” in  
1035 Alhama de Granada, a medieval necropolis was discovered. More than 20 individuals  
1036 were found, all buried with a southeast-northwest orientation and in lateral decubitus  
1037 position on the right side, following the Islamic tradition. The associated ceramics place  
1038 the necropolis within the 12th and 13th centuries CE. We analyzed 2 individuals from  
1039 this site:

- 1040 • I7458/CEF0073/UEI513: 1100–1300 CE

1041 • I7457/CEF0010/UEI211: 1100–1300 CE

1042 **Cueva Romero (Huéscar, Granada, Andalusia, Spain)**

1043 *Contact: Juan Manuel Jiménez Arenas, Isidro Jorge Toro Moyano*

1044 The site occupies a wide area along the fluvial terraces located on the banks of the  
1045 Huéscar river. Archaeological analysis has documented several phases of occupation  
1046 (86). The earliest one dates to the Late Neolithic-Early Copper Age and is defined by a  
1047 silo associated with a circular hut, the second corresponds to an Iron Age horizon in the  
1048 context of secondary deposition and the third corresponds to a short occupation during  
1049 the Roman period. Finally, a medieval necropolis with nine pit burials has been  
1050 documented.

1051 We analyzed three individuals from the medieval necropolis:

1052 • I7497/Burial 2 (no. 1003): 1000–1100 CE. This burial includes a mixed cover made  
1053 of sandstone and conglomerate. The body was in lateral decubitus position on the right  
1054 side, legs slightly flexed, arms resting on the pubis and face oriented to the southeast. The  
1055 burial was oriented on the southwest-northeast axis. Based on these characteristics the  
1056 burial can be dated to the Medieval period.

1057 • I7498/Burial 9 (no. 8016): 1000–1100 CE. This is a single pit burial with a cover  
1058 made with three sandstone slabs and large conglomerates. The space between the slabs  
1059 was filled with small sandstone pieces and silex pebbles. The body was in lateral  
1060 decubitus position on the right side, arms resting on the pubis and legs slightly flexed.  
1061 The associated materials, including numerous fragments of cooking pots and ceramic  
1062 platters with the imprints of fingers, places the burials around the 11th century CE. At the  
1063 constructive level, the pit covers made with sandstone slabs are the most reliable indicator  
1064 for the dating of the burials within the Zirid period.

1065 • I7499/Sepultura 7 (no. 5019): 1000–1100 CE. This is a single pit burial with a cover  
1066 made of six sandstone slabs and large conglomerates. The space between the slabs was  
1067 filled with small sandstone pieces and silex pebbles. The body was in lateral decubitus  
1068 position on the right side following a southwest-northeast axis, arms resting on the pubis  
1069 and extended legs.

1070 **El Castellón (Montefrío, Granada, Andalusia, Spain)**

1071 *Contact: Juan Manuel Jiménez Arenas, Isidro Jorge Toro Moyano*

1072 This site is located at the El Castellón hill, occupying a strategic area dominating the  
1073 valley. Between 1977 and 1985 the excavation uncovered 115 well-preserved cist burials  
1074 with large slabs, oriented on a north-south axis and reused several times (87). The simple  
1075 burials generally correspond to young individuals. Grave goods were found in 16 graves,  
1076 including earrings, bronze rings, glass beads, four Visigothic buckles, one bronze belt  
1077 with two animal figures holding a large cup (interpreted as having a Byzantine origin),  
1078 and ceramic olpes (flask). These objects place the cemetery within the 6th and 7th  
1079 centuries CE, although the available date indicates a slightly earlier chronology.

1080 We analyzed nine individuals from this necropolis:

- 1081 • I3577/sepultura 31: 400–600 CE
- 1082 • I3574/sepultura 48: 400–600 CE
- 1083 • I3579/sepultura 2: 400–600 CE
- 1084 • I3583/sepultura 80: 400–600 CE
- 1085 • I3578/sepultura 29: 400–600 CE
- 1086 • I3575/sepultura 44 individuo 1: 400–600 CE
- 1087 • I3582/sepultura 77: 400–600 CE
- 1088 • I3581/sepultura 71: 400–600 CE
- 1089 • I3576/sepultura 27: 408–538 cal CE (1595±25 BP, PSUAMS-2117)

1090 **El Maraute (Torrenueva, Granada, Andalusia, Spain)**

1091 *Contact: Juan Manuel Jiménez Arenas, Isidro Jorge Toro Moyano*

1092 This necropolis is located on top of a hill within the Torrenueva town limits (88). The  
1093 bodies were in lateral decubitus position on the right side oriented west-east, facing the  
1094 south and with flexed limbs, except one adult individual found in a prone position with  
1095 the head oriented south, hands united below the body and crossed legs. This generally  
1096 corresponds to the Islamic funerary rite.

1097 In the same stratigraphic level, a trapezoidal house with internal divisions was  
1098 documented. This house had a kitchen area and a space with lime floor with abundant

1099 ceramics for presenting food dated to the 10th and 11th centuries CE, such as “ataifores”  
1100 with green and manganese epigraphy (al-mulk) and fragments of kitchen ceramics.

1101 We analyzed one individual from this site:

- 1102 • I7500/Individuo 2: 900–1100 CE

### 1103 **Paseillos universitarios-Fuentenueva (Granada, Andalusia, Spain)**

1104 *Contact: Juan Manuel Jiménez Arenas, Isidro Jorge Toro Moyano*

1105 The villa of the “Paseillos universitarios” is located in the city of Granada. The earliest  
1106 phase has a Late Roman chronology (3rd-5th centuries CE) featuring an *horreum*, silos  
1107 and one *torcularium* (89), and is associated to a necropolis from which the individuals  
1108 analyzed in this study were sampled:

- 1109 • I3980/Individuo 221: 432–601 cal CE (1520±20 BP, PSUAMS-2110)
- 1110 • I3981/Individuo 234: 400–600 CE

### 1111 **Nécropolis de Torna Alta (Mondújar (Lecrín), Granada, Andalusia, Spain)**

1112 *Contact: Juan Manuel Jiménez Arenas, Isidro Jorge Toro Moyano*

1113 A few meters from the Cerrillo de Mondújar, in the field known as Torna Alta, a series  
1114 of surveys were made in different farming terraces. Three burials were found and  
1115 consequently an excavation of the area was carried out, identifying a total of 53 burials  
1116 (90). The orientation and cover structures indicated an Islamic origin. The excavation  
1117 determined that the necropolis had one short phase of occupation, following the  
1118 traditional typology without external indications and in some cases with double slate or  
1119 flat stone as cover. All these features, which match descriptions in the 16th century book  
1120 “Libro de Apeo de Mondújar”, and the finding of a Castilian coin dated to the 16th century  
1121 CE above the layer of the site, are consistent with an assignment to the 16th century and  
1122 its interpretation as belonging to the *morisco* population (former Muslims converted to  
1123 Christianity until their expulsion around 1610 CE). We analyzed eight individuals from  
1124 this site:

- 1125 • I3807/Individuo 34: 1500–1600 CE.
- 1126 • I7426/Individuo 32: 1500–1600 CE
- 1127 • I3809/Individuo 5: 1500–1600 CE

1128 • I7423/Individuo 34bis: 1500–1600 CE

1129 • I3810/Individuo 9: 1500–1600 CE

1130 • I7424/Individuo 8: 1500–1600 CE

1131 • I3808/Individuo 2: 1500–1600 CE

1132 • I7425/Individuo 16: 1500–1600 CE

1133 **Plaza Einstein (Granada, Andalusia, Spain)**

1134 *Contact: Juan Manuel Jiménez Arenas, Isidro Jorge Toro Moyano*

1135 The Roman villa of Camino de Ronda-Plaza Einstein is located in the city of Granada  
1136 and is associated to a necropolis, both dated to the 3rd and 4th centuries CE (89). A final  
1137 phase features several pits cutting the structures of the villa and three silos, all of them  
1138 filled with common ware with comb-incised decoration and African TSA (Terra sigillata  
1139 africana) type D tableware.

1140 We analyzed 4 individuals from this site:

1141 • I4054/Sondeo G2/UE217: 200–400 CE. Genetically a brother of I3983.

1142 • I4055/Tumba 49: 200–400 CE

1143 • I3983/Tumba 19: 265–427 cal CE (1660±25 BP, PSUAMS-2081)

1144 • I3982/Tumba 7: 200–400 CE

1145 **Necrópolis de las Delicias (Ventas de Zafarraya, Granada, Andalusia, Spain)**

1146 *Contact: Juan Manuel Jiménez Arenas, Isidro Jorge Toro Moyano*

1147 This necropolis is located within the Ventas de Zafarraya urban area, in the mountainside  
1148 of the Sierra de Alhama close to the El Boquete de Zafarraya, a natural pass from the  
1149 Malaga coast to the interior since antiquity. During the 1985 excavation, 33 tombs were  
1150 found (87, 91, 92). Three of them, not included in this study, were of clear Roman  
1151 tradition.

1152 The funerary rite of all the tombs was inhumation. The number of buried individuals  
1153 varies from one to four, with east-west orientation most common.

1154 A total of 16 graves had grave goods or some object of personal use such as glass bowls,  
1155 belt buckles, shells, iron rings, necklace beads, glasses with horizontal striae decoration,

1156 a rectangular belt brooch with decoration of cells filled with vitreous phase of Ostrogothic  
1157 influence, and a brooch and two sheets of Byzantine origin. The funerary ritual, the  
1158 constructive typology and the grave goods place this necropolis within the 5th-7th  
1159 centuries CE.

1160 We analyzed two individuals from this site:

- 1161 • I3584/Tumba XIX: 400–700 CE
- 1162 • I3585/Tumba XVIII: 677–866 cal CE (1250±25 BP, PSUAMS-2074)

1163 **La Angorrilla (Alcalá del Río, Sevilla, Andalusia, Spain)**

1164 *Contact: Domingo C. Salazar-García, Álvaro Fernández Flores*

1165 The archaeological site of La Angorrilla, which was excavated during the beginning of  
1166 the 21st century, is located on the southwest of the municipality of Alcalá del Río (Sevilla,  
1167 Spain). Its entire necropolis can be dated from the end of the 8th century to the middle of  
1168 the 6th century BCE (93). This "Tartessian" (or "orientalizante") necropolis shows a  
1169 variety of burial types in simple pits, mainly inhumations but a few primary and  
1170 secondary incinerations are also present. The tombs present rectangular shape and they  
1171 are oriented in west-east direction, a common feature amongst the necropolis of the  
1172 Phoenician archaic period in the Iberian Peninsula (93).

1173 We analyzed four individuals from this site:

- 1174 • I12173/ROD.03/25; UE 2007: 700–500 BCE
- 1175 • I12171/ROD.03/25; UE 1457: 700–500 BCE
- 1176 • I12560/S-EVA17170, ROD.03/25; UE 404, Tibia: 700–500 BCE
- 1177 • I12561/S-EVA17196, ROD.03/25; UE 1205, Tibia: 700–500 BCE

1178 **Mandubi Zelaia (Ezkio-Itsaso, Gipuzkoa, Basque Country, Spain)**

1179 *Contact: Javier Fernández-Eraso, José Antonio Mujika-Alustiza*

1180 This dolmen was discovered by J. Etxaniz and excavated between 1998–2000 by José  
1181 Antonio Mujika-Alustiza (94, 95). During excavation, two levels were discovered in the  
1182 interior of the chamber. The upper level contained with several individuals and grave  
1183 goods: a bronze awl, four arrowheads, two bone necklace beads and pottery sherds. The  
1184 lower level contained burials on the base slab of the chamber, four arrowheads, two bone



1185 awls and one bone chisel. Radiocarbon analysis of four individuals yielded the following  
1186 dates: 3502–3105 cal BCE (4585±40 BP, GrA-28313), 3498–3096 cal BCE (4560±50  
1187 BP, GrN-26174), 3347–3097 cal BCE (4500±30 BP, Beta 382963), 3348–2938 cal BCE  
1188 (4460±50 BP, GrN-26173), 3321–2921 cal BCE (4420±30 BP, Beta 382965).

1189 We analyzed five individuals from this site:

- 1190 • I7605/Mandubi Zelaia-13G-15.4 (x.32; y.9; z.158): 3500–2900 BCE
- 1191 • I7603/Mandubi Zelaia-13G-12.9 (x.10; y.74; z.152): 3500–2900 BCE
- 1192 • I7602/Mandubi Zelaia-13G-12.15 (x.4; y.74; z.151): 3500–2900 BCE
- 1193 • I7604/Mandubi Zelaia-13G-14.5: 3500–2900 BCE
- 1194 • I7606/Mandubi Zelaia-13H-16.37: 3500–2900 BCE

1195 **Jentillarri (Enirio-Aralar, Gipuzkoa, Basque Country, Spain)**

1196 *Contact: Javier Fernández-Eraso, José Antonio Mujika-Alustiza*

1197 Jentillarri is a gallery dolmen formed by 18 slabs. It was excavated in 1917 by José Miguel  
1198 de Barandiaran, Enrique de Eguren and Telesforo de Aranzadi (95). Human remains from  
1199 27 individuals were excavated, as well as pottery, awls and three arrowheads. We  
1200 analyzed four individuals from this site:

- 1201 • I11300/Ar-J11: 3400–3000 BCE
- 1202 • I11301/Ar-J14: 3341–3030 cal BCE (4480±30 BP, Beta 484117)
- 1203 • I11248/Ar-J6: 3400–3000 BCE
- 1204 • I11249/Ar-J10: 3400–3000 BCE

1205 **Ondarre (Aralar, Gipuzkoa, Basque Country, Spain)**

1206 *Contact: Javier Fernández-Eraso, José Antonio Mujika-Alustiza*

1207 This Bronze Age cist was excavated by José Antonio Mujika-Alustiza in 2011 (96). It  
1208 contains a small 150 cm long, 90-110 cm wide and 50-60 cm height chamber, formed by  
1209 eight disturbed limestone slabs and one sandstone slab.

1210 Fieldwork recovered several human bones corresponding to at least 4 individuals (one  
1211 infantile, one juvenile, one young adult and one mature adult), pottery sherds belonging

1212 to 6-7 undecorated vessels (two bowls, a carinated vessel and a S-shaped container), one  
1213 deteriorated pendant and a bipyramidal quartz crystal.

1214 We analyzed one individual from this site:

- 1215 • I1982/Ond zis 3D-2.19: 1729–1531 cal BCE (3340±30 BP, Beta-350136)

1216 **La Braña-Arintero (León, Castilla y León, Spain)**

1217 *Contact: Julio Manuel Vidal Encinas*

1218 This site was described in Olalde et al. 2014 (97). We analyzed a phalanx from LaBraña2  
1219 individual, who is genetically a brother of LaBraña1.

- 1220 • I0843/LaBraña2: 6010–5796 cal BCE (7030±50 BP, Beta-226473)

1221 **Camino de las Yeseras (San Fernando de Henares, Community of Madrid, Spain)**

1222 *Contact: Corina Liesau, Concepción Blasco, Patricia Ríos*

1223 This site was described in Olalde et al. 2018 (9). We analyzed one new individual from  
1224 Funerary Area 3, who corresponds to the only complete skeleton in the tomb:

- 1225 • I4246/RISE697, sample #7, Fondo 5 UE05 Muerto 1: 2473–2030 cal BCE [2473–  
1226 2299 cal BCE (3910±30 BP, PSUAMS-2119), 2280–2030 cal BCE (3650±40 BP, Beta-  
1227 184837)]

1228 **Fuente la Mora (Valladolid, Castilla y León, Spain)**

1229 *Contact: Domingo C. Salazar-García, Ángel Esparza Arroyo, Javier Velasco Vázquez,*  
1230 *Germán Delibes de Castro*

1231 The site of Fuente la Mora is a “pits site” with occupational levels from the Neolithic to  
1232 the Early Iron Age. Some of the excavated structures have been attributed to the  
1233 archaeological culture Cogotas I (Central Iberian Meseta Middle-Late Bronze Age, ca.  
1234 1850-1150 cal BCE). Three of them contained human remains: three primary burials of  
1235 an infant and two adults. The individual sampled for DNA analysis was a 20-25-year-old  
1236 female:

- 1237 • I3491/S-EVA 26054: 1850–1150 BCE

1238 **La Requejada (San Román de Hornija, Valladolid, Castilla y León, Spain)**

1239 *Contact: Germán Delibes de Castro, Ángel Esparza Arroyo, Javier Velasco Vázquez*

1240 La Requejada is a site located at a fluvial terrace of the river Duero. Excavations revealed  
1241 a ‘pits site’ with numerous structures dug on gravel and filled with refuse material such  
1242 as ceramic sherds, lithic objects, animal bones, etc (98). Furthermore, a pit burial was  
1243 found with the remains of three individuals synchronously buried (61, 99): a young adult  
1244 female (SRH-01), a senile female (SRH-02) and an infantile male (SRH-03). All the  
1245 materials and structures belonged to a short occupation phase of the Late Bronze Age  
1246 Cogotas I culture ~1400–1300 BCE. We generated data from SRH-02 and SRH-03.

1247 • I12208/SRH-02: 1368–1211 BCE

1248 • I12209/SRH-03: 1368–1211 BCE

1249 **Humanejos (Parla, Community of Madrid, Spain)**

1250 *Contact: Rafael Garrido-Pena, Raúl Flores-Fernández. Ana M. Herrero-Corral*

1251 This site was described in Szécsényi-Nagy et al. 2017 (58). A total of 11 Copper Age  
1252 individuals from this site were analyzed in Olalde et al 2018 (9). We analyzed one new  
1253 individual dated to the Bronze Age.

1254 • I6618/Hume 1A, 443: 1879–1693 cal BCE (3458±24 BP, MAMS-32475)

1255 **Tordillos (Aldeaseca de la Frontera, Salamanca, Castilla y León, Spain)**

1256 *Contact: Domingo C. Salazar-García, Ángel Esparza Arroyo, Javier Velasco Vázquez,*  
1257 *Germán Delibes de Castro*

1258 The site of Tordillos presents, like other ‘pits sites’ of the archaeological culture Cogotas  
1259 I (Central Iberian Meseta Middle-Late Bronze Age, ca. 1850–1150 cal BCE), contains  
1260 hundreds of dug structures that were originally grain storage pits and that are filled with  
1261 waste material (potsherds, animal bones, ashes). Nine pits with human remains from 20  
1262 skeletons in secondary position were also found, some of which were previously exposed  
1263 as indicated by canid bite marks and erosive processes detected during the  
1264 bioarchaeological study (100).

1265 We analyzed 2 individuals from this site:

1266 • I3492/S-EVA 26043: 1850–1150 BCE

1267 • I3493/S-EVA 26050: 1420–1283 cal BCE (3090±25 BP, PSUAMS-2072)

1268 **Galls Carboners (Mont-ral, Tarragona, Catalonia, Spain)**

1269 *Contact: Josep Maria Vergès, Marina Lozano*

1270 The Cova dels Galls Carboners site is located in the Prades Mountains, at 965 m a.s.l., on  
1271 the western margin of the Brugent river valley. Although the cave is located in a steep  
1272 area, it is 10 km away from Camp de Tarragona littoral plain connected with Francolí  
1273 river, of which the Brugent river is tributary, and 25 km from the Mediterranean Sea. The  
1274 NE oriented cave entrance is open to 5.5 meters high in an almost vertical rocky wall.  
1275 The cave is 70 meters long. To get to the inner-most part, where individuals have been  
1276 recovered, one has to bend or crawl after passing through a 40 cm diameter crawl. The  
1277 collective burial was excavated in different periods, the first in the 1970's and the second  
1278 between 2009 and 2010. Along with human remains belonging to a minimum of 17  
1279 individuals of different ages (adults and subadults), some ceramic fragments and  
1280 ornamentation beads made using shell fragments were recovered (101). Our direct dating  
1281 of a human tooth points to a Chalcolithic date of 3020-2909 cal BCE (4355±20 BP).  
1282 However, direct dates of a human phalanx and human teeth place most of the remains  
1283 from this site in the Middle Bronze Age ~1750–1500 BCE.

1284 We analyzed seven individuals from this site:

1285 • I4565/GC.I-1-c.n10: 3020–2909 cal BCE (4355±20 BP, PSUAMS-2866)

1286 • I4558/GC.2.126.n146: 1700–1500 BCE

1287 • I4563/GC.2.150.n170 and GC.2.149.n169: 1700–1500 BCE

1288 • I4559/GC.2.127.n147: 1700–1500 BCE

1289 • I4560/GC.2.132.n152: 1700–1500 BCE

1290 • I4561/GC.2.135.n155: 1700–1500 BCE

1291 • I4562/GC.2.138.n158: 1738–1623 cal BCE (3375±20 BP, PSUAMS-3191)

1292 **Mas Gassol (Alcover, Tarragona, Catalonia, Spain)**

1293 *Contact: Josep Maria Vergès*

1294 The Mas Gassol site is located on the north-western margin of the Camp de Tarragona  
1295 plain, at 235 meters a.s.l., at the foothills of the Prades Mountains, 18 km away from the

city of Tarragona on the Mediterranean coast. The human remains reported in this study come from a small necropolis, dated between the 3rd and 5th centuries CE, associated to a Roman *villa rustica* (countryside villa), a farm-house that functioned as a residence of the landowner, his family and his servants (retainers and farm labourers), as well as a farming management center. Tarragona (*Tarraco*) was the oldest Roman settlement of the Iberian Peninsula (218 BCE) and became capital of the Roman province of *Hispania Citerior* (197–27 BCE) and later *Hispania Tarraconensis* (27 BCE – 476 CE). Its hinterland (named *Ager Tarraconensis*) was occupied by many *villae* dedicated to agriculture and livestock exploitation.

The necropolis of Mas Gassol was composed of six graves, five funerary boxes made using *tegulae* and limestone slabs from local quarries, and one wood coffin. The graves contain 10 individuals: 8 adults and 2 children. In three cases, the funerary box contains more than one individual: 2 adults in two cases and 2 adults and 1 child in the other case. The wooden coffin contains the remains of a child of 5-6 years of age. All the graves are oriented NW-SE, with the head on the NW side, looking towards the rising of the sun (102).

We analyzed 4 individuals from this site:

- I7158/MGA'92 UE 108: 200–500 CE
- I6492/MGA'92 UE 105: 200–500 CE
- I6490/MGA'92-Resta II: 200–500 CE
- I6491/MGA'92-Resta III: 200–500 CE

**Coveta del Frare (La Font de la Figuera, València/Valencia, Valencian Community, Spain)**

*Contact: Pablo García Borja, Mario Sanz Tormo*

This site is located east of the hill known as “El Frare” or “Moleta del Frare”. It is a 5-meter-deep, 11-meter-wide rock shelter with a 0.8-1-meter-height entrance oriented towards the northeast. In 1968, a group of people who lived near the site found many archaeological remains, including human skulls belonging to at least 4 individuals. Archaeological study of those materials confirmed the presence of four individuals, two dated to the Chalcolithic and the other two to the Bronze Age (103). The analyzed sample belonged to a male individual from the Early Bronze Age:

1327 • I3494/CF-1: 1920–1753 cal BCE (3515±30 BP, CNA-1661.1.1)

1328 **Cueva de la Cocina (Dos Aguas, València/Valencia, Valencian Community, Spain)**

1329 *Contact: Oreto García-Puchol, Sarah B. McClure, Joaquim Juan-Cabanilles, Agustín A.*

1330 *Diez-Castillo*

1331 Cocina cave is an archaeological site with Holocene human occupations located in the

1332 municipality of Dos Aguas in eastern Spain. The cave opens to the La Ventana ravine and

1333 is surrounded by the rugged landscape of the southern Iberian ranges, close to the

1334 Mediterranean Sea (ca. 30 km). Humans occupied the site during the Holocene with

1335 evidence of Mesolithic hunter-gatherers as well as several discontinuous archaeological

1336 levels from the Early Neolithic to the Bronze Age (104).

1337 Research at Cocina Cave began in the 1940's (1941 to 1945), when Pericot excavated

1338 roughly 80 square meters at the entrance of the cave. This work produced the rich

1339 archaeological material currently deposited in the Valencian Museum of Prehistory/SIP,

1340 and identified a remarkable collection of portable art (105). In the 1970s, Javier Fortea

1341 leveraged the archaeological materials from Cocina Cave to shed light on the

1342 development of late Mesolithic hunter-gatherers and the transition to agriculture in the

1343 Neolithic (106). The investigation revealed the site's potential for characterizing late

1344 hunter-gatherer socioecological dynamics and the processes linked with the start of the

1345 Neolithic in the region. Fortea also excavated in the cave for seven field seasons (1974 to

1346 1981) in order to investigate the hypothesis of a gradual acculturation process to explain

1347 how last hunter-gatherers became farmers and herders (107). He focused the excavation

1348 in a large area located in the inner part of the cave using up-to-date excavation techniques,

1349 although most of the results remained unpublished (107, 108).

1350 Since 2014, an international research team led by Oreto García-Puchol, Sarah B. McClure

1351 and Joaquim Juan Cabanilles has been working at the site in the framework of two

1352 research projects -*MESO-COCINA* (Har2012-33111) and *EVOLPAST* (Har2015-68962),

1353 funded by government of Spain, to explore the site deposits in the context of the

1354 Neolithization process in Western Mediterranean. These studies are analyzing cultural

1355 and biotic assemblages recovered in the previous archaeological seasons with new

1356 methodological advances including three dimensional environmental modeling (108).

1357 The project also includes new excavations in order to resolve specific questions about

1358 cultural and sedimentary history, chronology, and stratigraphy (104, 109).

This analysis recently produced (104, 110) an accurate chronological framework for the Mesolithic levels making it possible to test hypotheses about the extent to which the early Neolithic sequence was shaped by acculturation or colonization model (or other possible scenarios), using data from both Pericot's and Fortea's excavations. The current revision of Pericot's archaeological and biological record has revealed the presence of human remains in the Mesolithic deposits.

Briefly, the chronology of archaeological deposits at the site starts with a long Mesolithic sequence that encompass the 7th millennium and the first centuries of the 6th millennium BCE including several episodes related to both regional phase A (with trapezes) and phase B (with triangles). At the moment, the Early Neolithic context is dated not before the last centuries of the 6th millennium BCE. The current radiocarbon dataset also reflects some Late Neolithic/Chalcolithic and Bronze Age occupations of the site (104).

We analyzed one individual from a tooth recovered in the 1941 Pericot's trench corresponding to a Mesolithic layer (layer 2):

- I8130/C. Cocina-25-7-41-capa 2: 6061-5934 cal BCE (7135±25 BP, PSUAMS-4429)

#### **Lloma de Betxí (Paterna, València/Valencia, Valencian Community, Spain)**

*Contact: Pablo García Borja, María Jesus de Pedro Michó*

This Bronze Age site was first discovered in 1928 but archaeological work began in 1984 under the direction of María Jesús de Pedro Michó and the patronage of the "Museu de Prehistòria de València". It is a small settlement located at a small hill and made out of stone. Its destruction due to a fire has preserved many domestic objects including pottery, flints, handmills, metal objects, counterbalance looms and fragments of ornaments. Different areas were identified including a warehouse and milling and loom spaces. Two human burials were discovered outside the living space: one senile male buried with a small dog and a male burial in fetal position with flexed arms and legs and delimited with a circular stone structure (111). The tooth analyzed with aDNA belonged to the second individual:

- I3997/LLBE-30593: 1864–1618 cal BCE (3400±40 BP, Beta-195318)

1387 **Cova de Sant Gomengo (La Font de la Figuera, València/Valencia, Valencian**  
1388 **Community, Spain)**

1389 *Contact: Pablo García Borja, Mario Sanz Tormo*

1390 This cave site is located on the northern slope of Mont Capurutxo in La Font de la Figuera.  
1391 In 1970 a group of locals found Late Neolithic/Chalcolithic and Iron Age archaeological  
1392 materials in the interior of the cave. The Late Neolithic material included pottery, a flint  
1393 arrowhead, a hoe made of polished stone and collar beads, and a set of human remains  
1394 including two mandibles (112). We analyzed one tooth from one of the mandibles:

- 1395 • I8566/C.560: 3800–2500 BCE

1396 **La Coveta Emparetà (Bocairent, València/Valencia, Valencian Community, Spain)**

1397 *Contact: Pablo García Borja, Isabel Collado Beneyto*

1398 This cave site is located on the northern slope of the “Serra Mariola”. It is a 10-meter-  
1399 long, 2.5-meter-wide cave with an irregular layout. It has a wide entrance oriented  
1400 towards the west dominating a large part of the valley. At least four burials were deposited  
1401 inside the cave (113), two dating to the Bronze Age. Two teeth recovered from the  
1402 superficial level and not associated with any mandible were selected for analysis:

- 1403 • I8567/C.E.-1: 3500–3300 BCE
- 1404 • I8568/C.E.-2: 3499–3353 cal BCE (4615±20 BP, PSUAMS-4432)

1405 **La Vital (Gandia, València/Valencia, Valencian Community, Spain)**

1406 *Contact: Yolanda Carrión Marco, David López-Serrano, Pablo García Borja*

1407 This open-air site is located at the river Serpis terraces in the city of Gandia. The  
1408 excavation has yielded numerous prehistoric remains dated from the Chalcolithic to the  
1409 Iron Age (114). In 2017, archaeological work was undertaken by the rescue archaeology  
1410 company “Estrats, Treballs d’Arqueologia SL” due to the construction of the “Acceso  
1411 Sur al Puerto de Gandía” by the “Ministerio de Fomento”. During the last dig a series of  
1412 prehistoric negative structures dated to the Chalcolithic were excavated. Inside one of  
1413 these pits three human skeletons were discovered, two of which were almost complete,  
1414 but their anatomic distribution suggested that they had been thrown in. No cultural  
1415 artifacts or other ritual signs were found. We sampled three teeth for analysis, two of  
1416 which belonged to the same individual:



1417 • I8131/A56-2017-UE5114 Diente 2, Diente 3: 2578–2457 cal BCE (3980±30 BP,  
1418 Beta-504712)

1419 • I8132/A56-2017-UE5114 Diente 1: 2600–2400 BCE

1420 **Carrer Sagunto 49 (València, València/Valencia, Valencian Community, Spain)**

1421 *Contact: Pablo García Borja, Guillermo Pascual Berlanga*

1422 Archaeological excavations were carried out at Sagunto street numbers 45, 47 and 49  
1423 (city of València) in 1997. An Islamic necropolis dated to the 12th-13th centuries CE was  
1424 found on the right banks of the Turia river. We analyzed seven individuals from this site:

1425 • I12644/UE 1617: 1100–1300 CE

1426 • I12645/UE 1813: 1100–1300 CE

1427 • I12646/UE 1637: 1100–1300 CE

1428 • I12647/UE 1996: 1100–1300 CE

1429 • I12648/UE 1117: 1100–1300 CE

1430 • I12649/UE 2194: 1100–1300 CE

1431 • I12650/UE 1384: 1100–1300 CE

1432 **Túmulo Mortòrum (Cabanès, Castelló/Castellón, Valencian Community, Spain)**

1433 *Contact: Gustau Aguilera Arzo, Pablo García Borja*

1434 The Túmulo del Mortòrum is a collective burial dated to the Bronze Age but has feature  
1435 that are reminiscent of megalithism, a tradition not attested in the province of  
1436 Castelló/Castellón. It is a tumulus structure with a simple chamber, no corridor and stone  
1437 cover (115). The tomb itself was pillaged by grave robbers but it was possible to recover  
1438 six individuals buried during the Bronze Age. We analyzed two individuals:

1439 • I8570/ID6: 1800–1000 BCE

1440 • I8571/ID4: 1800–1000 BCE

1441 **Cova dels Diablets (Alcalá de Xivert, Castelló/Castellón, Valencian Community,**  
1442 **Spain)**

1443 *Contact: Gustau Aguilera Arzo, Pablo García Borja*

1444 The Cova dels Diablets controls a small interior valley in the foothills of the “Serra d'Irta”  
1445 in Alcalá de Xivert. The cave had occupation levels dated to the end of the Paleolithic  
1446 (Epi-Magdalenian), Early Neolithic and Chalcolithic (116). The human remains  
1447 comprised four individuals from the later Chalcolithic period. We sampled one tooth from  
1448 the “nivel 1 cuadro Q1”:

- 1449 • I8569/Q1-N-1: 2871–2626 cal BCE (4141±21 BP, MAMS-18651)

1450 **Palau Castell de Betxí (Betxí, Castelló/Castellón, Valencian Community, Spain)**

1451 *Contact: Gustau Aguilera Arzo, Pablo García Borja*

1452 In 2017, during the restoration works of the Palace-Castle of Betxí, five Islamic  
1453 inhumations were discovered. Their chronology was confirmed by radiocarbon dating of  
1454 individual UE 119A, and showed that they belonged to a necropolis in use before the  
1455 construction of the Medieval fortress during the 14<sup>th</sup> century CE. We analyzed two  
1456 individuals from this site:

- 1457 • I12514/UE 119A: 1020–1155 cal CE (960±30 BP, Beta-459794)  
1458 • I12515/UE 102: 1000–1200 CE. Genetic data indicate that this individual is a 2nd-  
1459 3rd-degree relative of I12514.

1460 **Plaza Parroquial (Vinaròs, Castelló/Castellón, Valencian Community, Spain)**

1461 *Contact: Gustau Aguilera Arzo, Pablo García Borja*

1462 During rescue excavations of the medieval wall of Vinaròs in the Plaza Parroquial, one  
1463 inhumation was found. The location suggested that the remains were earlier than the  
1464 construction of the wall, which was confirmed by radiocarbon dating:

- 1465 • I12516/UE 30001-3: 901–1116 cal CE (1030±30 BP, Beta-372984)

1466 **Gruta do Medronhal (Arrifana, Coimbra, Portugal)**

1467 *Contact: Ana Maria Silva*

1468 In the 1940s, human bones, metallic artifacts (n=37) and non-human bones were  
1469 discovered in the natural cave of Medronhal (Arrifana, Coimbra). All these findings are

1470 currently housed in the Department of Life Sciences of the University of Coimbra and  
1471 are analyzed by a multidisciplinary team. The artifacts suggest a date at the beginning of  
1472 the 1<sup>st</sup> millennium BC, which is confirmed by radiocarbon date of a human fibula: 890–  
1473 780 cal BCE (2650±40 BP, Beta–223996). This natural cave has several rooms and  
1474 corridors with two entrances. No information is available about the context of the human  
1475 remains. Nowadays these remains are housed mixed and correspond to a minimum  
1476 number of 11 individuals, 5 adults and 6 non-adults.

1477 We analyzed two individuals from this site:

- 1478 • I7688/GM-23: 1200–700 BCE
- 1479 • I7687/GM-504: 1200–700 BCE

### 1480 **Monte da Cabida 3 (São Manços, Évora, Portugal)**

1481 *Contact: Ana Maria Silva*

1482 The Necropolis of Monte da Cabida 3 (São Manços, Évora, Portugal) was discovered in  
1483 2004. Excavations performed during the year of 2007 revealed human remains buried in  
1484 cists and pit burials, all dated to the Bronze Age (117). The human bone samples we  
1485 analyze here were recovered from two pit burials (I7689 and I7691), and one from a  
1486 rectangular cist (I7692). This last tomb contained two adults, and the individual analyzed  
1487 here was the final interment. Bones from a previous deposition were found dispersed  
1488 within the tomb.

1489 We analyzed 3 individuals from this site:

- 1490 • I7689/MC-3-Sep.14-960: 2200–1700 BCE
- 1491 • I7691/MC3-945-NÃ\_2: 2200–1700 BCE
- 1492 • I7692/MC3-Sep9: 2200–1700 BCE

### 1493 **Perdigões (Reguengos de Monsaraz, Évora, Portugal)**

1494 *Contact: Ana Maria Silva, António C. Valera*

1495 At the Perdigões ditched enclosure, twelve pits were identified and excavated during the  
1496 field campaigns of 2007/8. In two of them, pits 7 and 11, partial human skeletal remains  
1497 were found in primary context and anatomical connection (118).

In pit 11, only a small segment of the west part of the subcircular pit was found undisturbed. Three very incomplete and highly fragmented non adult skeletons (UE 76, 77 and 78) were unearthed. A Suidae paw and a cockle shell were found associated. UE 76 was a non-adult that died around 16/17 years based on dental age (root development of third upper molar). This skeleton was deposited on its right side, SW – NE orientated. A hand bone of this individual confirm the Late Neolithic chronology of these remains (3020–2910 cal BCE (4370 ± 40 BP, Beta-289263)). Non-adult 77, placed on the left side, flexed, N – S oriented, died at around age 5, based on dental calcification. With the exception of two teeth with linear enamel hypoplasia (physiological stress indicator), no other signs of pathology were detected. Non-adult 78 was lying on its left side, head orientated north. Age at death estimation of this individual based on several teeth fall between 12.7 and 14.8 years. The left radius allowed an estimation of 12 years. With the exception of an enamel hypoplasia in pit form observed in the lower left central incisor, no other signs of pathology were noted (119).

We analyzed two individuals from this site:

- I3432/Pit 11, UE77: 3082–2909 cal BCE (4365±25 BP, PSUAMS-1882)
- I5429/Pit 11, UE78: 3010–2887 cal BCE (4310±20 BP, PSUAMS-2692)

#### **Monte Canelas 1 (Alcalar, Faro, Portugal)**

*Contact: Ana Maria Silva*

This site was described in Martiniano et al. 2017 (6). We analyzed one new individual:

- I5076/MCI.228: 3335–3026 cal BCE (4465±25 BP, PSUAMS-3902)

#### **Cova das Lapas (Alcobaça, Leiria, Portugal)**

*Contact: Ana Maria Silva, Ana Catarina Sousa and Victor S. Gonçalves*

Cova das Lapas is a very small cave located in the Limestone Massif of Estremadura that was intensively used as a burial space. The excavation fieldworks were directed under direction of Victor S. Gonçalves in 1984, 1986 and 1987. The sequence of absolute dating and votive artifacts indicates that this necropolis was used over a relatively short period between 3245–3263 and 3036–2913 BCE. It was possible to identify several individualized and coupled burials and a complex sequence of management of the space with successive depositions and ossuaries. The votive artifacts include the characteristic elements of the magic-religious complex of the first and second phases of Megalithism:

1529 geometric armatures (all trapezes), blades, daggers, scarce ceramics and one engraved  
1530 schist plaque placed in the chest of a young person, which is very uncommon.

1531 We analyzed one individual from this site:

- 1532 • I5428/CLA6: 3300–2900 BCE

### 1533 **Casas Velhas (Melides, Setúbal, Portugal)**

1534 *Contact: Ana Maria Silva*

1535 The necropolis of Casas Velhas was discovered during the 1970s. Excavations were  
1536 undertaken by the Museum of Archaeology and Ethnography of the District of Setúbal  
1537 (Portugal) during 1975 and 1996 under the direction of Carlos Tavares da Silva and  
1538 Joaquina Soares. This necropolis is composed by 35 graves, mostly small stone cists. The  
1539 cists, highly disturbed by agriculture, were mostly composed of four upright slabs of  
1540 limestone or ferruginous breccia. The maximum lengths of these tombs were less than  
1541 1m. The cemetery belongs to the Southwest Iberian Bronze Age that was widespread  
1542 across the south of Portugal (Alentejo and Algarve) and southwest Spain, including the  
1543 regions of Huelva, Badajoz and Seville (120, 121). In funerary terms, this culture was  
1544 characterized by individual burials deposited in lateral fetal position, mostly inside small  
1545 stone cists, sometimes with funerary ceramic vessels, metallic objects and/or faunal  
1546 remains. These burials are predominantly individual, but double, triple and quadruple  
1547 (usually not simultaneous) interments are also documented (122). Casas Velhas  
1548 represents the site with best preserved human remains in Portugal for this culture and  
1549 period (122, 123). Radiocarbon dating of human bones from two cists confirmed the  
1550 Bronze Age chronology of these remains (cist 14 - 1670-1410 cal BCE (3255±55BP,  
1551 OxA-5531); and cist 35 - 1680-1415 cal BCE (3260±60BP, Beta-127904)) (124, 125).

1552 Preliminary results indicate that of the 35 graves, 20 contained human bone, 19 of which  
1553 were available for detailed anthropological analysis. Of these, 15 were individual tombs,  
1554 3 double and 1 triple, corresponding to a minimum number of 24 individuals, 22 adults  
1555 and 2 non-adults. Cist 30 contained the bones of two adults. The last interment of this  
1556 tomb belonged to an adult female more than 30 years old, the sample analyzed here  
1557 (I8045). This female was deposited in crouched position, lying on the right side,  
1558 orientated East (head) – West. In front of the pelvic region of this skeleton a ceramic  
1559 vessel was recovered. The bones from the left forelimb of an adult individual of *Bos*  
1560 *taurus* (radius, ulna, lunate and scaphoid bone) were also recovered from this cist,  
1561 although only the exact position of the *Bos* radius is known, apparently associated with

1562 the last interment. The other individual was identified through the duplication of some  
1563 teeth, belonging to an adult of unknown sex.

- 1564 • I8045/CV-Sep30.8: 1700–1300 BCE

#### 1565 **Bolores (Torres Vedras, Lisboa, Portugal)**

1566 *Contact: Katina Lillios*

1567 This site is described in Szécsényi-Nagy et al (58). We successfully analyzed 2  
1568 individuals:

- 1569 • I11614/MS024: 2800–2600 BCE
- 1570 • I11592/MS002: 2800–2600 BCE

#### 1571 **Cabeço da Arruda I (Torres Vedras, Lisboa, Portugal)**

1572 *Contact: Ana Maria Silva*

1573 This site is described in Martiniano et al (6). We successfully analyzed 3 individuals:

- 1574 • I11599/MS009: 3400–2800 BCE [layer date based on a long bone from a likely  
1575 different individual 3330–2885 cal BCE (4370±70 BP, Beta–123363)]
- 1576 • I11601/MS011: 3400–2800 BCE [layer date based on a long bone from a likely  
1577 different individual 3330–2885 cal BCE (4370±70 BP, Beta–123363)]
- 1578 • I11600/CA122A, CabecoArruda122A: 3400–2800 BCE [layer date based on a long  
1579 bone from a likely different individual 3330–2885 cal BCE (4370±70 BP, Beta–123363)].  
1580 This is a sample from the same individual as CabecoArruda122A, who was analyzed in  
1581 Martiniano et al (6).

#### 1582 **Tholos of Paimogo I (Lourinhã, Lisboa, Portugal)**

1583 *Contact: Ana Maria Silva*

1584 Paimogo I (or Pai Mogo I) is a corbel-vaulted tomb located in Lourinhã (Portugal), 1 km  
1585 from the Atlantic coast. The site was discovered in 1968, and excavated in 1971 (126).  
1586 The tomb consists of a nearly elliptic burial chamber (diameter 4.85 m East-West and 4.5  
1587 m North-South) and a corridor 6.6 m length. An extensive array of objects, dated to the  
1588 Late Neolithic and Chalcolithic were recovered, such as decorated pre-Beaker and Beaker  
1589 ceramics, groundstones and flaked stone tools, bone tools, limestone idols, other

1590 limestone objects, and copper implements (*126, 127*). Several radiocarbon dates were  
1591 obtained on human bones, which produced consistent date ranges between the end of 4th  
1592 millennium to the middle of 3rd millennium: 3095–2575 cal BCE (4250±90 BP, Sac-  
1593 1556) and 2619–2475 cal BCE (4030±25 BP, UGAM-22150) (*128*).

1594 Little information is available about the context of the human remains recovered from  
1595 this burial. These were found commingled and fragmented but with good preservation.  
1596 The first anthropological study performed by Silva revealed a minimal number of 413  
1597 individuals: 290 adults and 123 non-adults (*128, 129*). This collection was further  
1598 analyzed for dietary evidences using stable isotopic data (*130*), strontium isotope analysis  
1599 to identify territorial mobility patterns (*131*), physiological stress indicators (*132*),  
1600 fractures patterns, among others.

1601 We successfully analyzed 2 individuals from this site:

- 1602 • I11604/MS014: 3100–2500 BCE  
1603 • I11605/MS015: 3100–2500 BCE

1604

## SI 2 - Direct AMS <sup>14</sup>C Bone Dates

Bone samples for the newly reported direct AMS <sup>14</sup>C dates (Table S3) from Penn State (PSUAMS) were manually cleaned to remove sediment, conservants and adhesives. Parts of bones with obvious signs of glues, written catalog numbers, etc. were avoided for sampling. All samples were physically broken down to 1-3 mm pieces to aid demineralization and then sonicated in successive solvent washes of methanol, acetone and dichloromethane (a substitute for the more toxic chloroform) and rinsed repeatedly in 18.2 MΩ·cm<sup>-1</sup> water. Samples were demineralized in 0.5N HCl for 2-3 days at ~5°C, and soaked in 0.1N NaOH at room temperature to remove contaminating soil humates. Samples were then rinsed to neutrality in 18.2 MΩ·cm<sup>-1</sup> water and gelatinized in 0.01N HCL for 12 hrs at 60°C (133). The resulting gelatin was lyophilized and weighed to determine percent crude gelatin yield as a measure of collagen preservation. After assessing gelatin yield and qualitative indicators of preservation (e.g., persistent coloration suggestive of incomplete humate removal, gelatin was further purified by ultrafiltration, using precleaned Centriprep® filters retaining >30 kDa gelatin. More poorly preserved samples were hydrolyzed in 1.5 mL of 6N HCl at 100°C for 24 hrs, and then run through Supelco ENVI-Chrom° solid phase extraction columns to remove humates and other polar contaminants (“XAD” purification; detailed methods described in Lohse et al. 2014 (134)).

The resulting material, >30 kDa gelatin or purified amino acid hydrolyzate, was submitted to the Yale Analytical and Stable Isotope Center for EA-IRMS analysis, with %C, %N and C:N ratios and δ<sup>13</sup>C and δ<sup>15</sup>N evaluated before AMS <sup>14</sup>C dating. C:N ratios for well-preserved samples fall between 2.9 and 3.6, indicating good collagen preservation (135); in practice the observed range tends to be between 3.1 and 3.4.

Pretreated samples were converted to CO<sub>2</sub> in 6 mm OD clear fused quartz tubing prebaked at 900°C for 3 hrs, along with ~60 mg of CuO wire and ~3 mm of Ag wire, and sealed under vacuum on a line backed with an oil free turbopump system. Ultrafiltered gelatin (~2.2 mg) was packed into 6” tubes and combusted for 3 hrs at 900°C, while hydrolyzed amino acids (~4.0 mg) were packed into 8” tubes and combusted for 3 hrs at 800°C. Sample CO<sub>2</sub> was converted to graphite by hydrogen reduction onto an Fe catalyst (5.5-6.5 mg) at 550°C for 3 hrs (136) with reaction water is drawn off with Mg(ClO<sub>4</sub>)<sub>2</sub> (137). Sample graphite is pressed into Al targets for AMS measurement along with graphite of 6 OXII primary standards, and bone backgrounds (SR-5156 Beaufort Whale) and secondaries (AD 1800s cow bone, 1850 BP bison bone, and 5670 BP sea lion bone) for



each run. AMS  $^{14}\text{C}$  measurements were made on a modified NEC 500kV 1.5SDH-1 compact AMS at the Penn State AMS  $^{14}\text{C}$  laboratory. Conventional  $^{14}\text{C}$  ages were corrected for fractionation during graphitization and measurement with  $\delta^{13}\text{C}$  values measured on the AMS following the conventions of Stuiver and Polach 1977 (138).

### SI 3 - Ancient DNA laboratory work

We performed laboratory work in dedicated clean rooms at the Reich's lab (Harvard Medical School). We extracted DNA (139–141) and built double-stranded and single-stranded DNA libraries (Table S2). Libraries were subjected to a partial uracil-DNA-glycosylase (UDG half) treatment to remove most of the ancient DNA damage while preserving the signal in the terminal nucleotides (1, 142–144). For single-stranded libraries we used E.coli UDG (USER from NEB) with the ssDNA2.0 protocol to achieve this; Adapter CL78 was replaced by TL181 (5'-AGATCGGAAGAAA[A][A][A][A][A][A]-3'; [A] = ortho methyl RNA), Splinter TL110 was replaced by TL159a (5'-[A][A][A]CTTCCGATCTNNNNNNNN[A]-3', [A] = ortho methyl RNA) and the extension primer CL130 was replaced by CL128 5'-GTGACTGGAGTTCAGACGTGTGCTCTTCC\*G\*A\*T\*C\*T-3'; \* = phosphor thioate. A subset of the double-stranded libraries were prepared with an automated liquid handler that uses silica magnetic beads instead of MinElute columns for cleanup steps). DNA libraries were enriched for human DNA using probes that target 1,233,013 SNPs ('1240k capture') (3, 12) and the mitochondrial genome. Captured libraries were sequenced on an Illumina NextSeq500 instrument with 2x76 cycles and 2x7 cycles (2x8 for single-stranded libraries) to read out the two indices (145).

#### Sampling and DNA extraction at the University of Huddersfield

We processed six samples (I11614, I11592, I11599, I11601, I11604, I11605) in clean rooms in the specialized Ancient DNA Facility at the University of Huddersfield, wearing full body suits, hairnets, gloves and face masks at all times. We constantly cleaned all tools and surfaces with LookOut® DNA Erase (SIGMA Life Sciences), as well as with bleach, ethanol and long exposures to UV light. We subjected six samples to UV-radiation for a total of 60 minutes (30 minutes each side) and cleaned sampling surfaces with 5 $\mu\text{m}$  aluminum oxide powder using a compressed air abrasive system. For the four petrous samples (two each from Bolores and Cabeço da Arruda I), we targeted the densest part of the bone; for the two tooth samples (both from Paimogo I), we removed the tooth root, using a circular saw attached to a hobby drill. We obtained bone and tooth root powder by crushing the excised petrous portion or tooth root in a MixerMill (Retsch

MM400). We extracted DNA from ~150 mg of powder following the protocol of Yang et al. 1998 (146), with modifications by MacHugh et al. 2000 (147). We included blank controls throughout extractions to monitor for possible modern DNA contamination. DNA extracts were shipped to Reich's lab.

#### SI 4 - Bioinformatics processing

Reads for each sample were extracted from raw sequence data according to sample-specific indices added during wetlab processing, allowing for one mismatch. Adapters were trimmed and paired-end sequences were merged into single ended sequences requiring 15 base pair overlap (allowing one mismatch) using a modified version of *SeqPrep 1.1* (<https://github.com/jstjohn/SeqPrep>) which selects the highest quality base in the merged region. Unmerged reads are discarded prior to alignment to both the human reference genome (hg19) and the RSRS version of the mitochondrial genome (148) using the 'samse' command in *bwa v0.6.1* (149). Duplicates were removed based on the alignment coordinates of aligned reads, as well as their orientation. Libraries were sequenced to saturation across multiple sequencing lanes where necessary, with complexity metrics established using *preseq* (150), merging where necessary. Subsequent authenticity of ancient DNA is established using several criteria: we discarded from further analysis libraries with a rate of deamination at the terminal nucleotide below 3%. We computed the ratio of X-to-Y chromosome reads, estimated mismatch rates to the consensus mitochondrial sequence, using *contamMix-1.0.10* (151) and ran X-chromosome contamination estimates using *ANGSD* (152) in males with sufficient coverage (Table S2). Libraries with evidence of contamination were discarded from genome-wide analyses or, in cases with sufficient data, restricted to sequences with cytosine deamination to remove potential contaminating sequences (Table S1).

We merged libraries from the same individual and required a minimum of 10,000 SNPs with at least one overlapping sequence for inclusion in genome-wide analyses. Individuals that were first-degree relatives of others in the dataset with higher coverage were also excluded for genome-wide analyses (Table S1).

#### SI 5 - Mitochondrial and Y-chromosome haplogroup determination

We determined mitochondrial DNA haplogroups (Table S1) for each individual using Haplogrep2 (153).

We performed Y-chromosome haplogroup determination (Table S4) using the nomenclature of the International Society of Genetic Genealogy (<http://www.isogg.org>) version 11.110 (21 April 2016). We restricted to sequences with mapping quality  $\geq 30$  and bases with quality  $\geq 30$ .

We comment here on the striking Y-chromosome patterns observed during the Copper Age-Bronze Age transition in Iberia. All the Bronze Age males from Iberia with sufficient coverage ( $n=30$ ) belonged to R1b-M269 (R1b1a1a2). Furthermore, all the R1b-M269 males with sufficient coverage ( $n=15$ ) could be further classified as R1b-P312 (R1b1a1a2a1a2). Only one Bronze Age male, esp005.SG (7), had DNA sequences overlapping R1b-DF27 (R1b1a1a2a1a2a) and he was positive for the mutation. Two Bronze Age males, I6470 and I3997, had DNA sequences overlapping R1b-Z195 (R1b1a1a2a1a2a1), with I6470 being negative and I3997 positive. Eleven Bronze Age males had DNA sequences overlapping R1b-Z225 (R1b1a1a2a1a2a5), with only VAD001 being positive for the mutation (one Iron Age male, I3320, is also positive for this mutation). We thus detect three Bronze Age males who belonged to DF27 (*I54*, *I55*), confirming its presence in Bronze Age Iberia. The other Iberian Bronze Age males could belong to DF27 as well, but the extremely low recovery rate of this SNP in our dataset prevented us to study its true distribution. All the Iberian Bronze Age males with overlapping sequences at R1b-L21 were negative for this mutation. Therefore, we can rule out Britain as a plausible proximate origin since contemporaneous British males are derived for the L21 subtype.

## SI 6 - Kinship analysis

We looked for kinship relationships between the individuals included in our study. We followed the same strategy as in Kennett et al 2017 (*I56*) and Loosdrecht et al 2018 (*I5*), which is similar to that in Monroy Kuhn et al 2018 (*I57*). For each pair of individuals, we computed the mean mismatch rate using all the autosomal SNPs with at least one sequencing read for both individuals in the comparison. In the cases with more than one read at a particular SNP for a given individual, we randomly sample one read for analysis. We then estimated relatedness coefficients  $r$  as in Kennett et al 2017 (*I56*):

$$r = 1 - ((x-b)/b)$$

with  $x$  being the mismatch rate and  $b$  the base mismatch rate expected for two genetically identical individuals, which we estimated by computing intra-individual mismatch-rates.

We also computed 95% confidence intervals using block jackknife standard errors. The inferred kinship relationships for each pair can be viewed in Table S1.

We illustrate this procedure with our Iberian Mesolithic individuals. We first split them into two groups according to their genomic population affinities (Table S7): one group comprised of individuals with lower affinity to El Mirón individual: LaBraña1, LaBraña2 and Canes1. The other group comprised of individuals with high El Mirón affinity: Car1, CMN2, CC1 and Chan. We computed pairwise mismatch rates between individuals in each of the groups and intra-individual mismatch rates (Table S6).

Then, we computed relatedness coefficients (Fig. S1) using base mismatch rates of 0.1138323 and 0.1069545 for the first and second groups, respectively. These values were obtained by averaging intra-individual mismatch rates of individuals with more than 100,000 SNPs to avoid extremely noisy estimates.

We obtained a relatedness coefficient of 0.51 for LaBraña1 and LaBraña2 (two males with overlapping radiocarbon dates and found at the same cave), which indicates that they were 1st-degree relatives. They had the same mtDNA and Y-chromosome haplotypes, suggesting a sibling relationship, which we confirm by the presence of long IBD segments on the X-chromosome (Fig. S2). This is not expected for a father-son relationship as the X-chromosome is inherited from the mother.

## **SI 7 - Genome-wide analysis datasets**

We built two datasets for genome-wide analyses:

- HO dataset, which includes 1331 ancient individuals together with 2562 present-day individuals from worldwide populations genotyped on the Human Origins Array (10, 11, 158). The ancient set includes newly reported individuals from Iberia and individuals that had previously been published (2, 4–10, 12, 13, 15, 17, 20, 97, 158–181) (Table S1), both from Iberia and other regions. We kept 591,642 autosomal SNPs after intersecting autosomal SNPs in the 1240k enrichment with the analysis set of 594,924 SNPs from a previous publication (10).
- HOIII dataset, which includes the same set of ancient individuals, 300 present-day individuals from 142 populations sequenced to high coverage as part of the Simons Genome Diversity Project (182), and 2535 present-day individuals sequenced as part of the 1000 Genomes Project Phase 3 (183). For this dataset,

1768 we used 1,054,671 autosomal SNPs, excluding SNPs of the 1240k array with  
1769 known functional effects or located on sex chromosomes.

1770 For each individual, each genomic position was represented by a randomly sampled  
1771 sequence, removing the first and the last two nucleotides of each sequence if the  
1772 sample was treated with UDG half and the first and the last ten nucleotides for  
1773 samples from the literature that were not treated with UDG.

1774 We repeated key analyses after removing 284,013 SNPs in CpG context (Table S5)  
1775 that could potentially be affected by aDNA damage, as methylated cytosines are  
1776 deaminated into thymines which are not removed by UDG half treatment.

### 1777 **SI 8 - Principal component analysis**

1778 We performed principal component analysis on the HO dataset using the ‘smartpca’  
1779 program in EIGENSOFT (184). We projected ancient individuals onto the components  
1780 computed on present-day individuals with lsqproject:YES and shrinkmode:YES. We ran  
1781 three analyses with different sets of present-day individuals:

1782 -A set with 989 present-day West Eurasians (Fig. 1C-D).

1783 -A set with 989 present-day West Eurasians and 70 present-day North Africans (Fig. S3).

1784 -A set with 989 present-day West Eurasians, 70 present-day North Africans and 136  
1785 present-day sub-Saharan Africans (Fig. S4).

### 1786 **SI 9 - $f$ -statistics**

1787 We computed  $f_4$ -statistics in ADMIXTOOLS (11) using the program *qpDstat* and *f4mode*:  
1788 YES. To assess statistical significance, we compute standard errors using a weighted  
1789 block jackknife approach (185) over 5 Mb blocks.

### 1790 **SI 10 - Estimation of $F_{ST}$ coefficients**

1791 We estimated  $F_{ST}$  using smartpca (184) with parameters *inbreed*: YES and *fstonly*: YES.

### 1792 **SI 11 - *qpAdm* admixture modeling**

1793 In this section we use *qpAdm* (12) (<https://github.com/DReichLab>) to fit the ancestry of  
1794 populations in the Iberia genetic time transect as a mixture of other populations from the  
1795 same area or from neighboring regions. This method models the ancestry of a *test*  
1796 population as mixture of a set of *source* populations that are differentially related to a set  
1797 *outgroup* populations. The software fits a matrix of  $f_4$ -statistics relating the *test*, *source*  
1798 and *outgroup* populations and outputs mixture proportions and formal P-values for

whether the tested model is a good fit to the data. For a more detailed explanation of this methodology see Supplementary Information section 7 of ref (158).

Following a similar strategy to the one in ref (167), we started with a set of populations that includes groups distantly related, both geographically and temporally, to our Iberian individuals, and more proximate groups that are plausible sources for the ancestry in them. We tested all possible 1-way, 2-way and 3-way combinations of populations in our initial set, using them as sources and leaving the remaining populations as outgroups in the model. We then checked whether a 1-way model was sufficient to explain the ancestry in the *test* population. If no 1-way model showed a good fit ( $p > 0.05$ ), we looked for plausible 2-way models and if not, for 3-way models. Unless otherwise noted, this is the strategy followed throughout SI 11.

### ***Mesolithic period***

To increase resolution, we decided to merge the data for the two Mesolithic individuals from the southeast (CMN2 and CC1), both with fewer than 25,000 covered SNPs. This prevented us from studying differences between these two roughly contemporaneous individuals.

Using  $f_4$ -statistics (Fig. S5) we showed that Iberian Mesolithic hunter-gatherers are differentially related to the El Mirón (4) individual (northwestern Spain, ~16000 cal BCE) and to contemporaneous individuals from central Europe such as KO1 (186), demonstrating the presence of genetic structure during this period. Therefore, we included KO1 and El Mirón in our *outgroup* population set together with other Upper Palaeolithic and later West Eurasians, an ancient East African (Mota) (168) and the oldest East Asian (Tianyuan) (177) and North African (Morocco\_Iberomaurusian) (15) individuals with available genome-wide data.

*Outgroup* set: Mota, Ust\_Ishim, Kostenki14, GoyetQ116-1, Vestonice16, MA1, El Mirón, EHG, KO1, Iran\_N, Israel\_Natufian, Morocco\_Iberomaurusian, Tianyuan.

None of the possible 1-way models fit the data, meaning that our *test* populations do not form a clade with any population in the *outgroup* set. The model El Mirón+KO1 is the only 2-way model that fits the data for the Iberian Mesolithic individuals and Loschbour (Table S7). We repeated the analysis substituting KO1 by Villabruna as representative of the WHG cluster. The model El Mirón+Villabruna does not fit the data for the La Braña brothers and Canes1 and thus we present in the main text models featuring El Mirón+KO1.

1834 The Iberian hunter-gatherer with the strongest shift towards KO1 is Canes1. Unlike the  
1835 other Mesolithic Iberians who belong to mtDNA U5b, this individual belongs to mtDNA  
1836 haplogroup U5a, which is more common in central European hunter-gatherers.

### 1837 ***Neolithic and Copper Age***

1838  
1839 The Early Neolithic period in Europe is characterized by the arrival of farmers from  
1840 Anatolia. Therefore, we added Anatolia\_N as a possible source in the *outgroup* set.

1841 *Outgroup* set: Mota, Ust\_Ishim, Kostenki14, GoyetQ116-1, Vestonice16, MA1, El  
1842 Mirón, EHG, KO1, Iran\_N, Israel\_Natufian, Morocco\_Iberomaurusian, Tianyuan,  
1843 Anatolia\_N

1844  
1845 Again, we were not able to successfully model any Neolithic/Copper Age group using  
1846 one population from the *outgroup* set. Central European populations can be modeled as  
1847 a 2-way mixture between Anatolia\_N and KO1, with the exception of Germany\_MN  
1848 (Table S8). In the case of populations from Iberia, southern France and Britain, no 2-way  
1849 combination fit the data, and most of them can only be modeled as a mixture of  
1850 Anatolia\_N, El Mirón and KO1 (Table S8).

### 1851 ***Copper Age outlier from Camino de las Yeseras***

1852  
1853 One Copper Age individual (C\_Iberia\_CA\_Afr; ID I4246) excavated at Camino de las  
1854 Yeseras in central Iberia clusters with North Africans and not with Europeans in PCA  
1855 (Fig. 1C, Fig. S3-4), and we wanted to check whether *qpAdm* detects the same genetic  
1856 signal. Previous studies have reported the presence of ancestry related to Early Neolithic  
1857 Europeans in Late Neolithic North Africans (8). Therefore, we included in our *outgroup*  
1858 set several Early Neolithic Europeans (Croatia\_EN, Iberia\_EN, Macedonia\_N,  
1859 Serbia\_EN, LBK\_EN, Romania\_EN, Hungary\_EN) under the population name  
1860 Europe\_EN to act as a possible ancestry source.

1861 *Outgroup* set: Mota, Ust\_Ishim, Kostenki14, GoyetQ116-1, Vestonice16, MA1, El  
1862 Mirón, Villabruna, WHG, EHG, Iran\_N, Israel\_Natufian, Levant\_N, Europe\_EN,  
1863 Morocco\_Iberomaurusian, Tianyuan

1864  
1865 The best 2-way and 3-way models both feature Europe\_EN and  
1866 Morocco\_Iberomaurusian, with ancestry proportion for Mota not significantly different  
1867 from 0 in the 3-way model (Table S9). This supports the conclusion that  
1868 C\_Iberia\_CA\_Afr, like Late Neolithic North Africans (8), has ancestry related to both  
1869 Early Neolithic Europeans and earlier North Africans, supporting a North African origin  
1870 for this individual.

Next, we added Early and Late Neolithic North Africans (8) to the *outgroup* set and found that all the successful models included Morocco\_LN as the main source of ancestry (Table S10). This confirms that C\_Iberia\_CA\_Afr was genetically close to populations living in Morocco during the Late Neolithic, but with less ancestry related to Early Neolithic Europeans as compared to the available Morocco\_LN individuals.

A North African origin is further supported by uniparental markers: Y-chromosome E1b1b1a and mtDNA haplogroup M1a1b1 (tables S1 and S4). Both E1b1b1a, and the higher ranking clade M1a occur most frequently in present-day North and East Africans (187, 188). Also, haplogroups M1 (albeit M1b) and E1b1b1 have been found in Late Pleistocene and Early Neolithic North Africans (8, 15) but are completely absent or very rare in Neolithic and Copper Age Iberians.

### ***Bronze and Iron Ages***

We started by modeling the earliest individuals with steppe ancestry in Iberia (Iberia\_CA\_Stp), dated to ~2500-2000 BCE. We used an *outgroup* set that included Neolithic and Copper Age populations from Europe that could be a source for the non-steppe-related ancestry in Iberia\_CA\_Stp, as well as European groups that could be a proximate source for the population that introduced steppe ancestry into Iberia.

*Outgroup set:* Mota, Ust\_Ishim, Kostenki14, GoyetQ116-1, Vestonice16, MA1, El Mirón, EHG, Iran\_N, Israel\_Natufian, Morocco\_Iberomaurusian, Anatolia\_N, Steppe\_EBA, Iberia\_EN, LBK\_EN, England\_Beaker, Germany\_Beaker, Netherlands\_Beaker, France\_Beaker, Iberia\_CA, Globular\_Amphora\_Poland

Only one 2-way model fits the ancestry in Iberia\_CA\_Stp with  $P\text{-value} > 0.05$ : Germany\_Beaker + Iberia\_CA (Table S11). Finding a Bell Beaker-related group as a plausible source for the introduction of steppe ancestry into Iberia is consistent with the fact that some of the individuals in the Iberia\_CA\_Stp group were excavated in Bell Beaker associated contexts (9). Models with Iberia\_CA and other Bell Beaker groups such as France\_Beaker ( $P\text{-value} = 7.31\text{E-}06$ ), Netherlands\_Beaker ( $P\text{-value} = 1.03\text{E-}03$ ) and England\_Beaker ( $P\text{-value} = 4.86\text{E-}02$ ) failed, probably because they have slightly higher proportions of steppe ancestry than the true source population. We can also discard Beaker complex individuals from the island of Britain as a plausible directly source for the steppe ancestry in Iberia because all the analyzed males with enough resolution in this group are derived for R1b-L21, a SNP for which Iberian males are ancestral.

For Iberia\_BA, we added Iberia\_CA\_Stp to the *outgroup* set as a possible source. The same Germany\_Beaker + Iberia\_CA model shows a good fit, but with less ancestry



attributed to Germany\_Beaker (Table S11). Another working model is Iberia\_CA+Iberia\_CA\_Stp, suggesting that Iberia\_BA is a mixture between the local Iberia\_CA population and the earliest individuals with steppe ancestry in Iberia.

To model Iron Age Iberian groups, we added three preceding populations: England\_MBA, Unetice\_EBA and Iberia\_BA (including NE\_Iberia\_BA, N\_Iberia\_BA and C\_Iberia\_BA when modeling E\_Iberia\_IA and N\_Iberia\_IA, and SW\_Iberia\_BA and SE\_Iberia\_BA when modeling SW\_Iberia\_IA) as possible sources in the population set. The three Iron Age groups, E\_Iberia\_IA from a non-Indo-European-speaking area, SW\_Iberia from a Tartessian cultural context and N\_Iberia\_IA from an Indo-European-speaking area, show a poor fit (P-values of 1.72E-04, 3.46E-02 and 4.37E-15, respectively) when modeled with Iberia\_BA as the only source, indicating some degree of genetic discontinuity between the Bronze Age and the Iron Age in the three areas. Several models successfully fit (Table S11), most featuring either Iberia\_CA or Iberia\_BA and populations from outside Iberia with high levels of steppe ancestry. Interestingly, N\_Iberia\_IA is always modeled with a higher contribution from populations outside Iberia than E\_Iberia\_IA or SW\_Iberia\_IA (Fig. S6).

For all the populations in this section with good coverage (Iberia\_CA\_Stp, Iberia\_BA, E\_Iberia\_IA, N\_Iberia\_IA), the model Iberia\_CA + Steppe\_EBA shows a poor fit (P-value<2.24E-02). This is not surprising because in this model all the European Neolithic-related ancestry in those populations is attributed to Iberia\_CA, when in fact a portion of it must be derived from incoming populations that were not entirely Steppe\_EBA in ancestry. However, using a fixed set of outgroups less sensitive to the differences between Neolithic European populations we can try to estimate the proportion of Steppe\_EBA-related ancestry in our populations of interest. Table S12 and Fig. S6 show these estimates using the following set of *outgroups*: Mota, Ust\_Ishim, Kostenki14, GoyetQ116-1, Vestonice16, MA1, EHG, Iran\_N, Israel\_Natufian, Anatolia\_N, LBK\_EN.

To study possible genetic differences between Bronze Age groups from different geographic areas, we repeated the *qpAdm* model in Table S12 stratifying by geographic region (Table S13). We found that Bronze Age groups in the south had less steppe ancestry (~15%) than groups in central and northern Iberia (~20%).

### ***Sex bias in Bronze Age Iberia***

Based on the observation of the complete replacement of Neolithic/Copper Age Y-chromosome haplogroups by haplogroup R1b-M269 during the Bronze Age, we tried to

study sex-biased admixture in the formation of the Iberian Bronze Age population. Given that males carry one X-chromosome and two copies of each of the autosomes, if the incoming population that admixed with the local Iberia\_CA population was heavily male-biased, the Iberian Bronze Age population is expected to have lower ancestry proportions from the incoming population on the X-chromosome than on the autosomes. Thus, we computed ancestry proportions with *qpAdm* on the autosomes and on the X-chromosome using Iberia\_CA as a local source of ancestry and Germany\_Becker as a non-local source. This Germany\_Becker group was very likely not genetically identical to the actual group that arrived in Iberia between 2500-2000 BCE, but due to the lack of data from closer regions such as southern France, we think that it is a useful proxy both chronologically and genetically. We used the conservative fixed set of *outgroups* with the addition of Steppe\_EBA: Mota, Ust\_Ishim, Kostenki14, GoyetQ116-1, Vestonice16, MA1, EHG, Iran\_N, Israel\_Natufian, Anatolia\_N, LBK\_EN, Steppe\_EBA. We computed standard errors over 10-Mb blocks. We obtained lower proportions of ancestry related to Germany\_Becker on the X-chromosome than on the autosomes (Table S14), although the Z-score for the differences between the estimates is 2.64, likely due to the large standard error associated to the mixture proportions in the X-chromosome.

Using the estimated admixture proportions on the X-chromosome and autosomes, we estimated the proportion of female and male ancestors in Iberia\_BA that were local, i.e. from the Iberia\_CA population, following the same approach as in (169). The computed log-likelihood surface (Fig. S7) points to a low proportion of male ancestors from the Iberia\_CA population, which agrees with the observed Y-chromosome pattern.

#### ***Admixture proportions for individuals in the Iberia\_CA\_Stp, Iberia\_BA and Iberia\_IA groups***

We computed admixture proportions (Table S15, Fig. 2B) for each individual in the Iberia\_CA\_Stp, Iberia\_BA and Iberia\_IA groups, using Iberia\_CA and Germany\_Becker as sources and the same fixed *outgroup* set as in the previous section: Mota, Ust\_Ishim, Kostenki14, GoyetQ116-1, Vestonice16, MA1, EHG, Iran\_N, Israel\_Natufian, Anatolia\_N, LBK\_EN, Steppe\_EBA.

#### ***Bronze Age outlier from Loma del Puerco***

In PCA analysis (Fig. 1C-D, Fig. S3), one Bronze Age individual (ID I7162) from Loma del Puerco (Chiclana de la Frontera, Cádiz), a site located in the southern tip of Spain, appears somewhat shifted from the main Bronze Age cluster. This shift cannot be

1976 attributed to statistical noise from low coverage because we recovered 366,033 genomic  
1977 positions. Therefore, we tried to understand the underlying cause of this shift with *qpAdm*  
1978 using the following *outgroup* set.

1979 *Outgroup* set: Mota, Ust\_Ishim, Kostenki14, GoyetQ116-1, Vestonice16, MA1, El  
1980 Mirón, EHG, Iran\_N, Israel\_Natufian, Morocco\_Iberomaurusian, Anatolia\_N,  
1981 Steppe\_EBA, Iberia\_EN, LBK\_EN, Germany\_Becker, Iberia\_CA,  
1982 Globular\_Amphora\_Poland, Iberia\_BA, C\_Iberia\_CA\_Afr, Morocco\_LN

1983  
1984 Given that Loma del Puerco lies only 70 kilometers north of the North African coast, we  
1985 included in the *outgroup* set the outlier individual from Camino de las Yeseras with a  
1986 North African origin (C\_Iberia\_CA\_Afr) and Morocco\_LN to account for the possibility  
1987 of recent North African ancestry in I7162 as the reason for the shift observed in the PCA.

1988 None of the 1-way models show a good fit, including Iberia\_BA (P-value=6.93E-08),  
1989 confirming that this individual does not form a clade with the rest of the Bronze Age  
1990 samples from Iberia. We found five 2-way models with a good fit (Table S16), all of the  
1991 them featuring Iberia\_BA and either an African individual/population or the Natufians.  
1992 Similar models including Iberia\_CA instead of Iberia\_BA show a very poor fit,  
1993 demonstrating that this individual has steppe ancestry like the rest of the Bronze Age  
1994 Iberians. Taking into account archaeological context, the most plausible model is a  
1995 mixture between Iberia\_BA-related ancestry and ancestry related to individuals like  
1996 C\_Iberia\_CA\_Afr, who could have been present not only in central Iberia like the one we  
1997 have sampled, but also in southern Iberia during the second half of the 3<sup>rd</sup> millennium  
1998 BCE and the first half of 2<sup>nd</sup> millennium BCE.

### 1999 ***The past 2500 years in northeast Iberia***

2000  
2001 Many of our individuals with working genome-wide data from northeast Iberia and dated  
2002 to the past ~2500 years were excavated from the site of Empúries, the most important  
2003 Greek colony in the Iberian Peninsula and later occupied by the Romans.

2004 In PCA (Fig. 1C-D), most of the individuals from Empúries form two clusters: one (which  
2005 we call Empúries1) plotting close to the Iron Age Iberia cluster that includes samples  
2006 from the nearby site of Ullastret and the other (which we call Empúries2) plotting close  
2007 to Bronze Age samples from the eastern Mediterranean such as the Mycenaean samples  
2008 from Greece (I67). The presence of two genetically distinct populations is further  
2009 supported by different patterns of  $F_{ST}$  estimated with present-day populations (Fig. S8)  
2010 and by Y-chromosome haplogroup composition (Table S4). Empúries2 was least  
2011 differentiated from populations from the central and eastern Mediterranean region and

2012 was dominated by Y-chromosome haplogroup J, present in high frequencies precisely in  
2013 those regions, whereas Empúries1 was least differentiated from western European  
2014 populations and contained only R1b lineages, similar to the Bronze and Iron Age  
2015 populations from Iberia. We find the two clusters in the three periods of the site for which  
2016 we have genetic data: the Greek, Hellenistic and Roman periods. This demonstrates that  
2017 the ancient town of Empúries was inhabited by local Iberians as well as by colonists from  
2018 the Eastern Mediterranean, which agrees with historical sources and archaeological  
2019 evidence.

2020 We confirm the eastern Mediterranean origin of the second cluster of individuals  
2021 (Empuries2) using *qpAdm* and the following *outgroup* set:

2022 *Outgroup* set: Mota, Ust\_Ishim, Kostenki14, GoyetQ116-1, Vestonice16, MA1, El  
2023 Mirón, EHG, Iran\_N, Israel\_Natufian, Morocco\_Iberomaurusian, Anatolia\_N,  
2024 Steppe\_EBA, Iberia\_EN, LBK\_EN, Iberia\_CA, Globular\_Amphora\_Poland, Iberia\_BA,  
2025 Iberia\_IA, Mycenaean, Minoan\_Lasithi

2026  
2027 Using this setup, all the 1-way models failed ( $P\text{-value} < 3.69\text{E-}14$ ) except for the  
2028 Mycenaean ( $P\text{-value} = 8.81\text{E-}01$ ), indicating that Empuries2 and the Mycenaean  
2029 samples form a clade with respect to the rest of the groups in the populations set to the  
2030 limits of our resolution. This result is perhaps not surprising given that the available  
2031 Mycenaean samples from southern Greece lived only ~700 years before the founding of  
2032 Empúries by Greeks from Phocaea ~575 BCE, according to historical sources.

2033 Next, we wished to study whether the different peoples that established themselves in  
2034 northeast Iberia over the past ~2500 years and dominated parts or the whole territory had  
2035 a significant impact on the overall Iberian gene pool. We analyzed individuals from  
2036 L'Esquerda (Roda de Ter, Barcelona) dated to the 7th-8th century CE and individuals  
2037 from Pla de l'Horta (Sarrià de Ter, Girona) dated to the 6th century CE, both from the  
2038 period of Visigoth domination and postdating the Greek and Roman presence in Iberia.  
2039 We began with the individuals from L'Esquerda (NE\_Iberia\_c.6-8CE\_ES) and used the  
2040 following *outgroup* set for our admixture modeling.

2041 *Outgroup* set: Mota, Ust\_Ishim, Kostenki14, GoyetQ116-1, Vestonice16, MA1, El  
2042 Mirón, EHG, Iran\_N, Israel\_Natufian, Morocco\_Iberomaurusian, Anatolia\_N,  
2043 Steppe\_EBA, Iberia\_EN, LBK\_EN, Iberia\_CA, Globular\_Amphora\_Poland, Iberia\_BA,  
2044 Iberia\_IA, Empuries2, England\_Saxon.SG, Bavaria\_Early\_Medieval.SG, TSI, Greek,  
2045 Bergamo

2046  
2047 To increase resolution, we added to the Iberia\_IA group the samples from Empúries that  
2048 cluster within the Iberia\_IA cluster. The other group of samples from Empúries with

Eastern Mediterranean origin (Empuries2) was included in the *outgroup* set because they could have contributed ancestry to later populations in northeast Iberia. Due to the lack of published aDNA data from the first millennium CE, we included present-day European populations such as TSI (Tuscans from the 1000 Genomes project), Greek and Bergamo that could serve as a proxy for the ancestry in our samples of interest. Modeling NE\_Iberia\_c.6-8CE\_ES as 1-way mixture with any of the populations from the set fails, including Iberia\_IA (P-value=3.01E-07). This demonstrates that the individuals from L'Esquerda do not form a clade with Iberia\_IA, and therefore additional layers of ancestry are needed to explain their genetic makeup. In Table S17 we show all 2-way models that include Iberia\_IA as one of the sources. The only models with good fit are those featuring present-day populations from Italy and Greece. This suggests that NE\_Iberia\_c.6-8CE\_ES has ancestry related to populations from the central and eastern Mediterranean that is not present in Iberia\_IA. The eastern outliers from Empúries showed a poor fit (P-value= 4.48E-04), suggesting that they were likely not the source of the central/eastern Mediterranean ancestry in NE\_Iberia\_c.6-8CE\_ES.

Next, we wanted to study the individuals from Pla de l'Horta (NE\_Iberia\_c.6CE\_PL), adding NE\_Iberia\_c.6-8CE\_ES to the population set as a possible source of ancestry. In fact, all the successful models include NE\_Iberia\_c.6-8CE\_ES as one of the sources (Table S18), confirming that both sites have similar ancestry makeup although they do not form a clade with respect to the other populations in the population set (P-value= 1.29E-03). The best 2-way models feature NE\_Iberia\_c.6-8CE\_ES and either Steppe\_EBA, Bavaria\_Early\_Medieval or Saxon, indicating that the individuals from Pla de l'Horta had higher steppe ancestry than the individuals from L'Esquerda, probably mediated by contemporaneous populations from central/northern Europe where this type of ancestry was present in higher proportions than in Iberia.

Finally, to explore the genetic impact of the Muslim conquest in northeast Iberia, we studied individuals from Sant Julià de Ramis (Girona), dated between the 8th and 12th centuries CE (NE\_Iberia\_c.8-12CE) and therefore largely postdating Muslim political control of the area. We added to the *outgroup* set the preceding population from the area (NE\_Iberia\_c.6-8CE\_ES) and, to account for a possible genetic contribution of the Muslim conquest, a North African ancient group (Morocco\_LN) and the individuals from southeast Iberia during the period of Muslim rule (SE\_Iberia\_c.10-16CE):

Mota, Ust\_Ishim, Kostenki14, GoyetQ116-1, Vestonice16, MA1, El Mirón, EHG, Iran\_N, Israel\_Natufian, Morocco\_Iberomaurusian, Anatolia\_N, Steppe\_EBA,

2083 Iberia\_EN, LBK\_EN, Iberia\_CA, Globular\_Amphora\_Poland, Iberia\_BA, Iberia\_IA,  
 2084 Empuries2, NE\_Iberia\_c.6-8CE\_ES, SE\_Iberia\_c.10-16CE, Morocco\_LN  
 2085  
 2086 No 1-way model fits the data, including the one featuring NE\_Iberia\_c.6-8CE\_ES (P-  
 2087 value=7.58E-04). Three 2-way models fit, with two being (Table S19) historically more  
 2088 plausible: NE\_Iberia\_c.6-8CE\_ES + SE\_Iberia\_c.10-16CE and NE\_Iberia\_c.6-8CE\_ES  
 2089 + Morocco\_LN. This suggests that the individuals from Sant Julià de Ramis harbored  
 2090 North African-related ancestry not present in the populations from the same area before  
 2091 the Muslim conquest.

## 2092 ***The past 2000 years in southeast Iberia***

2093  
 2094 We recovered aDNA data from individuals excavated at 13 sites in the present-day  
 2095 provinces of Granada, València/Valencia and Castelló/Castellón, and dated between the  
 2096 3rd and 16th centuries CE, covering the periods of Roman, Visigothic, Byzantine and  
 2097 Islamic domination in southeast Iberia.

2098 We grouped the individuals under three population names: SE\_Iberia\_c.3-4CE,  
 2099 SE\_Iberia\_c.5-8CE and SE\_Iberia\_c.10-16CE. All the individuals that we analyzed are  
 2100 clearly shifted towards present-day and ancient North Africans in PCA (Fig. S3-4), which  
 2101 suggests that North African genetic input was already present in this region several  
 2102 centuries before the Islamic conquest of the Iberian Peninsula beginning in the 8th century  
 2103 CE. Two individuals from SE\_Iberia\_c.10-16CE plot on a very different position (Fig.  
 2104 S3-4) and thus were not included in the three groups. For *qpAdm* analysis, we began by  
 2105 using the following *outgroup* set:

2106 *Outgroup* set: Mota, Ust\_Ishim, Kostenki14, GoyetQ116-1, Vestonice16, MA1, El  
 2107 Mirón, EHG, Iran\_N, Israel\_Natufian, Morocco\_Iberomaurusian, Anatolia\_N,  
 2108 Steppe\_EBA, Iberia\_EN, LBK\_EN, Iberia\_CA, Globular\_Amphora\_Poland, Iberia\_BA,  
 2109 Iberia\_IA/NE\_Iberia\_c.6-8CE\_ES, Guanche, Morocco\_LN, Levant\_EBA  
 2110

2111 This set includes Upper Paleolithic North Africans (Morocco\_Iberomaurusian),  
 2112 Late\_Neolithic North Africans (Morocco\_LN) and indigenous Canary Islanders  
 2113 (Guanche), all of which could serve as a proxy for North African populations before the  
 2114 Arab expansion, and Levant\_EBA to account for Levantine-related ancestry. We also use  
 2115 either Iron Age Iberia (Iberia\_IA) or early Medieval Iberian individuals from the  
 2116 northeast (NE\_Iberia\_c.6-8CE\_ES) to act as a proxy for Iberia-related ancestry. For the  
 2117 three groups, the best 2-way models include NE\_Iberia\_c.6-8CE and the Guanche or  
 2118 Morocco\_LN (Table S20). However, with the exception of SE\_Iberia c.3-4 CE, these  
 2119 models show a poor fit to the data, meaning that they do not successfully explain the

ancestry in these groups. Using present-day North Africans such as Mozabite or Saharawi instead of the ancients does not improve the fit. Instead, the models slightly improve when Levant\_EBA is used as a third source, although they do not achieve a P-value  $>0.05$  for SE\_Iberia\_c.5-8CE (Table S20).

The lack of models with a good fit to the data might be a consequence of the limited number of available proximate sources of ancestry in key regions. For instance, in North Africa the only ancient populations with available data are Morocco\_Iberomaurusian, Morocco\_EN, Morocco\_LN and the Guanches, and we use Morocco\_LN and the Guanches as proxies for North African populations before the Arab expansion. However, they might not be good representatives of the true North African population that contributed ancestry to our Iberian test populations. Similarly, the local Iberian ancestry component in our test populations could have some genetic differences to the populations that we are using as sources for this component. Another potential issue is the presence of genetic heterogeneity within the populations we are trying to model. In PCA (Fig. S3-4), all the individuals in SE\_Iberia\_c.3-4CE, SE\_Iberia\_c.5-8CE and SE\_Iberia\_c.10-16CE plot in an intermediate position between present-day populations from Europe, the Levant and North Africa, but they do not form a tight cluster, which could represent significant ancestry differences. Thus, we analyzed each individual separately, with the caveat that for low-coverage individuals we had less power to reject poorly-fitting models and to estimate admixture proportions. We used a fixed set of *outgroups*: Mota, Ust\_Ishim, Kostenki14, GoyetQ116-1, Vestonice16, MA1, El Mirón, EHG, Iran\_N, Israel\_Natufian, Morocco\_Iberomaurusian, Anatolia\_N, Steppe\_EBA, Iberia\_EN, LBK\_EN, Iberia\_CA, Globular\_Amphora\_Poland, Iberia\_BA; and tested models including either Iberia\_IA or NE\_Iberia\_c.6-8CE\_ES as a local Iberian ancestry source, the Guanches or Morocco\_LN as a North African ancestry source and one of the following Levantine populations as proxies for the extra ancestry not modeled by the Iberian and North African populations: present-day Palestinian, present-day Druze, present-day Jordanian and Levant\_EBA. In Table S21 we provide the best-fitting model for each individual. An interesting observation is the fact that many individuals require ancestry from Levantine populations on top of the Iberian and North African-related ancestry for the model to fit. This could represent eastern Mediterranean ancestry input into the region, either independently or through North African populations with more Levantine-related ancestry than the one we used as a North African ancestry source.

As previously mentioned, two individuals dated to the 10th (I7427) and 16th (I3810) century CE plot on a very different position in the PCA (Fig. S3-4), reflecting a very different ancestry profile. We were able to model them as mixture of ancestry related to previous populations from the same region (SE\_Iberia c.3-4CE) and ancestry related to present-day sub-Saharan African populations (Table S22). The high proportions of sub-Saharan African ancestry explain their marked shift in PCA and agree with uniparental markers with sub-Saharan African origin in both individuals.

## **SI 12 - Allele frequency estimation of SNPs of phenotypic importance**

Our dense genetic time transect allowed us to follow the trajectory of genetic variants with phenotypic importance over time. Due to the presence of missing data in ancient individuals, chances are high that a particular SNP will not be covered by any DNA sequence in several individuals. Therefore, we group our Iberian individuals in 5 broad time periods to increase the accuracy of the allele frequency estimation. The groups are Mesolithic, Neolithic, Copper Age, Bronze-Iron Age and Historical (which includes individuals from 500 BCE to 1600 CE). We used allele counts at each SNP to perform maximum likelihood estimations of allele frequencies in ancient populations as in ref. (2), and computed confidence intervals using the Agresti-Coull method implemented in the `binom.confint` function of the R-package *binom*.

In Fig. S9, we show derived allele frequency estimates for four SNPs with functional importance: SNP rs4988235 in *LCT* responsible for lactase persistence, SNP rs12913832 in *HERC2/OCA2* responsible for blue eyes, and SNPs rs16891982 and rs1426654 in *SLC45A2* and *SLC24A5*, respectively, associated with reduced skin pigmentation in Europeans. A striking observation is the complete absence of the lactase persistence allele in Iberia (present at 0.46 frequency in present-day Iberians) until recent historical times, which suggests very recent selection.

We wished to examine whether the obtained allele frequencies could be affected by reference bias (i.e., the preferential recovery of the allele present in the reference genome over the alternative allele). To estimate this possible bias, we identified ancient individuals with 1240k data from previous studies that presented at least one read with the reference allele and one read with the derived allele at the SNP of interest, which indicates that they were very likely heterozygous at that position. Then, we counted the number of reads with the reference and alternative allele in those individuals and



computed a reference bias estimate. In the case of rs4988235 it was not possible to estimate reference bias due to the limited number of heterozygous individuals. For rs12913832 (152 reference reads, 145 alternative reads; 0.5118) and rs16891982 (946 reference reads, 947 alternative reads; 0.4997) we found no evidence of reference bias. In contrast, for rs4988235 (102 reference reads, 45 alternative reads; 0.6939) we found evidence of reference bias as ~70% of the reads in heterozygous individuals carried the reference allele. Thus, we applied a correction for this bias in the maximum likelihood estimation of rs4988235, shown in Fig. S9.

### **SI 13 - Date of the Carigüela pre-Neolithic individual**

We successfully obtained sequencing data from the Car1 individual from the Carigüela cave in Piñar, Granada Province. The archaeological excavation strongly points to a pre-Neolithic context, but several attempts to generate a radiocarbon date have not been successful. Therefore, we tried to narrow down the age of this individual using the genetic data.

In PCA, the Car1 individual plots close to the other Iberian Mesolithic individuals (Fig. 1C), confirming that his genome-wide ancestry signal is the one expected for an individual who lived before the arrival of Neolithic farmers.

It has been previously shown (4) that Neanderthal ancestry has steadily decreased during the last 45,000 years. Thus, we computed the % of Neanderthal introgression for the ancient European individuals analyzed in Fu et al. 2016 (4) with at least 200,000 SNPs and for the Car1 individual, using  $f_4$ -statistics as in Fu et al. 2016 (4). We obtained 2.22% of Neanderthal ancestry for Car1 (Fig. S10), similar to other European individuals that lived around 8000 BCE.

Lastly, we looked at the mitochondrial genome of Car1. He belonged to haplogroup U5b1, also present in one Iberian Mesolithic sample from Cingle del Mas Nou (Castelló/Castellón, Spain). The appearance of the U5b1 lineage has been dated to 15530±4890 years ago (148) using data from present-day individuals. In the ancient DNA literature, the oldest known U5b1 individuals to date are from Late Glacial Oberkassel (Germany, 12220–11920 and 11620–11340 BCE) (151, 189) and Bichon (Switzerland, 11820–11610 BCE) (164), becoming prevalent in Europe during the Mesolithic (4).

Based on these lines of evidence, we conclude that the Car1 individual likely lived during the Mesolithic period, 9700–5500 BCE. We caution, however, that a direct radiocarbon date would provide the most accurate estimation of the age of this individual.



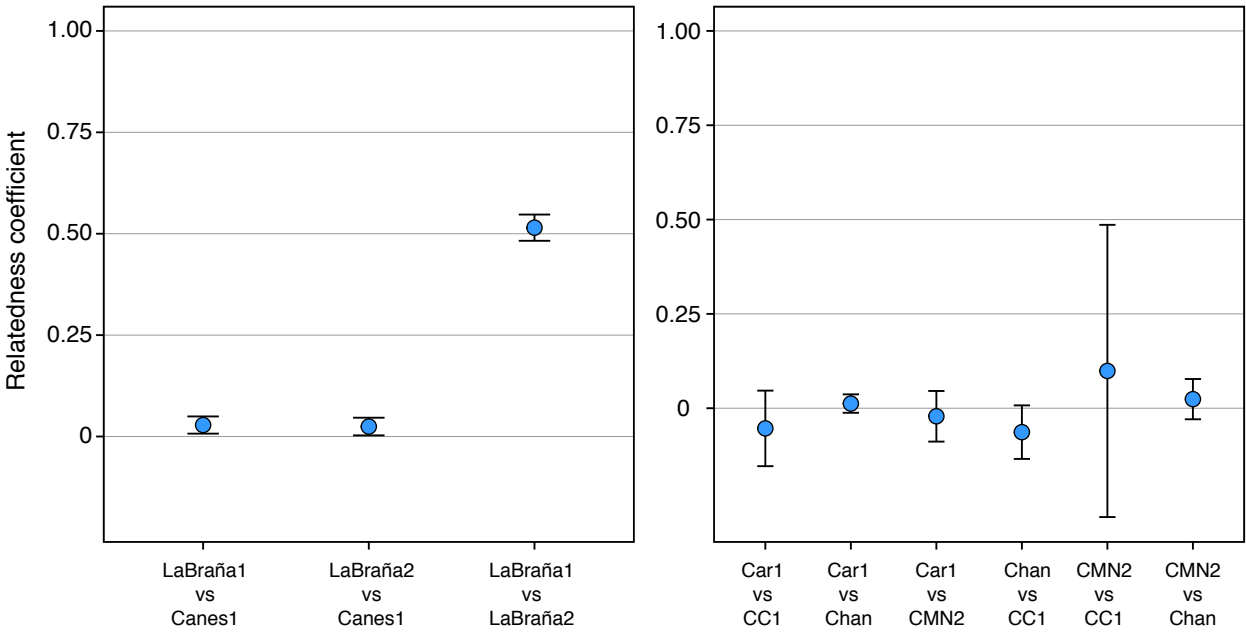


**Fig. S1.** Genetic relatedness among Mesolithic individuals. Relatedness coefficients estimated on the autosomes for pairs of Iberian Mesolithic individuals. Error bars correspond to 95% confidence intervals.

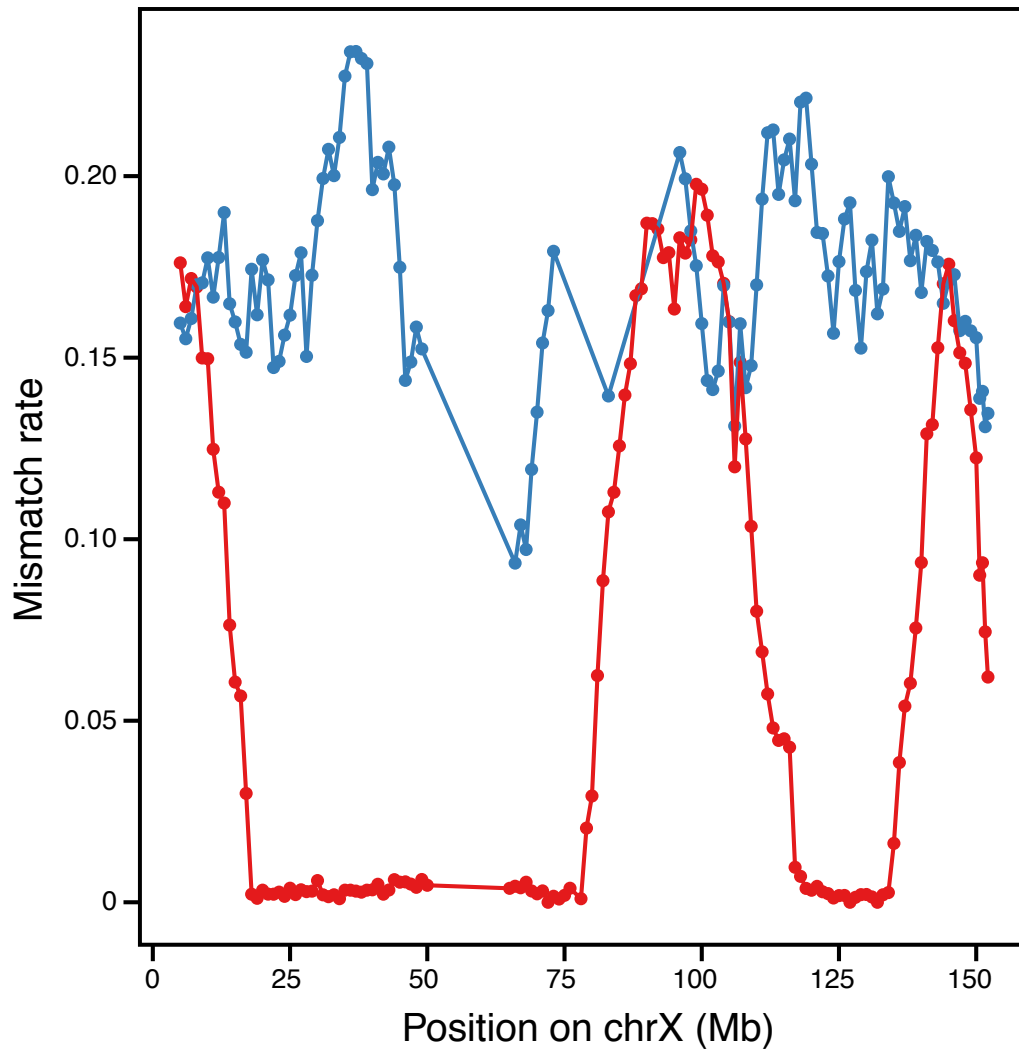


**Fig. S2.** Mismatch rate at 1240k sites between LaBraña1 and LaBraña2 males (red) and between two unrelated Iberian hunter-gatherers (blue) along the X chromosome. Analysis was performed on sliding windows of 10 Mb, moving by 1 Mb each step.

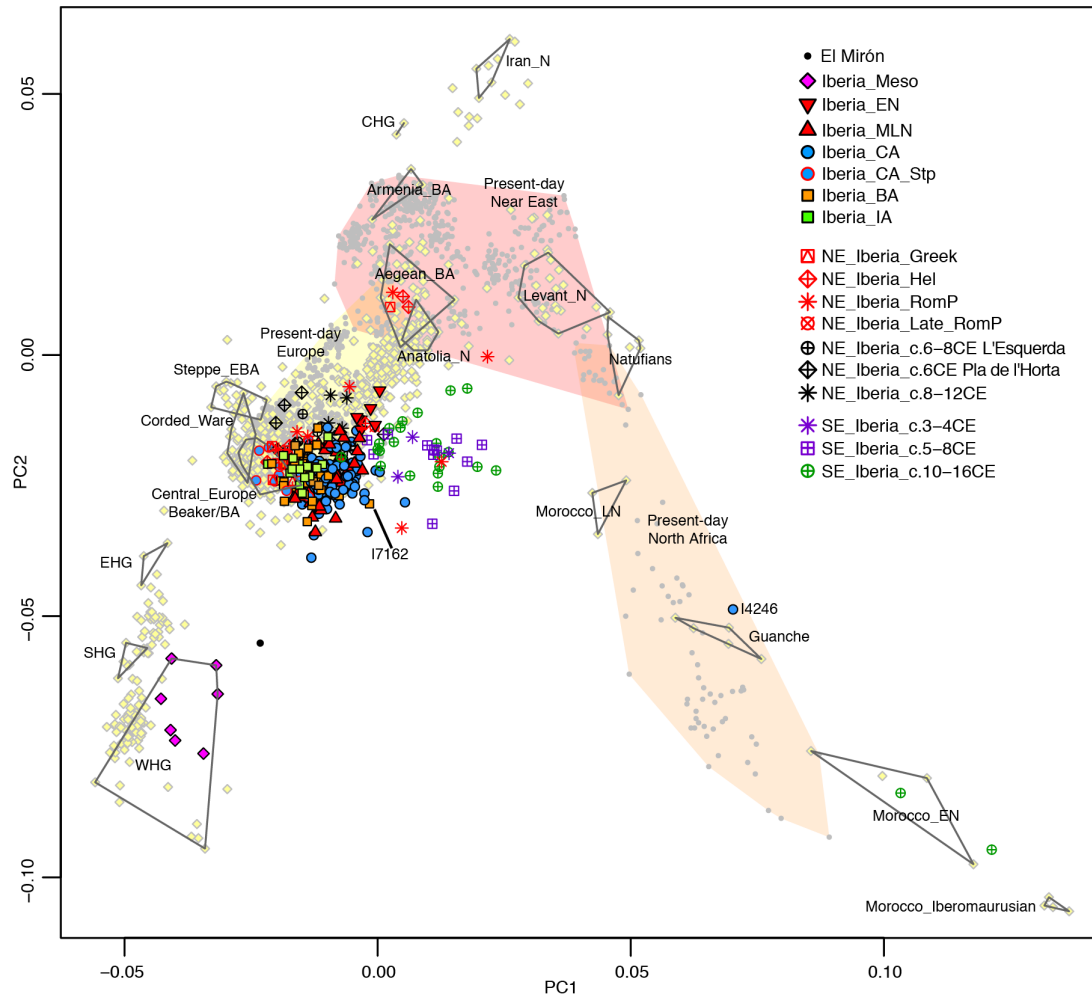


**Fig. S3.** Principal component analysis of 1,059 present-day west Eurasian and North African individuals (grey dots), with ancient individuals from Iberia and other regions (pale yellow) projected onto the first two principal components. WHG, western hunter-gatherers; EHG, eastern hunter-gatherers; SHG, Scandinavian hunter-gatherers; CHG, Caucasus hunter-gatherers; E, Early; M, Middle; L, Late; N, Neolithic; CA, Copper Age; BA, Bronze Age; IA, Iron Age; Meso, Mesolithic; Hel, Hellenistic; RomP, Roman Period; NE, Northeast; SE, Southeast.

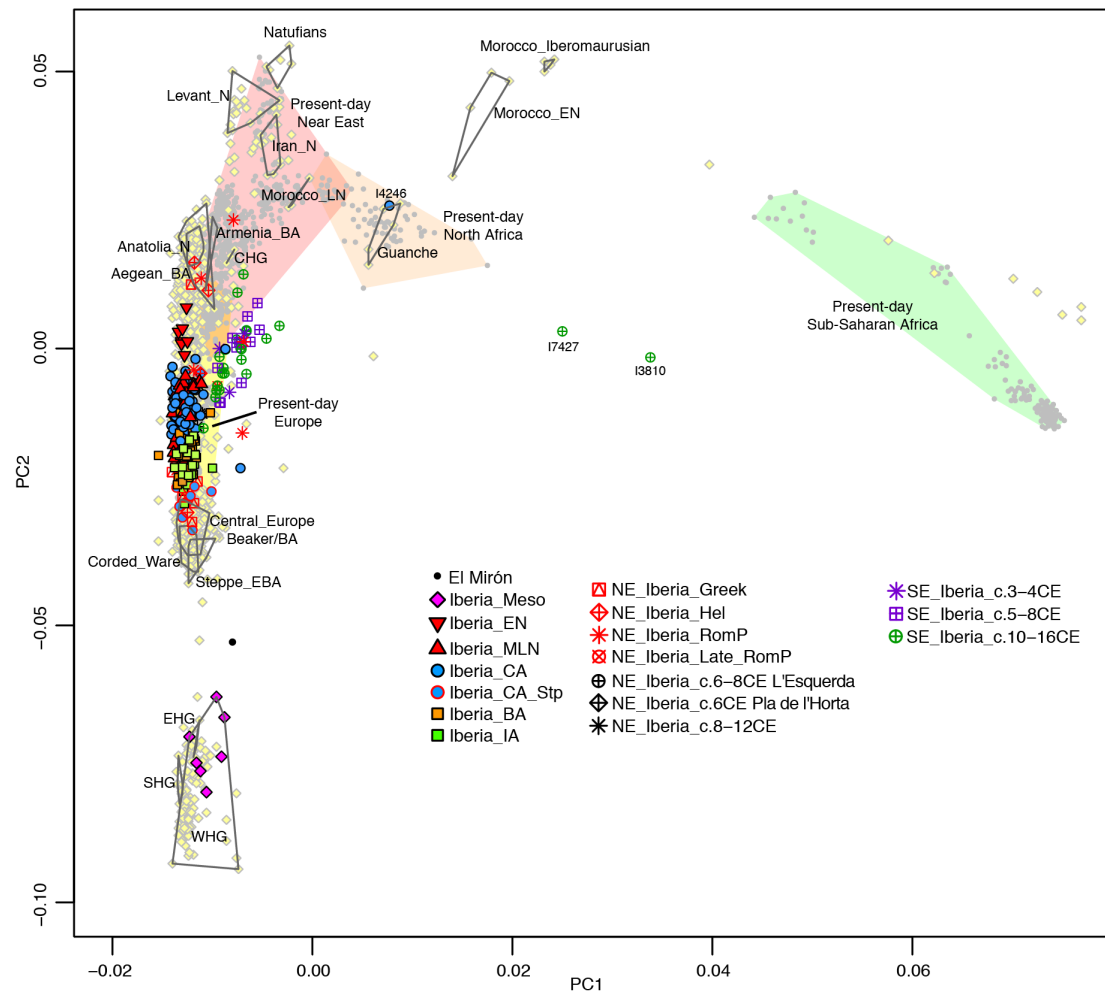


**Fig. S4.** Principal component analysis of 1,195 present-day west Eurasian, North African and Sub-Saharan African individuals (grey dots), with ancient individuals from Iberia and other regions (pale yellow) projected onto the first two principal components. WHG, western hunter-gatherers; EHG, eastern hunter-gatherers; SHG, Scandinavian hunter-gatherers; CHG, Caucasus hunter-gatherers; E, Early; M, Middle; L, Late; N, Neolithic; CA, Copper Age; BA, Bronze Age; IA, Iron Age; Meso, Mesolithic; Hel, Hellenistic; RomP, Roman Period; NE, Northeast; SE, Southeast.

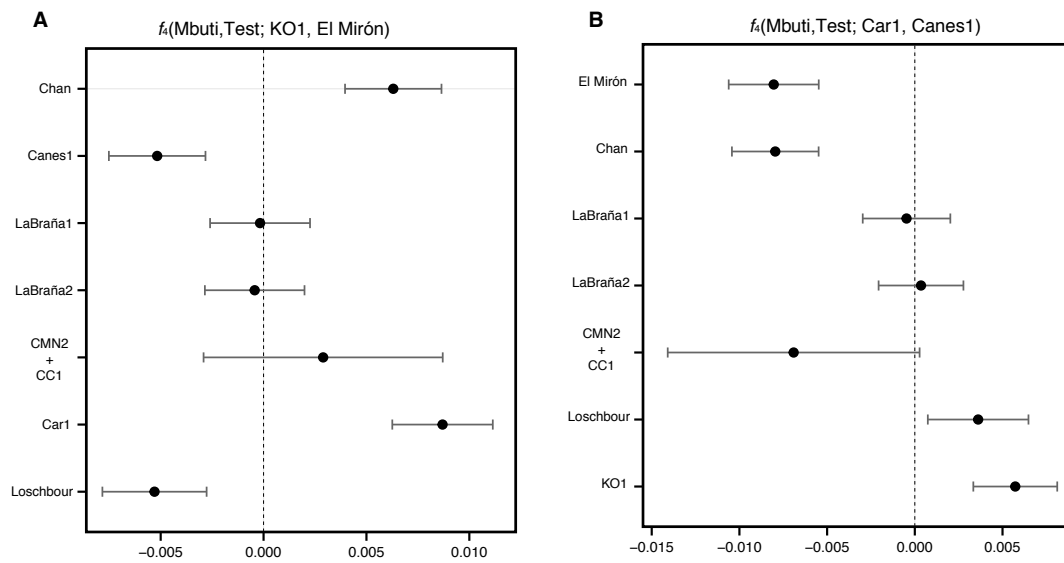


**Fig. S5.**  $f$ -statistics of the form (A)  $f_4(\text{Mbuti, Test; KO1, El Mirón})$  and (B)  $f_4(\text{Mbuti, Test; Car1, Canes1})$ . Bars indicate  $\pm 3$  standard errors.

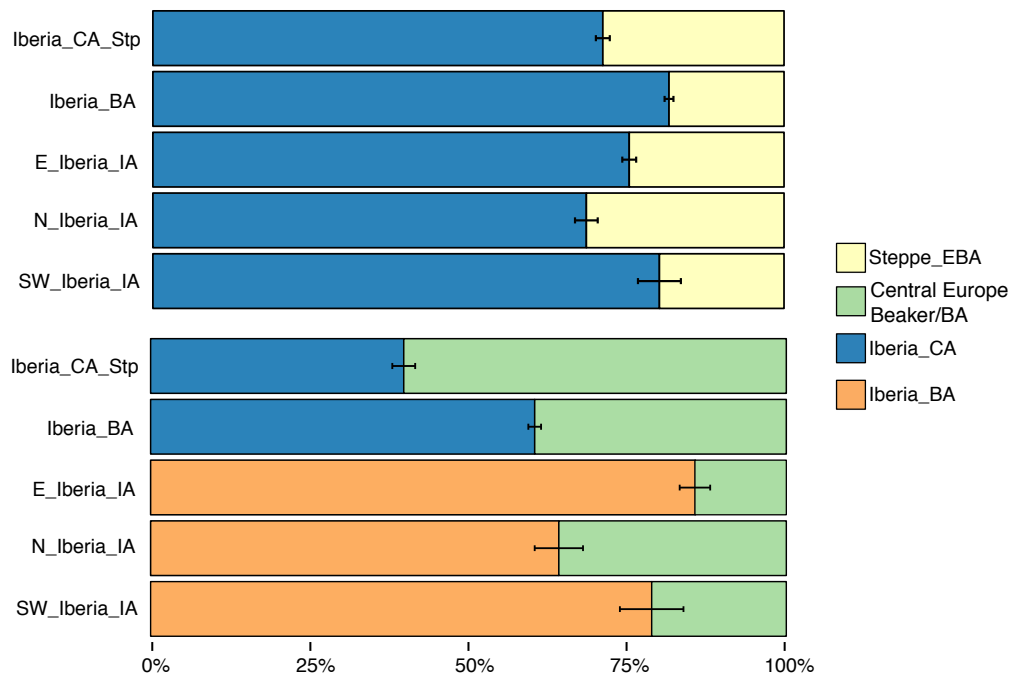


**Fig. S6.** Genome-wide admixture proportions using *qpAdm*. The top panel shows the model Iberia\_CA+Steppe\_EBA and the bottom panel shows more proximate admixture models for the same five populations. Error bars indicate  $\pm 1$  standard errors. CA, Copper Age; EBA, Early Bronze Age; BA, Bronze Age; IA, Iron Age; SW\_Iberia, southwest Iberia; N\_Iberia, northern Iberia; E\_Iberia, eastern Iberia.



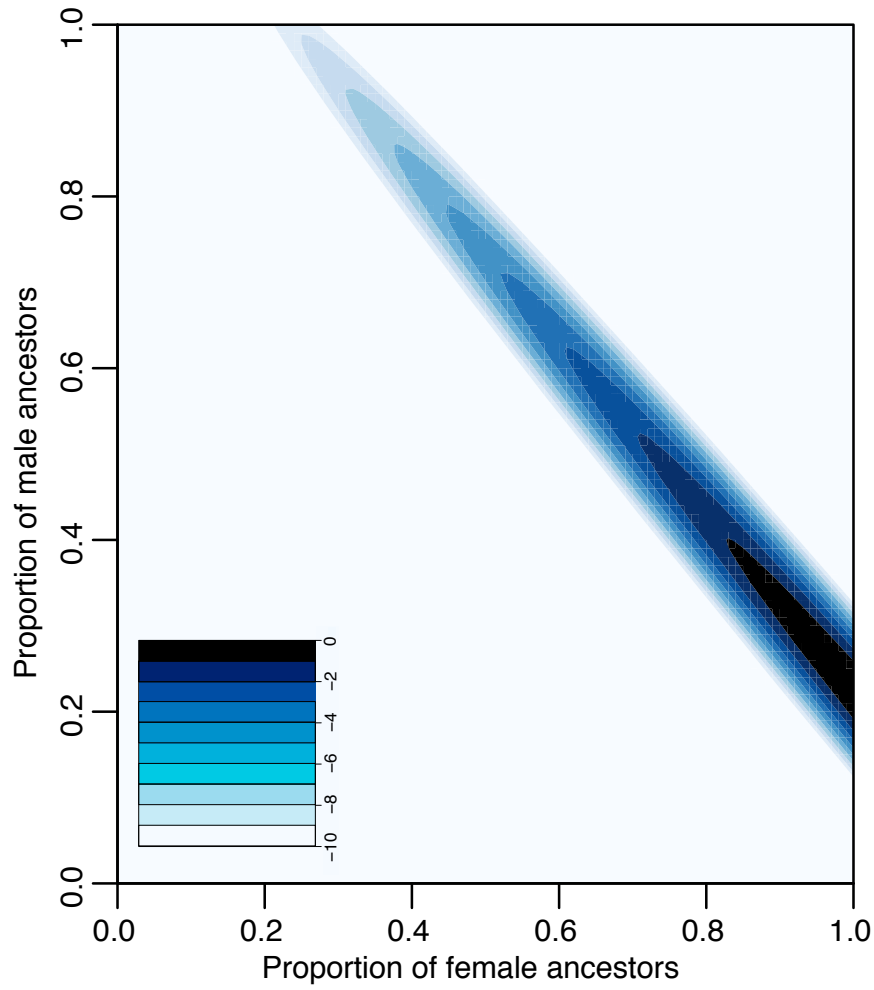


**Fig. S7.** Sex bias in Bronze Age Iberia. Log-likelihood surface for the proportion of female (x axis) and male (y axis) ancestors from the Iberia\_CA population. The log-likelihood scale ranges from 0 to  $-10$ , in which 0 is the feasible point with the highest likelihood.

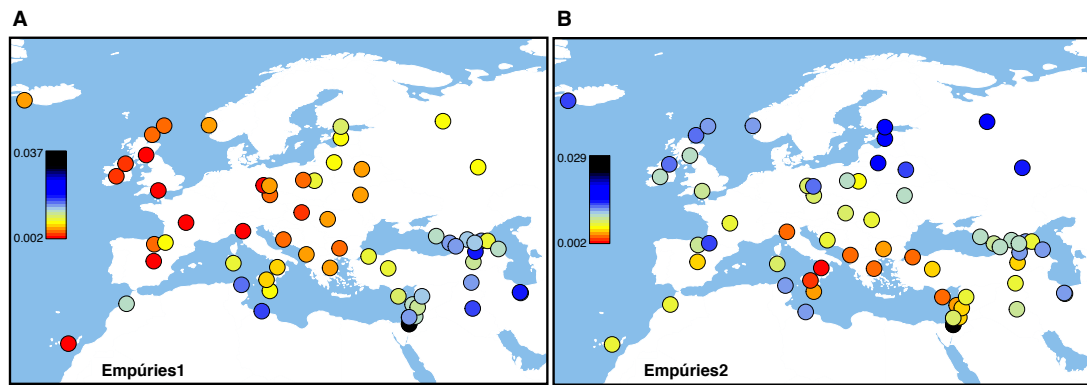


**Fig. S8.** Genetic differentiation measured by  $F_{ST}$  between present-day West Eurasians and (A) Empúries1 or (B) Empúries2 groups.

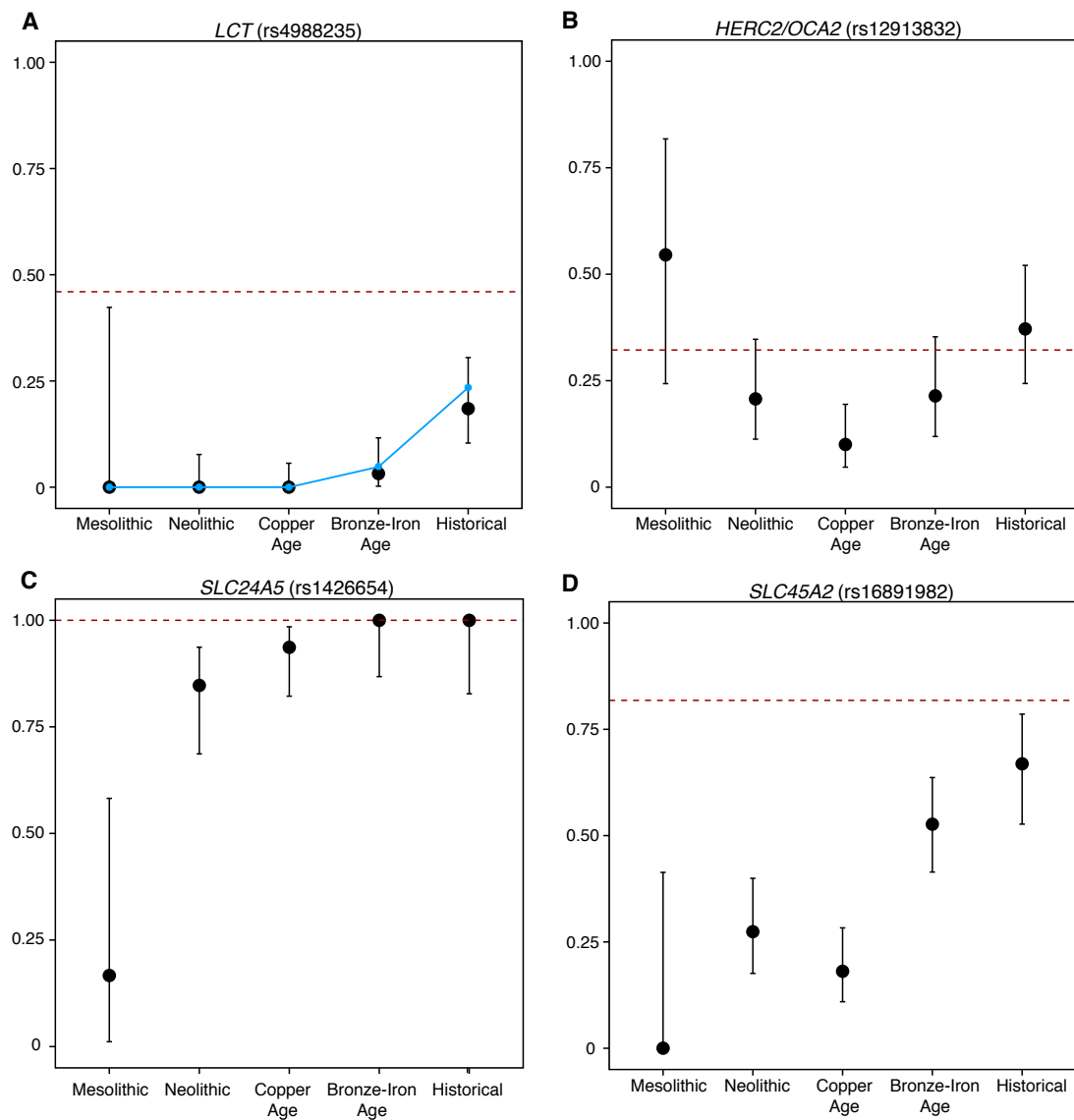


**Fig. S9. Derived allele frequencies at four SNPs of functional importance.** Error bars represent 95% confidence intervals. The red dashed lines show allele frequencies in the 1000 Genomes Project (<http://www.internationalgenome.org/>) 'IBS' population (present-day people from Spain). The blue solid line in (A) represents the derived allele frequencies after correcting for reference bias.

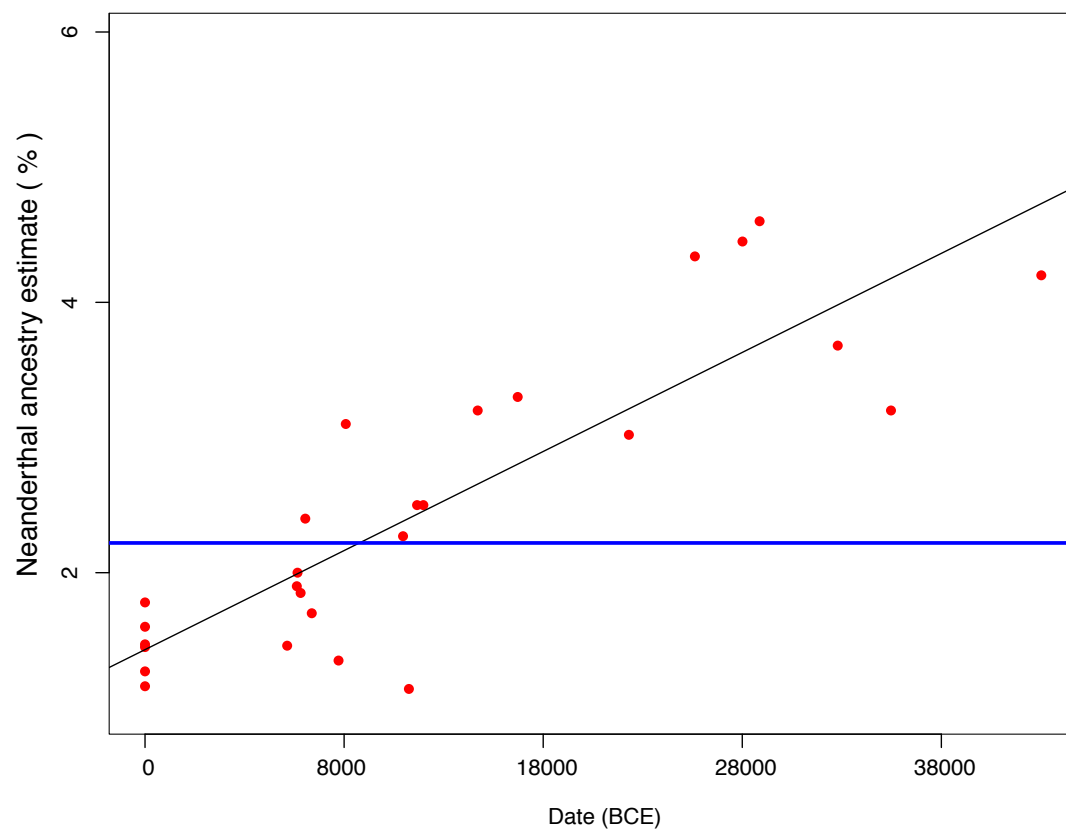


**Fig. S10. Neanderthal ancestry for the Car1 individual from Carigüela cave in the context of other ancient and present-day Europeans.** Neanderthal ancestry for 21 ancient Europeans and six present-day populations (Dai, Han, French, Karitiana, English and Sardinian). Each dot represent one individual. The black line represents the least squares fit. The blue horizontal line represents the estimated Neanderthal ancestry for the Car1 individual.

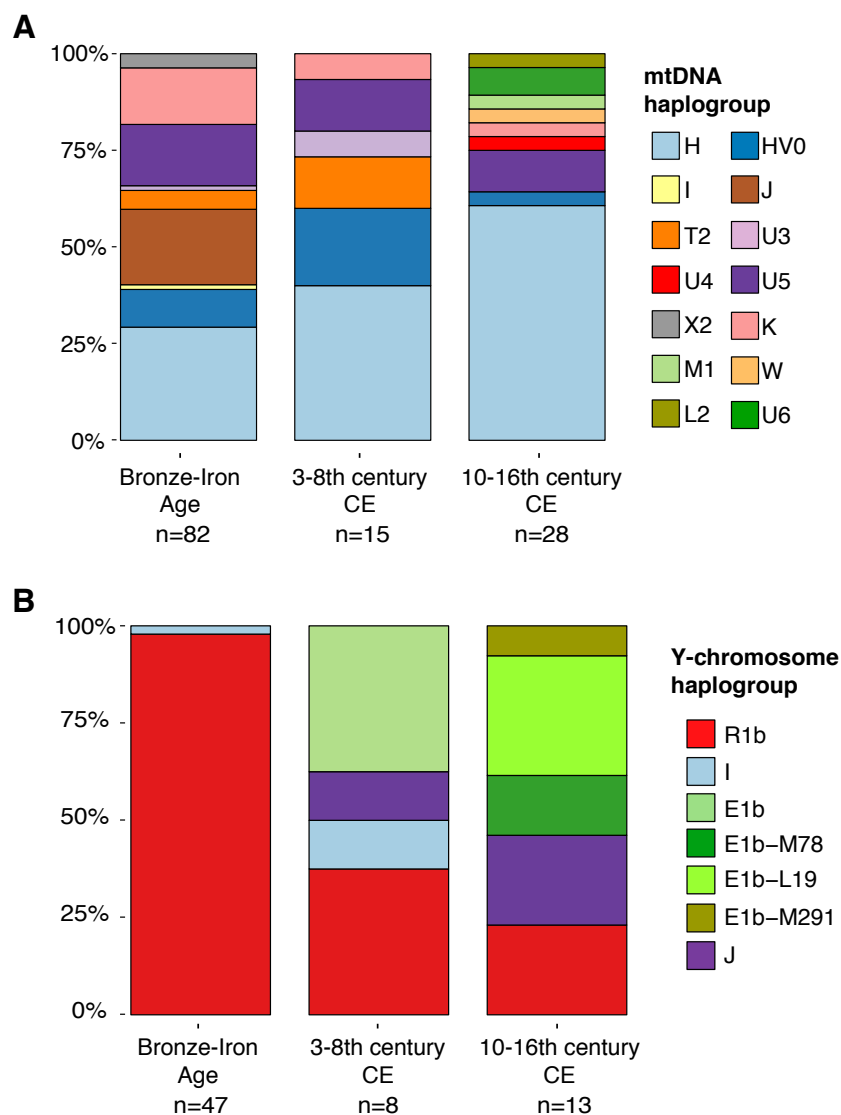


**Fig. S11. (A) Mitochondrial and (B) Y chromosome haplogroup composition of individuals from southeast Iberia during the past 2000 years. The general Iberian Bronze and Iron Age population is included for comparison.**

2288 **Table S1.** Ancient individuals from the Iberian Peninsula included in this study.  
2289  
2290 **Table S2.** New DNA libraries sequenced in this study.  
2291  
2292 **Table S3.** New radiocarbon dates generated in this study.  
2293  
2294 **Table S4.** Y-chromosome calls for the Iberian males.  
2295  
2296 **Table S5.** Comparison between key statistics computed using all SNPs and after  
2297 removing SNPs in CpG context.

2298 **Table S6.** Mismatch rates between Iberian Mesolithic individuals.

<b>Individual 1</b>	<b>Individual 2</b>	<b>Mismatch rate</b>	<b>SE</b>	<b>SNPs</b>
LaBraña2	LaBraña2	0.1148088	0.00102	804276
LaBraña1	LaBraña1	0.1106495	0.00095	857356
Canes1	Canes1	0.1160385	0.00102	579144
LaBraña1	LaBraña2	0.1690504	0.00188	892225
LaBraña2	Canes1	0.2248682	0.00126	738526
LaBraña1	Canes1	0.2244443	0.00123	752748
Car1	Car1	0.1068768	0.00123	156133
CMN2	CMN2	0.0704225	0.00998	710
CC1	CC1	0.0374449	0.00944	454
Chan	Chan	0.1070321	0.00106	948893
Car1	CMN2	0.2161954	0.00366	12979
Car1	Chan	0.2125906	0.00133	450321
Car1	CC1	0.2196306	0.00546	6388
Chan	CC1	0.2206930	0.00387	12497
CMN2	Chan	0.2113349	0.00291	23432
CMN2	CC1	0.2033426	0.02113	359

2299

2300

2301 **Table S7.** Working 2-way models for Iberian Mesolithic hunter-gatherers and Loschbour. These  
 2302 values were used for Fig. 2A.

<i>Test</i>	<i>Source1</i>	<i>Source2</i>	<i>P-value</i>	<b>Mixture proportions</b>		<b>SE</b>	
				<i>Source1</i>	<i>Source2</i>	<i>Source1</i>	<i>Source2</i>
LaBraña1	El Mirón	KO1	2.34E-01	0.448	0.552	0.046	0.046
LaBraña2	El Mirón	KO1	1.63E-01	0.490	0.510	0.042	0.042
Canes1	El Mirón	KO1	1.17E-01	0.268	0.732	0.047	0.047
Chan	El Mirón	KO1	6.26E-01	0.874	0.126	0.045	0.045
CMN2+CC1	El Mirón	KO1	5.22E-01	0.801	0.199	0.137	0.137
Carl	El Mirón	KO1	5.10E-01	0.927	0.073	0.046	0.046
Loschbour	El Mirón	KO1	8.65E-01	0.320	0.680	0.051	0.051

2303  
 2304



2305 **Table S8.** Working 2-way and 3-way models for Neolithic and Copper Age groups from Iberia,  
2306 central Europe and Britain. These values were used for Fig. 2A.  
2307  
2308

<i>Test</i>	<i>Source1</i>	<i>Source2</i>	<i>Source3</i>	<i>P-value</i>	<b>Mixture proportions</b>			<b>SE</b>		
					<i>Source 1</i>	<i>Source 2</i>	<i>Source 3</i>	<i>Source 1</i>	<i>Source 2</i>	<i>Source3</i>
C_Iberia_MLN	El Mirón	KO1	Anatolia_N	9.07E-01	0.118	0.218	0.664	0.025	0.027	0.022
C_Iberia_CA	El Mirón	KO1	Anatolia_N	9.35E-01	0.079	0.216	0.705	0.016	0.019	0.013
NE_Iberia_EN	GoyetQ116-1	KO1	Anatolia_N	5.89E-01	0.083	0.087	0.831	0.026	0.024	0.021
	Ust_Ishim	KO1	Anatolia_N	5.04E-01	0.061	0.136	0.803	0.017	0.019	0.025
	Vestonice16	KO1	Anatolia_N	4.93E-01	0.089	0.091	0.820	0.026	0.024	0.022
	El Mirón	KO1	Anatolia_N	3.27E-01	0.079	0.076	0.845	0.025	0.026	0.021
	Iran_N	KO1	Anatolia_N	2.40E-01	0.061	0.120	0.819	0.033	0.019	0.038
	Tianyuan	KO1	Anatolia_N	2.23E-01	0.053	0.132	0.815	0.019	0.019	0.025
	Kostenki14	KO1	Anatolia_N	1.98E-01	0.074	0.102	0.824	0.026	0.023	0.023
	Morocco	KO1	Anatolia_N	1.96E-01	0.048	0.161	0.791	0.016	0.021	0.031
	Iberomaurusian									
	EHG	KO1	Anatolia_N	1.24E-01	0.026	0.151	0.823	0.027	0.034	0.025
	El Mirón	EHG	Anatolia_N	6.29E-02	0.103	0.063	0.834	0.023	0.022	0.020
	Israel_Natufian	KO1	Anatolia_N	5.70E-02	0.066	0.141	0.793	0.052	0.024	0.069
NE_Iberia_MLN	El Mirón	KO1	Anatolia_N	3.86E-01	0.058	0.188	0.754	0.021	0.022	0.016
NE_Iberia_CA	El Mirón	KO1	Anatolia_N	6.88E-01	0.089	0.175	0.736	0.031	0.032	0.025
	GoyetQ116-1	KO1	Anatolia_N	1.50E-01	0.134	0.188	0.677	0.034	0.032	0.024
N_Iberia_EN	El Mirón	KO1	Anatolia_N	9.76E-01	0.000	0.106	0.893	0.035	0.036	0.031
	El Mirón	EHG	Anatolia_N	1.32E-01	0.060	0.037	0.904	0.035	0.033	0.030
	GoyetQ116-1	KO1	Anatolia_N	7.26E-02	0.061	0.115	0.824	0.037	0.035	0.030
N_Iberia_MLN	GoyetQ116-1	KO1	Anatolia_N	9.31E-02	0.100	0.263	0.636	0.022	0.022	0.016
	EHG	KO1	Anatolia_N	7.64E-02	0.008	0.379	0.613	0.021	0.027	0.020
	El Mirón	KO1	Anatolia_N	4.73E-02	0.066	0.264	0.670	0.020	0.023	0.016
N_Iberia_CA	El Mirón	KO1	Anatolia_N	5.99E-01	0.095	0.233	0.672	0.018	0.020	0.015
NW_Iberia_MLN	El Mirón	EHG	Anatolia_N	2.22E-01	0.208	0.264	0.528	0.114	0.098	0.092
	EHG	KO1	Anatolia_N	1.03E-01	0.182	0.446	0.372	0.110	0.131	0.112
	El Mirón	KO1	Anatolia_N	2.35E-02	0.365	-0.016	0.651	0.212	0.195	0.102
SE_Iberia_MLN	El Mirón	KO1	Anatolia_N	3.75E-01	0.114	0.143	0.742	0.021	0.022	0.017
SE_Iberia_CA	El Mirón	KO1	Anatolia_N	3.72E-01	0.097	0.157	0.746	0.019	0.022	0.015
SW_Iberia_EN	El Mirón	KO1	Anatolia_N	8.53E-01	0.052	0.074	0.874	0.049	0.051	0.040
	El Mirón	EHG	Anatolia_N	7.23E-01	0.070	0.070	0.860	0.044	0.043	0.038
	El Mirón	Iran_N	Anatolia_N	5.76E-01	0.133	0.005	0.862	0.038	0.060	0.066
	GoyetQ116-1	KO1	Anatolia_N	4.55E-01	0.075	0.096	0.829	0.049	0.047	0.038
	MA1	ElMirón	Anatolia_N	4.32E-01	0.023	0.100	0.877	0.044	0.042	0.040
	Iran_N	KO1	Anatolia_N	3.44E-01	0.001	0.156	0.843	0.063	0.037	0.068
	Tianyuan	KO1	Anatolia_N	3.30E-01	0.024	0.138	0.838	0.037	0.036	0.046
	Kostenki14	KO1	Anatolia_N	3.14E-01	0.031	0.132	0.836	0.048	0.043	0.042
	Vestonice16	KO1	Anatolia_N	3.13E-01	0.025	0.136	0.839	0.051	0.047	0.041
	Ust_Ishim	KO1	Anatolia_N	3.12E-01	0.000	0.147	0.853	0.036	0.035	0.047
SW_Iberia_MLN	El Mirón	KO1	Anatolia_N	6.18E-03	0.078	0.132	0.790	0.028	0.032	0.024
SW_Iberia_CA	El Mirón	KO1	Anatolia_N	6.83E-01	0.124	0.155	0.721	0.017	0.019	0.014
England_N	El Mirón	KO1	Anatolia_N	9.78E-01	0.058	0.202	0.740	0.018	0.020	0.015
Scotland_N	El Mirón	KO1	Anatolia_N	2.97E-01	0.041	0.201	0.758	0.015	0.017	0.012
France_MLN	El Mirón	KO1	Anatolia_N	7.35E-01	0.054	0.205	0.741	0.028	0.032	0.023
	GoyetQ116-1	KO1	Anatolia_N	2.18E-01	0.093	0.214	0.692	0.027	0.030	0.022
LBK_EN	KO1	Anatolia_N		6.71E-01	0.076	0.924		0.009	0.009	
Germany_MN	Tianyuan	KO1	Anatolia_N	4.40E-01	0.096	0.245	0.659	0.023	0.023	0.029
	mota	KO1	Anatolia_N	1.96E-01	0.043	0.298	0.659	0.020	0.024	0.036
	Iran_N	KO1	Anatolia_N	1.09E-01	0.110	0.240	0.650	0.037	0.024	0.042
	KO1	Anatolia_N		1.55E-03	0.263	0.737		0.024	0.024	

Hungary_EN	KO1	Anatolia_N	4.43E-01	0.090	0.910	0.012	0.012
Hungary_LCA	KO1	Anatolia_N	9.31E-01	0.164	0.836	0.010	0.010
Globular_Amphora Poland	KO1	Anatolia_N	1.51E-01	0.280	0.720	0.020	0.020

---

2309

2310

2311 **Table S9.** Best 2-way and 3-way model for the Iberian Copper Age outlier (C\_Iberia\_CA\_Afr).  
 2312

				Mixture proportions			SE		
<i>Source1</i>	<i>Source2</i>	<i>Source3</i>	P-value	<i>Source1</i>	<i>Source2</i>	<i>Source3</i>	<i>Source1</i>	<i>Source2</i>	<i>Source3</i>
Europe_	Morocco		1.60E-02	0.451	0.549		0.027	0.027	
EN	Iberomauru								
	sian								
Mota	Europe_EN	Morocco	5.85E-02	0.034	0.549	0.417	0.060	0.054	0.102
		Iberomau							
		rusian							

2313  
 2314

**Table S10.** Working models for the Iberian Copper Age outlier (C\_Iberia\_CA\_Afr) when including Morocco\_EN and Morocco\_LN in the *outgroup* set.

				Mixture proportions			SE		
<i>Source1</i>	<i>Source2</i>	<i>Source3</i>	P-value	<i>Source1</i>	<i>Source2</i>	<i>Source3</i>	<i>Source1</i>	<i>Source2</i>	<i>Source3</i>
Morocco Iberomaurusian	Morocco_EN	Morocco_LN	7.36E-01	0.021	0.164	0.814	0.084	0.105	0.037
Mota	Israel_Natufian	Morocco_LN	3.51E-01	0.039	0.065	0.895	0.022	0.055	0.068
Mota	Morocco_EN	Morocco_LN	3.38E-01	0.013	0.024	0.963	0.021	0.012	0.021
Mota	Morocco Iberomaurusian	Morocco_LN	3.07E-01	0.013	0.015	0.972	0.022	0.014	0.020
Mota	Morocco_LN		2.32E-01	0.024	0.976		0.020	0.020	

2320 **Table S11.** Working models for Iberia\_CA\_Stp, Iberia\_BA and Iberia IA groups. Models in bold  
2321 were used for Fig. S6 and mentioned in the main text.  
2322

<i>Test</i>	<i>Source1</i>	<i>Source2</i>	P-value	Mixture proportions		SE	
				<i>Source1</i>	<i>Source2</i>	<i>Source1</i>	<i>Source2</i>
Iberia_CA_Stp	<b>Germany_Beaker</b>	<b>Iberia_CA</b>	<b>6.06E-01</b>	<b>0.602</b>	<b>0.398</b>	<b>0.018</b>	<b>0.018</b>
Iberia_BA	<b>Germany_Beaker</b>	<b>Iberia_CA</b>	<b>3.90E-01</b>	<b>0.396</b>	<b>0.604</b>	<b>0.010</b>	<b>0.010</b>
	Iberia_CA	Iberia_CA_Stp	2.96E-01	0.332	0.668	0.024	0.024
E_Iberia_IA	England_MBA	Iberia_BA	6.64E-01	0.135	0.865	0.022	0.022
	England_Beaker	Iberia_BA	6.03E-01	0.123	0.877	0.020	0.020
	Netherlands_Beaker	Iberia_BA	5.87E-01	0.114	0.886	0.019	0.019
	<b>France_Beaker</b>	<b>Iberia_BA</b>	<b>5.32E-01</b>	<b>0.144</b>	<b>0.856</b>	<b>0.024</b>	<b>0.024</b>
	Unetice_EBA	Iberia_BA	3.10E-01	0.119	0.881	0.021	0.021
	Steppe_EBA	Iberia_BA	2.73E-01	0.059	0.941	0.011	0.011
	France_Beaker	Iberia_CA	2.71E-01	0.493	0.507	0.017	0.017
	Germany_Beaker	Iberia_BA	2.69E-01	0.143	0.857	0.026	0.026
	EHG	Iberia_BA	2.36E-01	0.048	0.952	0.009	0.009
	England_Beaker	Iberia_CA	2.09E-01	0.434	0.566	0.013	0.013
	Netherlands_Beaker	Iberia_CA	1.92E-01	0.422	0.578	0.012	0.012
	England_MBA	Iberia_CA	1.87E-01	0.474	0.526	0.014	0.014
N_Iberia_IA	England_MBA	Iberia_BA	5.59E-01	0.322	0.678	0.034	0.034
	Netherlands_Beaker	Iberia_BA	3.09E-01	0.286	0.714	0.029	0.029
	<b>France_Beaker</b>	<b>Iberia_BA</b>	<b>2.43E-01</b>	<b>0.358</b>	<b>0.642</b>	<b>0.038</b>	<b>0.038</b>
	France_Beaker	Iberia_CA	2.35E-01	0.639	0.361	0.026	0.026
	Netherlands_Beaker	Iberia_CA	2.25E-01	0.545	0.455	0.022	0.022
	England_Beaker	Iberia_BA	2.14E-01	0.300	0.700	0.03	0.03
	England_MBA	Iberia_CA	2.10E-01	0.604	0.396	0.023	0.023
	England_Beaker	Iberia_CA	1.10E-01	0.562	0.438	0.021	0.021
	Steppe_EBA	Iberia_BA	5.50E-02	0.162	0.838	0.017	0.017
SW_Iberia_IA	Unetice_EBA	Iberia_CA	8.34E-01	0.395	0.605	0.040	0.040
	Germany_Beaker	Iberia_BA	6.99E-01	0.260	0.740	0.059	0.059
	Unetice_EBA	Iberia_BA	6.78E-01	0.192	0.808	0.047	0.047
	Steppe_EBA	Iberia_BA	6.77E-01	0.105	0.895	0.028	0.028
	<b>France_Beaker</b>	<b>Iberia_BA</b>	<b>6.77E-01</b>	<b>0.212</b>	<b>0.788</b>	<b>0.050</b>	<b>0.050</b>
	Steppe_EBA	Iberia_CA	5.71E-01	0.228	0.772	0.026	0.026
	MA1	Iberia_BA	5.27E-01	0.110	0.890	0.028	0.028
	Netherlands_Beaker	Iberia_BA	5.11E-01	0.179	0.821	0.044	0.044
	England_Beaker	Iberia_BA	5.09E-01	0.171	0.829	0.047	0.047
	Germany_Beaker	Iberia_CA	4.94E-01	0.479	0.521	0.047	0.047
	England_MBA	Iberia_BA	4.69E-01	0.197	0.803	0.051	0.051
	EHG	Iberia_BA	3.72E-01	0.089	0.911	0.024	0.024
	Iran_N	Iberia_BA	3.48E-01	0.147	0.853	0.037	0.037
	France_Beaker	Iberia_CA	3.11E-01	0.410	0.590	0.042	0.042

Netherlands_Beaker	Iberia_CA	2.44E-01	0.362	0.638	0.037	0.037
England_Beaker	Iberia_CA	1.94E-01	0.368	0.632	0.038	0.038
England_MBA	Iberia_CA	1.42E-01	0.401	0.599	0.041	0.041
ElMiron	Iberia_BA	1.28E-01	0.081	0.919	0.042	0.042
EHG	Iberia_CA	1.00E-01	0.199	0.801	0.021	0.021
Kostenki14	Iberia_BA	7.91E-02	0.073	0.927	0.031	0.031

2323

2324

2325 **Table S12.** Mixture proportions for the model Iberia\_CA+Steppe\_EBA. These values were used  
 2326 for Fig. S6.

<i>Test</i>	<i>Source1</i>	<i>Source2</i>	<i>P-value</i>	<b>Mixture proportions</b>		<b>SE</b>	
				<i>Source1</i>	<i>Source2</i>	<i>Source1</i>	<i>Source2</i>
Iberia_CA_Stp	Iberia_CA	Steppe_EBA	4.01E-01	0.713	0.287	0.011	0.011
Iberia_BA	Iberia_CA	Steppe_EBA	1.66E-01	0.818	0.182	0.007	0.007
E_Iberia_IA	Iberia_CA	Steppe_EBA	1.24E-01	0.754	0.245	0.011	0.011
N_Iberia_IA	Iberia_CA	Steppe_EBA	2.57E-01	0.687	0.313	0.018	0.018
SW_Iberia_IA	Iberia_CA	Steppe_EBA	9.30E-01	0.803	0.197	0.034	0.034

2327  
 2328

2329 **Table S13.** Mixture proportions for the model Iberia\_CA+Steppe\_EBA in Bronze Age groups  
 2330 from different regions.

<i>Test</i>	<i>Source1</i>	<i>Source2</i>	<i>P-value</i>	<b>Mixture proportions</b>		<b>SE</b>	
				<i>Source1</i>	<i>Source2</i>	<i>Source1</i>	<i>Source2</i>
C_Iberia_BA	Iberia_CA	Steppe_EBA	1.29E-01	0.808	0.192	0.012	0.012
N_Iberia_BA	Iberia_CA	Steppe_EBA	2.69E-01	0.799	0.201	0.012	0.012
NE_Iberia_BA	Iberia_CA	Steppe_EBA	9.19E-02	0.806	0.194	0.012	0.012
SE_Iberia_BA	Iberia_CA	Steppe_EBA	4.35E-01	0.854	0.146	0.014	0.014
SW_Iberia_BA	Iberia_CA	Steppe_EBA	7.64E-03	0.856	0.144	0.017	0.017

2331  
 2332



2333 **Table S14.** Mixture proportions for Iberia\_BA using the model Iberia\_CA+ Germany\_Beaker.  
 2334

	<i>Source1</i>	<i>Source2</i>	<b>P-value</b>	<b>Mixture proportions</b>		<b>SE</b>	
				<i>Source1</i>	<i>Source2</i>	<i>Source1</i>	<i>Source2</i>
Autosomes	Iberia_CA	Germany_Beaker	6.14E-01	0.611	0.389	0.012	0.012
X-chromosomes	Iberia_CA	Germany_Beaker	1.27E-01	0.827	0.173	0.081	0.081

2335

2336

2337 **Table S15.** Admixture proportions for individuals in the Iberia\_CA\_Stp, Iberia\_BA and  
2338 Iberia\_IA populations. These values were used for Fig. 2B.  
2339

Ind	Label	P-value	Iberia_CA	Germany_Beaker	SE
I0462	C_Iberia_CA_Stp	2.53E-01	0.229	0.771	0.111
EHU002	C_Iberia_CA_Stp	9.30E-01	0.371	0.629	0.049
I3239	NW_Iberia_CA_Stp	9.39E-01	0.226	0.774	0.085
I3243	NW_Iberia_CA_Stp	7.54E-01	0.239	0.761	0.094
I3238	NW_Iberia_CA_Stp	8.81E-01	0.365	0.635	0.056
I0461	C_Iberia_CA_Stp	5.19E-02	0.544	0.456	0.046
I6471	C_Iberia_CA_Stp	7.81E-01	-0.145	1.145	0.097
I6472	C_Iberia_CA_Stp	4.89E-01	0.499	0.501	0.057
I6539	C_Iberia_CA_Stp	5.74E-01	0.485	0.515	0.048
I6588	C_Iberia_CA_Stp	4.02E-01	0.270	0.730	0.067
EHU001	C_Iberia_CA_Stp	8.76E-01	0.096	0.904	0.049
I5665	C_Iberia_CA_Stp	3.69E-01	0.501	0.499	0.045
I3484	C_Iberia_CA_Stp	6.19E-01	0.644	0.356	0.075
I7689	SW_Iberia_BA	9.71E-01	0.840	0.160	0.188
I7691	SW_Iberia_BA	2.64E-01	0.678	0.322	0.073
I7692	SW_Iberia_BA	2.40E-01	0.645	0.355	0.077
I3756	C_Iberia_BA	4.28E-01	0.655	0.345	0.044
I6623	C_Iberia_CA_Stp	1.86E-01	0.297	0.703	0.046
I3494	SE_Iberia_BA	4.60E-01	0.744	0.256	0.042
I12809	C_Iberia_BA	6.54E-01	0.507	0.493	0.083
I12855	C_Iberia_BA	5.09E-01	0.677	0.323	0.124
I6618	C_Iberia_BA	4.73E-02	0.681	0.319	0.046
I8144	SE_Iberia_BA	4.64E-01	0.534	0.466	0.064
VAD001	N_Iberia_BA	3.12E-02	0.498	0.502	0.047
I1310	NE_Iberia_BA	7.15E-02	0.654	0.346	0.048
I1312_d	NE_Iberia_BA	5.84E-01	0.499	0.501	0.056
I1313_d	NE_Iberia_BA	9.26E-01	0.688	0.312	0.049
I3997	SE_Iberia_BA	1.81E-03	0.694	0.306	0.044
I4562	NE_Iberia_BA	2.48E-01	0.559	0.441	0.042
I3487	SE_Iberia_BA	2.42E-01	0.754	0.246	0.065
I6470	C_Iberia_BA	5.11E-01	0.522	0.478	0.045
I10939	SW_Iberia_BA	6.27E-01	0.702	0.298	0.049
I10940	SW_Iberia_BA	3.45E-01	0.544	0.456	0.095
I10941	SW_Iberia_BA	1.18E-01	0.638	0.362	0.050
VAD005	N_Iberia_BA	3.67E-01	0.524	0.476	0.050
I1982	N_Iberia_BA	7.70E-01	0.462	0.538	0.141
VAD002	N_Iberia_BA	1.64E-01	0.583	0.417	0.070
VAD003	N_Iberia_BA	3.33E-01	0.575	0.425	0.109
I3486	SE_Iberia_BA	1.13E-01	0.650	0.350	0.089
I3488	SE_Iberia_BA	3.52E-01	0.793	0.207	0.074
I4559	NE_Iberia_BA	6.19E-01	0.545	0.455	0.048
I4560	NE_Iberia_BA	9.25E-01	0.549	0.451	0.045
I4561	NE_Iberia_BA	4.25E-01	0.552	0.448	0.044
I1836	NE_Iberia_BA	2.71E-01	0.597	0.403	0.050
I2471	N_Iberia_BA	9.37E-01	0.577	0.423	0.059
I1840	N_Iberia_BA	6.19E-01	0.610	0.390	0.046
I1977	N_Iberia_BA	3.42E-02	0.585	0.415	0.064
I2472	N_Iberia_BA	5.35E-01	0.677	0.323	0.060
I8136	SE_Iberia_BA	1.43E-01	0.685	0.315	0.044

I3490	C_Iberia_BA	4.09E-01	0.585	0.415	0.053
I3491	C_Iberia_BA	1.09E-01	0.606	0.394	0.071
I3492	C_Iberia_BA	4.43E-01	0.483	0.517	0.058
I8045	SW_Iberia_BA	7.14E-01	0.627	0.373	0.104
VAD004	N_Iberia_BA	1.75E-02	0.572	0.428	0.050
I8570	SE_Iberia_BA	9.86E-01	0.648	0.352	0.048
I8571	SE_Iberia_BA	4.70E-01	0.766	0.234	0.095
I3493	C_Iberia_BA	1.76E-02	0.518	0.482	0.048
I2470	N_Iberia_BA	1.14E-01	0.583	0.417	0.049
I12208	C_Iberia_BA	7.83E-02	0.598	0.402	0.043
I12209	C_Iberia_BA	3.93E-01	0.581	0.419	0.043
I7687	SW_Iberia_BA	7.75E-01	0.537	0.463	0.117
I7688	SW_Iberia_BA	9.49E-01	0.391	0.609	0.123
I2469	N_Iberia_BA	7.79E-01	0.420	0.580	0.069
I12641	E_Iberia_IA	5.82E-01	0.430	0.570	0.071
I12640	E_Iberia_IA	3.94E-01	0.461	0.539	0.073
I12171	SW_Iberia_IA	7.90E-01	0.505	0.495	0.068
I12561	SW_Iberia_IA	7.87E-01	0.582	0.418	0.091
I4556	E_Iberia_IA	9.24E-01	0.412	0.588	0.060
I3322	E_Iberia_IA	9.22E-01	0.504	0.496	0.045
I12642	E_Iberia_IA	4.83E-01	0.678	0.322	0.172
I12879	E_Iberia_IA	2.83E-03	0.359	0.641	0.053
I12410	E_Iberia_IA	9.18E-01	0.499	0.501	0.043
I12877	E_Iberia_IA	4.13E-01	0.596	0.404	0.093
I12878	E_Iberia_IA	5.67E-01	0.562	0.438	0.057
I3757	N_Iberia_IA	3.59E-01	0.467	0.533	0.060
I3323	E_Iberia_IA	5.89E-01	0.548	0.452	0.049
I3758	N_Iberia_IA	6.02E-01	0.307	0.693	0.043
I3759	N_Iberia_IA	6.13E-01	0.407	0.593	0.044
I3324	E_Iberia_IA	1.49E-01	0.389	0.611	0.049
I3326	E_Iberia_IA	5.81E-01	0.021	0.979	0.070
I3327	E_Iberia_IA	4.46E-01	0.495	0.505	0.053
I3320	E_Iberia_IA	3.68E-01	0.434	0.566	0.045
I3321	E_Iberia_IA	9.25E-01	0.518	0.482	0.044

2340  
2341

**Table S16.** Working 2-way model for the Iberian Bronze Age outlier (ID I7162).

			Mixture proportions		SE	
<i>Source1</i>	<i>Source2</i>	P-value	<i>Source1</i>	<i>Source2</i>	<i>Source1</i>	<i>Source2</i>
Iberia_BA	Morocco_LN	7.40E-01	0.534	0.466	0.050	0.050
Morocco						
Iberomaurusian	Iberia_BA	5.50E-01	0.112	0.888	0.018	0.018
Iberia_BA	C_Iberia_CA_Afr	5.65E-01	0.759	0.241	0.031	0.031
Israel_Natufian	Iberia_BA	3.54E-01	0.292	0.708	0.039	0.039
mota	Iberia_BA	8.33E-02	0.133	0.867	0.016	0.016

**Table S17.** 2-way models for NE\_Iberia\_c.6-8CE\_ES (L'Esquerda) including Iberia\_IA as one of the sources. The models in bold were used for Fig. 2C.

<i>Source1</i>	<i>Source2</i>	<b>P-value</b>	<b>Mixture proportions</b>		<b>SE</b>	
			<i>Source1</i>	<i>Source2</i>	<i>Source1</i>	<i>Source2</i>
<b>Iberia_IA</b>	<b>Greek</b>	<b>3.29E-01</b>	<b>0.794</b>	<b>0.206</b>	<b>0.027</b>	<b>0.027</b>
Iberia_IA	Bergamo	1.33E-01	0.731	0.269	0.039	0.039
Iberia_IA	TSI	4.89E-02	0.737	0.263	0.043	0.043
Iberia_IA	Bavaria_Early Medieval.SG	5.70E-03	0.819	0.181	0.033	0.033
Iberia_IA	Saxon.SG	2.87E-03	0.818	0.182	0.034	0.034
Iberia_IA	Steppe_EBA	1.14E-03	0.926	0.074	0.018	0.018
Iberia_IA	Empuries2	4.48E-04	0.858	0.142	0.034	0.034
Iberia_IA	Iran_N	2.64E-04	0.908	0.092	0.019	0.019
Iberia_IA	MA1	9.93E-05	0.955	0.045	0.013	0.013
Iberia_IA	EHG	3.68E-05	0.959	0.041	0.014	0.014
Iberia_IA	Anatolia_N	7.38E-06	-0.009	1.009	0.024	0.024
Iberia_IA	Kostenki14	1.79E-06	0.987	0.013	0.014	0.014
Iberia_IA	Israel_Natufian	1.04E-06	0.985	0.015	0.020	0.020
Iberia_IA	LBK_EN	7.62E-07	0.975	0.025	0.025	0.025
Iberia_IA	Ust_Ishim	8.73E-09	0.976	0.024	0.012	0.012
Iberia_IA	mota	8.46E-11	0.986	0.014	0.009	0.009
Iberia_IA	Morocco Iberomaurusian	6.07E-13	0.970	0.030	0.011	0.011

2351 **Table S18.** Best 2-way and 3-way models for NE\_Iberia\_c.6CE\_PL (Pla de l'Horta). The models  
 2352 in bold were used for Fig. 2C.

				Mixture proportions			SE		
<i>Source1</i>	<i>Source2</i>	<i>Source3</i>	P-value	<i>Source1</i>	<i>Source2</i>	<i>Source3</i>	<i>Source1</i>	<i>Source2</i>	<i>Source3</i>
NE_Iberia_c.6-8CE_ES	Steppe_EBA		1.22E-01	0.914	0.086		0.020	0.020	
NE_Iberia_c.6-8CE_ES	Bavaria_Early Medieval.SG		3.61E-02	0.832	0.168		0.042	0.042	
NE_Iberia_c.6-8CE_ES	Saxon.SG		2.87E-02	0.864	0.136		0.045	0.045	
NE_Iberia_c.6-8CE_ES	Steppe_EBA	LBK_EN	1.96E-01	0.853	0.114	0.033	0.069	0.033	0.040
NE_Iberia_c.6-8CE_ES	Steppe_EBA	TSI	9.35E-02	0.781	0.091	0.127	0.059	0.019	0.054
<b>NE_Iberia_c.6-8CE_ES</b>	<b>Bavaria_Early Medieval.SG</b>	<b>TSI</b>	<b>9.20E-02</b>	<b>0.732</b>	<b>0.226</b>	<b>0.041</b>	<b>0.067</b>	<b>0.050</b>	<b>0.054</b>
NE_Iberia_c.6-8CE_ES	Steppe_EBA	Bavaria_Early Medieval.SG	6.19E-02	0.881	0.069	0.050	0.053	0.036	0.080
NE_Iberia_c.6-8CE_ES	Steppe_EBA	Empuries2	5.58E-02	0.819	0.104	0.077	0.054	0.022	0.040
NE_Iberia_c.6-8CE_ES	Steppe_EBA	Anatolia_N	5.39E-02	0.792	0.136	0.072	0.059	0.030	0.033

2353

2354

2355 **Table S19.** Working 2-way models for NE\_Iberia\_c.8-12CE (Sant Julià de Ramis). The models  
 2356 in bold were used for Fig. 2C.

			Mixture proportions		SE	
<i>Source1</i>	<i>Source2</i>	P-value	<i>Source1</i>	<i>Source2</i>	<i>Source1</i>	<i>Source2</i>
NE_Iberia_c.6-8CE_ES	SE_Iberia_c.10-16CE	3.33E-01	0.678	0.322	0.059	0.059
<b>NE_Iberia_c.6-8CE_ES</b>	<b>Morocco_LN</b>	<b>1.36E-01</b>	<b>0.827</b>	<b>0.173</b>	<b>0.038</b>	<b>0.038</b>
NE_Iberia_c.6-8CE_ES	Israel Natufian	1.21E-01	0.888	0.112	0.023	0.023

2357  
 2358

2359 **Table S20.** 2-way and 3-way admixture models for populations from the southeast over the past  
2360 2000 years.

<i>Test</i>	<i>Source1</i>	<i>Source2</i>	<i>Source3</i>	<i>P-value</i>	Mixture proportions			SE		
					<i>Source 1</i>	<i>Source 2</i>	<i>Source 3</i>	<i>Source 1</i>	<i>Source 2</i>	<i>Source 3</i>
SE_Iberia c.3-4 CE	NE_Iberia c.6-8CE_ES	Morocco _LN		7.87E-02	0.554	0.446		0.031	0.031	
SE_Iberia c.5-8 CE	NE_Iberia c.6-8CE_ES	Morocco _LN		1.22E-06	0.532	0.468		0.026	0.026	
SE_Iberia c.10-16CE	NE_Iberia c.6-8CE_ES	Guanche		2.76E-02	0.773	0.227		0.012	0.012	
SE_Iberia c.3-4 CE	NE_Iberia c.6-8CE_ES	Morocco _LN	Levant_ EBA	9.45E-02	0.542	0.393	0.065	0.031	0.047	0.041
SE_Iberia c.5-8 CE	NE_Iberia c.6-8CE_ES	Guanche	Levant_ EBA	6.92E-05	0.699	0.193	0.108	0.026	0.018	0.036
SE_Iberia c.10-16CE	NE_Iberia c.6-8CE_ES	Guanche	Levant_ EBA	2.11E-01	0.699	0.188	0.113	0.022	0.015	0.030

2361

2362



2363 **Table S21.** Admixture models for individuals in the SE\_Iberia\_c.3-4CE, SE\_Iberia\_c.5-8CE and  
2364 SE\_Iberia\_c.10-16CE populations. These ancestry proportions were used for Fig. 2D.  
2365

Ind ID	Population	Source1	Source2	Source3	P-value	Mixture proportions			SE		
						Source 1	Source 2	Source 3	Source 1	Source 2	Source 3
I3982	SE_Iberia_c.3-4CE	NE_Iberia_c.6-8CE_ES	Morocco_LN	Levant_EBA	1.03E-01	0.543	0.435	0.022	0.046	0.067	0.050
I3983	SE_Iberia_c.3-4CE	NE_Iberia_c.6-8CE_ES	Morocco_LN	Levant_EBA	6.51E-02	0.480	0.410	0.110	0.041	0.068	0.058
I4055	SE_Iberia_c.3-4CE	NE_Iberia_c.6-8CE_ES	Morocco_LN		3.88E-01	0.433	0.567	0.000	0.102	0.102	0.000
I3980	SE_Iberia_c.5-8CE	NE_Iberia_c.6-8CE_ES	Morocco_LN	Levant_EBA	7.73E-01	0.269	0.568	0.162	0.041	0.080	0.077
I3981	SE_Iberia_c.5-8CE	NE_Iberia_c.6-8CE_ES	Morocco_LN	Levant_EBA	1.28E-01	0.489	0.504	0.007	0.048	0.090	0.067
I3574	SE_Iberia_c.5-8CE	NE_Iberia_c.6-8CE_ES	Morocco_LN		4.63E-01	0.539	0.461	0.000	0.092	0.092	0.000
I3575	SE_Iberia_c.5-8CE	NE_Iberia_c.6-8CE_ES	Morocco_LN		4.68E-01	0.331	0.669	0.000	0.043	0.043	0.000
I3581	SE_Iberia_c.5-8CE	NE_Iberia_c.6-8CE_ES	Morocco_LN		4.60E-01	0.459	0.541	0.000	0.042	0.042	0.000
I3576	SE_Iberia_c.5-8CE	NE_Iberia_c.6-8CE_ES	Morocco_LN	Levant_EBA	1.62E-01	0.481	0.447	0.071	0.041	0.066	0.058
I3583	SE_Iberia_c.5-8CE	NE_Iberia_c.6-8CE_ES	Morocco_LN	Levant_EBA	7.42E-01	0.281	0.668	0.051	0.058	0.105	0.082
I3577	SE_Iberia_c.5-8CE	NE_Iberia_c.6-8CE_ES	Morocco_LN		1.75E-01	0.290	0.710	0.000	0.086	0.086	0.000
I3578	SE_Iberia_c.5-8CE	NE_Iberia_c.6-8CE_ES	Guanche		3.41E-01	0.681	0.319	0.000	0.043	0.043	0.000
I3579	SE_Iberia_c.5-8CE	NE_Iberia_c.6-8CE_ES	Morocco_LN	Levant_EBA	4.46E-01	0.548	0.229	0.223	0.102	0.204	0.143
I3582	SE_Iberia_c.5-8CE	NE_Iberia_c.6-8CE_ES	Morocco_LN	Levant_EBA	2.34E-01	0.442	0.557	0.001	0.048	0.090	0.066
I3585	SE_Iberia_c.5-8CE	NE_Iberia_c.6-8CE_ES	Morocco_LN	Levant_EBA	6.20E-02	0.662	0.317	0.022	0.058	0.091	0.056
I7500	SE_Iberia_c.10-16CE	NE_Iberia_c.6-8CE_ES	Guanche		1.28E-01	0.795	0.205	0.000	0.060	0.060	0.000
I12516	SE_Iberia_c.10-16CE	NE_Iberia_c.6-8CE_ES	Morocco_LN		1.89E-01	0.699	0.301	0.000	0.066	0.066	0.000
I12514	SE_Iberia_c.10-16CE	NE_Iberia_c.6-8CE_ES	Morocco_LN		7.59E-01	0.556	0.444	0.000	0.047	0.047	0.000
I12515	SE_Iberia_c.10-16CE	NE_Iberia_c.6-8CE_ES	Morocco_LN		3.28E-01	0.602	0.398	0.000	0.051	0.051	0.000
I7497	SE_Iberia_c.10-16CE	NE_Iberia_c.6-8CE_ES	Morocco_LN	Levant_EBA	5.51E-01	0.466	0.464	0.070	0.071	0.115	0.112
I7498	SE_Iberia_c.10-16CE	NE_Iberia_c.6-8CE_ES	Morocco_LN	Levant_EBA	1.39E-01	0.589	0.294	0.117	0.050	0.078	0.062
I7499	SE_Iberia_c.10-16CE	NE_Iberia_c.6-8CE_ES	Morocco_LN	Jordanian	5.00E-02	0.431	0.286	0.283	0.042	0.081	0.079
I7457	SE_Iberia_c.10-16CE	NE_Iberia_c.6-8CE_ES	Guanche	Levant_EBA	9.74E-02	0.678	0.242	0.080	0.052	0.037	0.068
I12644	SE_Iberia_c.10-16CE	Iberia IA	Morocco_LN	Jordanian	3.04E-02	0.333	0.486	0.181	0.038	0.073	0.059
I12645	SE_Iberia_c.10-16CE	NE_Iberia_c.6-8CE_ES	Morocco_LN	Levant_EBA	3.84E-01	0.327	0.478	0.195	0.118	0.171	0.128

I12647	SE_Iberia c.10-16CE	NE_Iberia c.6-8CE_ES	Guanche	Levant_EBA	8.15E-02	0.753	0.150	0.097	0.047	0.031	0.060
I12648	SE_Iberia c.10-16CE	NE_Iberia c.6-8CE_ES	Guanche		8.20E-02	0.936	0.064	0.000	0.085	0.085	0.000
I12649	SE_Iberia c.10-16CE	NE_Iberia c.6-8CE_ES	Morocco_LN		9.68E-01	0.674	0.326	0.000	0.089	0.089	0.000
I8145	SE_Iberia c.10-16CE	NE_Iberia c.6-8CE_ES	Morocco_LN		9.14E-01	0.571	0.429	0.000	0.176	0.176	0.000
I8146	SE_Iberia c.10-16CE	NE_Iberia c.6-8CE_ES	Guanche	Levant_EBA	3.15E-01	0.445	0.358	0.197	0.068	0.045	0.086
I8147	SE_Iberia c.10-16CE	Iberia IA	Guanche	Levant_EBA	4.12E-01	0.720	0.176	0.103	0.124	0.100	0.172
I3808	SE_Iberia c.10-16CE	NE_Iberia c.6-8CE_ES	Morocco_LN	Levant_EBA	4.39E-02	0.379	0.367	0.255	0.046	0.079	0.065
I3809	SE_Iberia c.10-16CE	NE_Iberia c.6-8CE_ES	Morocco_LN		1.16E-01	0.461	0.539	0.000	0.133	0.133	0.000
I7423	SE_Iberia c.10-16CE	Iberia IA	Morocco_LN	Levant_EBA	8.51E-01	0.317	0.637	0.045	0.056	0.116	0.088
I7424	SE_Iberia c.10-16CE	NE_Iberia c.6-8CE_ES	Morocco_LN	Levant_EBA	1.19E-01	0.559	0.336	0.105	0.051	0.090	0.065
I7425	SE_Iberia c.10-16CE	NE_Iberia c.6-8CE_ES	Guanche	Levant_EBA	1.98E-01	0.629	0.286	0.086	0.046	0.033	0.057

---

2366

2367

2368 **Table S22.** Admixture models for the two outlier individuals from the SE\_Iberia\_c.10-16CE  
 2369 population. These ancestry proportions were used for Fig. 2D.

<i>Test</i>	<i>Source1</i>	<i>Source2</i>	<i>P-value</i>	<b>Mixture proportions</b>		<b>SE</b>	
				<i>Source1</i>	<i>Source2</i>	<i>Source1</i>	<i>Source2</i>
I7427	SE_Iberia c.3-4CE	Gambian	6.61E-01	0.630	0.370	0.021	0.021
I3810	SE_Iberia c.3-4CE	Gambian	2.68E-01	0.517	0.483	0.023	0.023

2370